Theses and Dissertations   Graduate School

1985

Chemical Studies on Oxomolybdenum(VI,IV) Complexes as Bioinorganic Models for the Molybdenum Oxidases

James Thomas Lyon III

COLLEGE OF HUMANITIES AND SCIENCES

VIRGINIA COMMONWEALTH UNIVERSITY

This is to certify that the dissertation prepared by JAMES
THOMAS LYON, III entitled CHEMICAL STUDIES ON OXOMOLYBDE-
NUM(VI,IV) COMPLEXES AS BIOINORGANIC MODELS FOR THE MOLYB-
DENUM OXIDASES has been approved by his committee as
satisfactory completion of the dissertation requirement for
the degree of Doctor of Philosophy.

Director of Dissertation

Committee Member

Committee Member

Committee Member

Committee Member

Department Chairman

College Dean

8/12/85
Date

Chemical Studies on Oxomolybdenum(VI,IV) Complexes
as Bioinorganic Models for the Molybdenum Oxidases

A dissertation submitted in partial fulfillment
of the requirements for the degree of Doctor of
Philosophy at Virginia Commonwealth University

By

James Thomas Lyon, III
B.S., University of North Carolina
at Greensboro, 1980

Director: Dr. Joseph Topich
Associate Professor of Chemistry
Virginia Commonwealth University
Richmond, Virginia
July, 1985

ACKNOWLEDGEMENTS

I would like to express my sincere appreciation to my advisor, Dr. Joseph Topich, for providing me with the knowledge and experience necessary to begin a scientific career. His guidance, patience and inspiration will never be forgotten.

I thank my parents Mr. and Mrs. James T. Lyon, Jr., and sister Jennifer A. Lyon, for their encouragement, and financial support throughout my graduate studies. Without their support this degree would not have been possible.

I would also like to thank the faculty members, staff, and graduate students of the Virginia Commonwealth University Chemistry Department for their friendship and support during my graduate career. Special thanks are extended to Dr. Fred M. Hawkridge and Kent Koller for their interest and helpful advice concerning the electrochemical aspects of my work.

The financial support which I have received through-out my graduate studies consisted of a teaching assistant-ship from Virginia Commonwealth University and a research assistantship from the National Institutes of Health, this support is greatly appreciated.

Finally, I thank Diane Holmes for her helpful comments and excellent typing skills in the completion of this dissertation.

TABLE OF CONTENTS

TABLE OF CONTENTS (continued)

TABLE OF CONTENTS (continued)

LIST OF TABLES

LIST OF TABLES (continued)

LIST OF FIGURES

LIST OF FIGURES (continued)

LIST OF FIGURES (continued)

ABSTRACT

CHEMICAL STUDIES ON OXOMOLYBDENUM(VI,IV) COMPLEXES
AS BIOINORGANIC MODELS FOR THE MOLYBDENUM OXIDASES

James T. Lyon, III, Ph.D.
Virginia Commonwealth University
Major Director: Dr. Joseph Topich

The synthesis, characterization, and chemical prop-
erties of $Mo(VI)O_2$(5-X-SSP) and $Mo(VI)O_2$(5-X-SSE), (5-X-
SSP^{2-} = 2-((5-X-salicylidene)amino)benzenethiolate; 5-X-
SSE^{2-} = 2-((5-X-salicylidene)amino)ethanethiolate; X = Br,
Cl, H, CH_3O), which contain tridentate (ONS) Schiff base
ligands is described. The chemical properties of these
molybdenum complexes are compared with those which possess
tridentate (ONO) Schiff base ligands. Cyclic voltammetry
was used to obtain cathodic reduction potentials (E_{pc}) for
the quasi-reversible reduction of the cis-dioxomolybdenum-
(VI) complexes. Although the reductions are quasi-revers-
ible, trends are observed in E_{pc} both within series and
when different series are compared. Cathodic reduction
potentials for the four series of complexes examined span
the range -1.53 to -1.05 V versus NHE. The oxygen atom
transfer reactions for $Mo(VI)O_2$(5-X-SSP) and $Mo(VI)O_2$(5-
X-SSE) with $PEtPh_2$ were studied in detail between 30 and
60°C. The applicable rate law is $+d[Mo(IV)OL]/dt = k_1[Mo-(VI)O_2L][PEtPh_2]$. The specific rate constants span the
range from 8.4 x 10^{-4} $M^{-1}s^{-1}$ (X = CH_3O) to 19.6 x 10^{-4}

$M^{-1}s^{-1}$ (X = Br) for Mo(VI)O$_2$(5-X-SSP) at 30°C and from 21.4 x 10^{-4} $M^{-1}s^{-1}$ (X = CH$_3$O) to 34.8 x 10^{-4} $M^{-1}s^{-1}$ (X = Br) for Mo(VI)O$_2$(5-X-SSE) at 60°C. Only oxomolybdenum(IV) complexes are observed as products of these reactions. This is a significant result. A linear dependence is observed between log(k$_{1X}$/k$_{1H}$) and the Hammett σ$_p$ parameter for the ligand X substituents for the two series Mo(VI)O$_2$(5-X-SSP) (ρ = +0.75) and Mo(VI)O$_2$(5-X-SSE) (ρ = +0.42). Activation parameter data were obtained for Mo(VI)O$_2$(5-H-SSP) (E$_a$ = 67.9 kJ/mol, ΔH‡ = 65.2 kJ/mol, ΔS‡ = -86.5 J/(mol-K)) and Mo(VI)O$_2$(5-H-SSE) (E$_a$ = 72.0 kJ/mol, ΔH‡ = 70.3 kJ/mol, ΔS‡ = -82.6 J/(mol-K)). There are three ligand features whose effect systematically alters both the cis-dioxomolybdenum-(VI) cathodic reduction potentials and specific rate constants. These include (1) the X-substituent on the salicylaldehyde portion of each ligand; (2) the degree of ligand delocalization; and (3) the substitution of a sulfur donor atom for an oxygen donor atom. Each of these effects is considered separately with regard to both the cis-dioxo-molybdenum(VI) cathodic reduction potentials and specific rate constants, then their cumulative effect is discussed. There exists a correlation between the specific rate constants and E$_{pc}$ for Mo(VI)O$_2$(5-X-SSP) and Mo(VI)O$_2$(5-X-SSE). Initial results are included on the reaction of Mo(IV)O(5-H-SSP) with NO$_3^-$. Spectral results suggest conversion of Mo(IV)O(5-H-SSP) to Mo(VI)O$_2$(5-H-SSP) by way of an oxygen atom transfer reaction.

I.   GENERAL INTRODUCTION

Molybdenum is presently attracting a great deal of interest due to its participation in a variety of important biological and industrial processes. Major deposits of naturally occurring molybdenum containing minerals, i.e., molybdenite (MoS_2) and wulfenite ($PbMoO_4$), are found in the North American Rockies, the Chilean Andes, and the Urals and Altai Mountains of the USSR (1). However, more than 50% of the worlds molybdenum reserves are located in the United States, primarily in Colorado, New Mexico, and Arizona (1).

The chemical properties of molybdenum are quite varied. The element is known to possess many stable and accessible oxidation states (-2 to +6), as well as coordination numbers which can vary from four to eight (2). Molybdenum is also known to form stable complexes with many organic and inorganic ligands, particularly those containing oxygen, nitrogen and/or sulfur donor atoms. Polynuclear complexes containing molybdenum-molybdenum bonds and/or bridging ligands are also known (3).

The chemical uses of molybdenum are constantly expanding. Sodium molybdate (Na_2MoO_4) is presently taking the place of chromates as a corrosion inhibitor in industrial cooling towers and automobile radiators (1,3). In addition, molybdates are increasingly being substituted for lead and chromium in anticorrosive paint pigments and MoS_2 is being extensively employed as a lubricant (3). Industrial

1

processes such as petroleum hydrodesulfurization (4), olefin epoxidation (5), and coal liquefaction (6) are carried out over molybdenum catalysts.

Molybdenum is also known to be an essential micronutrient for a variety of microorganisms, plants, and mammals (2,7,8). At present it is the only second row transition element known to be essential for life (9). Molybdenum is most likely incorporated into living systems as the molybdate anion (MoO_4^{2-}) and it appears that the level of molybdenum in organisms is governed by the availability of the element in soil and/or food and water (2).

Nature has incorporated molybdenum into a variety of redox enzymes which catalyze important biological redox reactions. These enzymes include among others nitrogenase (10,11), nitrate reductase (12,13), xanthine oxidase/dehydrogenase (8,14), aldehyde oxidase (8,15), and sulfite oxidase (8,16,17). A tabulation of enzyme data including sources, molecular weights, prosthetic groups, and respective substrate half-reactions are provided in Table 1. Nitrogenase and nitrate reductase are important reducing enzymes involved in the nitrogen cycle of plants. Xanthine oxidase/dehydrogenase, aldehyde oxidase and sulfite oxidase are primarily mammalian enzymes which may participate in biological processes in man (8). Xanthine oxidase appears to play a role in the disease processes, xanthinuria, gout and uricemia (7,8). It may also be involved in the absorption of iron (18,19). Sulfite oxidase is apparently linked

Table 1. Molybdenum Containing Enzymes (2,7)

Enzyme	Typical Source	Molecular Weight	Mo Content	Prosthetic Groups	Substrate Reaction
Nitrogenase	*Klebsiella*			Fe-S	$N_2 \rightarrow NH_3$
Mo-Fe protein	*pneumoniae*	218,000	2		
Fe protein		66,800	0		
Nitrate Reductase	*Escherichia coli*	200,000	1	heme,$4Fe_4S_4$	$NO_3^- \rightarrow NO_2^-$
Xanthine Oxidase	Cow's Milk	275,000	2	FAD,$4Fe_2S_2$	$RH \rightarrow ROH$
Xanthine dehydrogenase	Turkey Liver	300,000	2	FAD,$4Fe_2S_2$	$RH \rightarrow ROH$
Sulfite Oxidase	Chicken Liver	108,000	2	heme	$SO_3^{2-} \rightarrow SO_4^{-2}$
Aldehyde Oxidase	Rabbit Liver	270,000	2	FAD,$4Fe_2S_2$	$RCHO \rightarrow RCOOH$

with sulfite detoxification and deficiencies are linked to neurological disorders and mental retardation (8).

The literature pertinent to molybdenum containing enzymes has been extensively reviewed (2,20-26). Experimental results obtained from biochemical studies (7,8), electron paramagnetic resonance spectroscopy (EPR), x-ray absorption spectroscopy (XAS), and extended x-ray absorption fine structure (EXAFS) (26), have contributed to a growing body of information directed towards elucidating the structure and redox function of the local molybdenum environment in the molybdenum enzymes. To date, EXAFS in conjunction with EPR studies have provided the most valuable insights in an area where X-ray crystal structures are not available.

Biochemical evidence (27,28) suggests that the molybdenum enzymes possess two fundamentally different types of "active sites". Nitrogenase contains molybdenum in a cofactor which includes Fe and S in stoichiometric ratios intimately associated with the molybdenum (27). This cofactor has been designated as the "iron-molybdenum cofactor" (FeMo-co). On the other hand, the remaining molybdenum enzymes appear to contain a molybdenum site which is structurally and spectroscopically distinct from nitrogenase in that it is free of iron and possess a novel pterin component (20,28,29). The active site in these enzymes has been designated as the "Mo-cofactor" (28).

An important consideration in the study of molybdenum enzymes is the relationship which exists between molecular structure and chemical reactivity. The following section is intended to be an overview of the known structural and reactivity properties of molybdenum in the well character- ized enzymes.

Molybdenum Enzymes

Nitrogenase

Nitrogenase is by far the most important molybdenum containing enyzme. In bacteria and blue-green algae this enzyme catalyzes the reduction of dinitrogen to ammonia which may then be utilized in the synthesis of amino acids, nucleic acids and other nitrogen containing compounds (27). The reduction takes place at atmospheric pressure and ambient temperature and has been termed 'nitrogen fixation' (30). In contrast, industrial reduction of dinitrogen, carried out in the Haber process requires high reaction temperatures and pressures. The ability of microorganisms to reduce dinitrogen under mild conditions has aroused a considerable amount of scientific interest in the nitro- genase enzyme. This interest derives not only from a desire to understand the fundamental biochemical process involved in nitrogen fixation, but also to mimic the nitrogen-fixing ability of living organisms with synthetic catalysts in order to develop new chemical routes to nitrogen based

compounds. The chemical and biochemical aspects of nitrogen fixation have been reviewed (11,24-26,30,31).

Bacteria which fix dinitrogen are either symbiotic or asymbiotic (25,26). Symbiotic bacteria (Rhizobium) fix dinitrogen only when they have infected the roots of certain plants, (i.e., the legumes) and changed to a degenerate form known as a bacterioid. In this role, the symbiotic bacteria provide the plant with a source of nitrogen (NH_3) in ex-change for carbohydrates. Asymbiotic bacteria have been isolated from a variety of sources including termites (32) and shipworms (33). These bacteria include aerobes (Azotobacter vinelandii), facultative aerobes (Klebsiella pneumoniae), and anerobes (Clostridium pasteurianum). There appears to be a great deal of similarity, in terms of composition and reactivity, in the nitrogenase enzyme isolated from these various sources.

The nitrogenase enzyme consists of two distinct and separately isolable proteins, component I and component II (27). Component I is a Fe-Mo protein (molybdoferredoxin) which has a molecular weight of approximately 220,000 daltons and is made up of a tetramer of two pairs of dif-ferent subunits. Each tetramer contains two molybdenum atoms per mole, 32-33 atoms of non-heme iron and 27-32 acid labile sulfide atoms. Component II, a Fe-S protein (azo-ferredoxin), is a dimer of equivalent subunits with a molecular weight of approximately 60,000 daltons possessing a Fe_4S_4 cluster. Each of these proteins are extremely

sensitive to oxygen and upon atmospheric exposure are irreversibly inactivated. The nitrogenase enzyme will only function catalytically when both components along with the reducing agent adenosine triphosphate (ATP) and Mg^{2+} are present (34). ATP in the presence of Mg^{2+} is hydrolyzed to adenosine 5'-diphosphate (ADP) and inorganic phosphate during enzyme turnover (26). The source of electrons in this process may be a ferredoxin or flavodoxin in vivo (2).

Previous studies (35-39) have led to a general consensus concerning the electron transfer sequence in nitrogenase. Initially a reductant (ferredoxin or $S_2O_4^{2-}$) reduces the Fe-S protein, which together with ATP hydrolysis reduces the Mo-Fe protein. The Mo-Fe protein goes on to reduce substrate. Dinitrogen is the physiological substrate but all preparations of nitrogenase when supplied with a reducing agent and ATP also exhibit hydrogenase activity towards substrates with multiple bonds, i.e., acetylenes, isonitriles and cyanide ion (40). In the absence of a suitable substrate, the enzyme will spontaneously produce H_2 and ATP is hydrolyzed to ADP and inorganic phosphate. H_2 evolution is not inhibited by carbon monoxide however, it appears that nitrogen fixation is competitively inhibited by CO. This suggests that the sites of nitrogen fixation and hydrogen evolution in nitrogenase are different. It has been shown (41) that the reduction of acetylene by nitrogenase (Azotobacter vinelandii) is ATP dependent as is nitrogen fixation. In D_2O this reaction is stereospecific

producing entirely cis-$C_2H_2D_2$ (41). The apparent similarity in enzymatic reduction of acetylene and dinitrogen has led to the proposal that the first step in nitrogen fixation may be a two electron reduction yielding a diimide intermediate (42). Further studies are required to substantiate this hypothesis.

A majority of the early research on nitrogenase was directed towards examining the features of the MoFe protein (component I). This response was based on evidence obtained from both chemical and spectroscopic studies which implicated the molybdenum in the FeMo-co as the active site for substrate binding and catalysis (27). A significant contribution towards determining the structure of the MoFe protein came from EPR (36,38,43) and Mossbauer (43) spectroscopic studies. The MoFe protein isolated from Clostridium pasteurianum in a "semi-reduced" state was found to exhibit a low temperature EPR signal with g-values near 4.3, 3.7, and 2.0 which were assigned to an S = 3/2 species. Initially Mo(III) was thought to be responsible for this signal. Additional EPR studies (44) on ^{57}Fe substituted enzyme isolated from Klebsiella pneumoniae revealed a 5-7 gauss broadening of the g = 2.0 resonance. The results of these experiments were consistent with Fe producing the S = 3/2 signal, but there remained the possibility that there may exist an EPR silent molybdenum species at the active site. Recent results obtained using enhanced nuclear double resonance (ENDOR) spectroscopy have indicated that both ^{57}Fe

(45) and ^{95}Mo (46) contribute to the S = 3/2 signal. Although these studies did not provide any direct structural information, it was concluded that the molybdenum in the MoFe protein of nitrogenase was in an even oxidation state.

To date, XAS and EXAFS spectroscopic studies (26) have provided the most valuable insight into the structural composition of nitrogenase. Cramer et al. (47) reported the initial XAS results on the lyophilized MoFe protein isolated from Clostridium pasteurianum. Subsequently, these workers investigated the MoFe protein from Azotobacter vinelandii, and the MoFe-co from Azotobacter vinelandii by XAS (48). The samples were shown to exhibit very similar spectra indicating a similar composition for each of the them. Qualitative conclusions drawn by Cramer et al. (48,49) concerning the MoFe protein and FeMo-co of nitrogenase were as follows: (1) the molybdenum coordination sites in the MoFe native protein and FeMo-co are similar; (2) molybdenum is coordinated primarily by sulfur and is in close proximity to an iron atom which is the only other metallic element contained in nitrogenase; and (3) Mo=O interactions are absent in the semi-reduced state of the enzyme and appear only upon exposure to atmospheric O_2.

Quantitative analysis of the EXAFS spectra, obtained by curve fitting procedures of the Fourier transform data (49) indicate three to four short Mo-S bonds at a distance of ~ 2.35 Å, two to three Mo-Fe bonds at ~ 2.72 Å, and one to two longer Mo-S' bonds at ~ 2.58 Å. The authors were

careful to note that in their experiment a lighter element such as nitrogen or oxygen could be present in the molybdenum coordination sphere and remain undetected in the analysis. The coordination distances and numbers for the nitrogenase MoFe protein are chemically reasonable and have been interpreted by comparison with known model complex structures as representing three or four bridging sulfides, one or two terminal RS^- groups and two or three μ-sulfido bridged iron atoms around the molybdenum (49). These results suggested a novel Mo-Fe-S(R) polynuclear cluster for the active site of nitrogenase.

Based on the original EXAFS data, Cramer et al. (47) initially proposed structure I, consisting of a $MoFe_3S_4$ cube, and structure II, possessing a linear $Fe-(S)_2-Mo-(S)_2-Fe$ cluster as possible models for the FeMo-co.

I   II
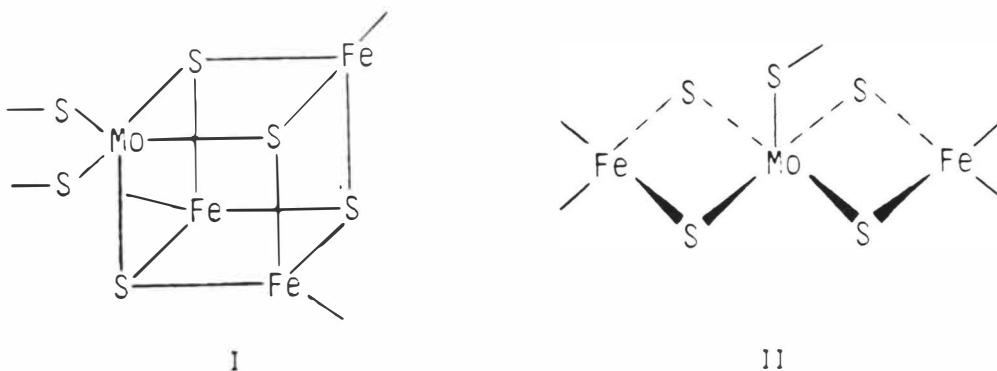
This led Wolff et al. (50) and Christou et al. (51) virtually simultaneously to synthesize and structurally characterize a series of related complexes which would possibly mimic the EXAFS results obtained for nitrogenase and the FeMo-co. These complexes were salts of the anions

$Mo_2Fe_6S_9(SC_2H_5)_8^{3-}$ (50) and $Mo_2Fe_6S_8(SR)_9^{3-}$ (where R = $-C_2H_5$ (50) and $-C_6H_5$ (51)). Each of these complexes possess two cubane $MoFe_3S_4$ cluster cores which are triply bridged to each other by two thiolate and one sulfide, (unsymmetrically bridged), or three thiolate ions, (symmetrically bridged). The crystal structure of $[Mo_2Fe_6S_9(SC_2H_5)_8]$ (50), an example of the former type, is shown in Figure 1 as a representative example for these types of cluster complexes.

Pertinent crystallographic bond distances within the $MoFe_3S_4$ cubes are given in Table 2 along with Mo-S and Mo-Fe bond lengths obtained from EXAFS results on the MoFe protein of nitrogenase (49). Examination of the data in Table 2 indicate that the shorter Mo-S distance and the Mo-Fe distance in the Mo-Fe protein closely approximate the crystallographic values for the model complexes. The EXAFS results for these "nitrogenase models" were important because they demonstrated that the immediate molybdenum environments in nitrogenase, $[Mo_2Fe_6S_8(SC_2H_5)_9]^{3-}$, and $[Mo_2Fe_6S_9(SC_2H_5)_8]^{3-}$, are very similar. This directly identified molybdenum in nitrogenase as being contained in a Mo-Fe-S cluster.

Based on available chemical (35-39) and spectroscopic (26) studies, the current understanding of the MoFe protein of nitrogenase is that it contains four Fe_4S_4 clusters and two FeMo-co clusters per subunit. At present, the major structural problem which has yet to be solved is the arrangement of metals and bridging ligands within the cluster

Figure 1. Structure of the $[Mo_2Fe_6S_9(SC_2H_5)_8]^{3-}$ cluster.
Model for molybdenum site in nitrogenase,
(reference 30).

$$\left[Mo_2Fe_6S_9(SC_2H_5)_8\right]^{3-}$$

S(4) 2.264 S(1) S(3) S(1) S(4)
Fe S(1) 2.340 Fe S(4)
S(4)
S(2) Fe S(1) Mo S(3) Mo S(1) Fe S(2)
Fe S(1) Mo S(3) Fe
2.282 Fe S(1) S(1) Fe
2.260
2.242 S(3) S(4)
S(4)

Mo····Mo 3.306 (3)
Fe····Mo 2.730 (2)
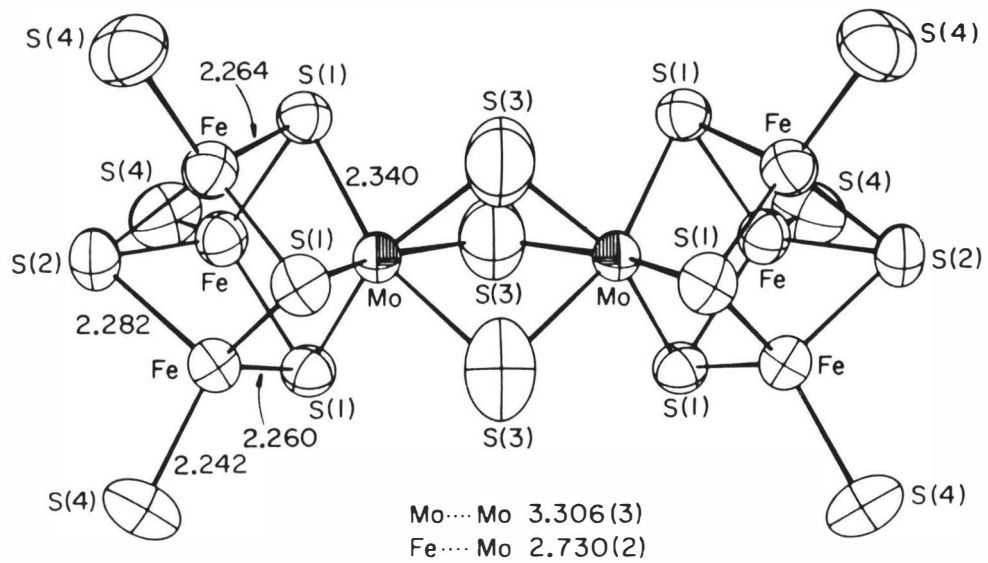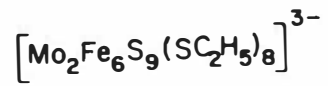
Table 2. Pertinent Crystallographic Distances (Å) in Fe_3MoS_4-Containing

Clusters Compared to EXAFS Results on the Nitrogenase [Fe-Mo] Protein

Bonds	$[N(C_2H_5)_4]_3^-$ $[Mo_2Fe_6S_9(SC_2H_5)_8]^a$	$[N(C_2H_5)_4]_3^-$ $[Mo_2Fe_6S_8(SC_2H_4OH)_9]^b$	Nitrogenase [Fe-Mo] Protein[c]
Mo-Fe	2.73	2.75	2.72
Mo-S $($sulfide bridge$)$ to Fe	2.34	2.39	2.35
Mo-S $($sulfide bridge$)$ to Mo	d	2.55	2.48

(a) reference (50); (b) reference (51); (c) reference (49) for protein from Clostridium pasteurianum; (d) distance could not be resolved.

of the FeMo-co (26). Although cubane structures such as $MoFe_6S_8$ and $MoFe_6S_9$ have been proposed (50,51) to comprise the FeMo-co, the arrangement of three iron atoms of the total six cannot be adequately accounted for (26). Until the unambiguous structure of the FeMo-co is determined, proposals related to substrate interactions and the mechanism of nitrogenase should be viewed as speculative.

NITRATE REDUCTASE

Nitrate reductase enzymes may be classified as two types (8): assimilatory, isolated from plants and fungi, and dissimilatory, found in denitrifing microorganisms. Both types of nitrate reductase enzymes catalytically reduce nitrate to nitrite, with the source of electrons provided by NADH, NADPH, or other reductants (2,8). The physiological role of these enzymes is dependent on the organism in which they are found.

Organisms which contain assimilatory nitrate reductases convert NO_3^- to NH_3 which can be incorporated into the synthesis of proteins, nucleic acids and other cell constituents (8). An example of this type of enzyme is nitrate reductase isolated from Chlorella vulgaris (52). The purified enzyme is a homotetramer with a molecular weight of 360,000 daltons. Each subunit contains bound FAD, heme and molybdenum (52). In contrast, the dissimilatory nitrate reductases use nitrate in the place of dioxygen as the terminal electron acceptor in an anerobic respiratory chain

(26). A representative example of this type of nitrate reductase is that isolated from <u>Escherichia coli</u>. This enzyme is a heterodimer with a molecular weight of 220,000 daltons and contains one molybdenum and four Fe_4S_4 clusters (52).

The nitrate reductase enzymes have not been examined in as much mechanistic detail as nitrogenase, however the electron transfer pathway for the enzyme from <u>Neurospora crassa</u> is suggested (2) to be:

$$NADPH \rightarrow FAD \rightarrow cyt\ b_{557} \rightarrow Mo \rightarrow NO_3^-$$
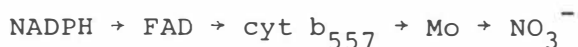
From a bioinorganic view it is significant that the molybdenum site of the enzyme interacts with the NO_3^- substrate. This suggestion has led to EPR studies (7,12), and more recently EXAFS analysis (54), each directed toward an understanding of the nature of the molybdenum coordination site.

Vincent and Bray (12) have reported that the dissimilatory nitrate reductase obtained from <u>Escherichia coli</u> yielded an Mo(V) EPR signal with g_{av} = 1.983 which was dependent on the pH of the sample, (e.g., at pH 7.8, g_{av} = 1.983; at pH 10.8, g_{av} = 10.8). This result led these workers to propose Mo(V) as a participating oxidation state during catalysis. Recently, Solomonson et al. (55) reported the first extensive EPR investigation of the molybdenum center in an assimilatory nitrate reductase from (<u>Chlorella vulgaris</u>). Interestingly, the low temperature (77 K) EPR

spectrum of the native _Chlorella vulgaris_ enzyme lacked any "resting" signals attributable to Mo(V). This implicated Mo(VI) in the oxidized enzyme. This result differed from that observed for the dissimilatory enzyme from _Escherichia coli_.

Although EPR studies provided information as to the oxidation state(s) of the molybdenum in nitrate reductase, they did not produce any detailed structural information concerning the active site environment. Recently, Cramer et al. (54) reported the first x-ray absorption study for _Chlorella vulgaris_ and _Escherichia coli_ nitrate reductase enzymes. Curve fitting analysis of the Fourier transform EXAFS data (54) indicated that the _Chlorella vulgaris_ enzyme molybdenum site in both oxidized (Mo(VI)) and reduced (Mo(IV)) forms was virtually identical to that of hepatic sulfite oxidase (vide infra), whereas the _Escherichia coli_ enzyme appeared to possess a novel site lacking oxo ligation. Proposed structures are shown below:
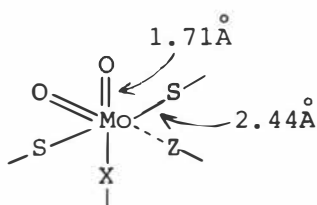
Oxidized   Reduced

Chlorella

$$2.36\text{Å} \xrightarrow{\ \ \ } \overset{\displaystyle \text{O,N} \ \overset{2.10\text{Å}}{\nearrow}}{\underset{\text{S} \diagdown \quad \text{X}}{\overset{\text{S} \diagup}{\text{Mo}}}} \cdots\cdots \overset{\text{O,N} \ _{2.79\text{Å}}}{\text{Fe,P,Mo[?]}}$$
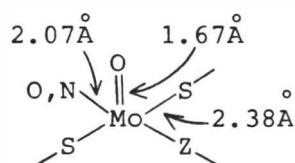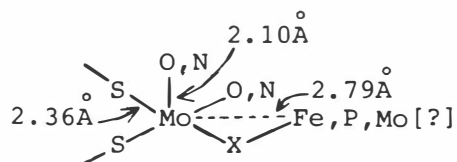
Reduced

E. coli

These structures appear to be credible representations of the active site of nitrate reductase enzymes. However, at present, it is unclear whether the ligand Z represents a sulfur donor or chloride atom ligated to the molybdenum in the Chlorella vulgaris enzyme. It may be that it is simply a ligand in close enough proximity to the molybdenum to bind during or after reduction. On reduction there is a significant change in the Mo=O bond length in the Chlorella vulgaris enzyme, this may indicate a redistribution of sulfur ligands, or alternatively, evidence for chloride binding. For the reduced Escherichia coli structure there appears to be a significant 2.8 Å interaction with a bridged iron neighbor, a bridged molybdenum, or even a phosphorous atom (54).

Xanthine Oxidase/Dehydrogenase

Xanthine oxidase and xanthine dehydrogenase are closely related to each other, and in some instances, are interconvertible forms of the same enzyme (56,57). The

enzymes catalyze the oxidation of xanthine (III) to uric acid (IV):

III   IV

$$(1)$$
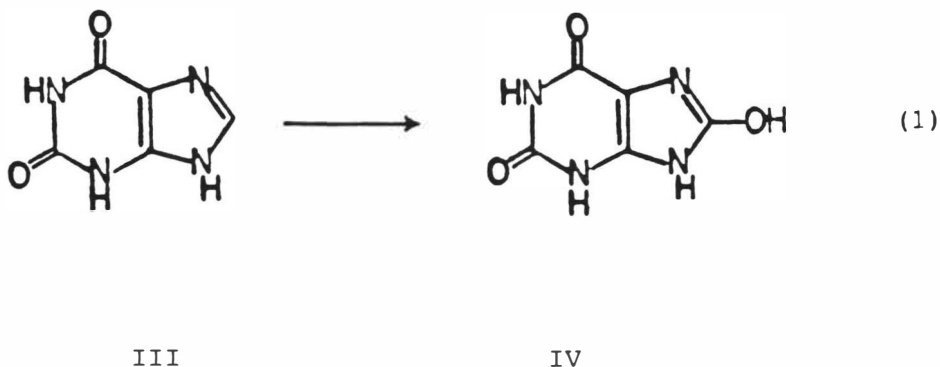
Xanthine oxidase and xanthine dehydrogenase have been isolated from a variety of microorganisms and mammals (7,8). Evidence suggests that xanthine oxidase in mammals may play a role in xanthinurea, gout and uricemia (7,8) although its exact role in these disease states has not been firmly established. Additionally, it appears that for certain bacteria and fungi, xanthine may serve as a primary nitrogen source (23). In these species xanthine oxidase/dehydrogenase would participate in nitrogen assimilation as does nitrogenase and nitrate reductase.

Xanthine oxidase/dehydrogenase enzymes are the best characterized of the molybdenum containing enzymes with respect to composition and mechanism (7,8). Xanthine oxidase isolated from cow's milk as well as other mammalian sources (liver) has a molecular weight of approximately

300,000 daltons and exists as a dimer of equivalent polypeptide subunits, each containing molybdenum, FAD, and two different types of Fe_2S_2 clusters (58,59). Currently there exists a considerable amount of agreement concerning the mechanism of substrate conversion for xanthine oxidase based on EPR (60-63) and EXAFS (64-66) spectroscopic studies. These studies suggest that xanthine oxidase, like many of the other molybdenum oxidases, utilizes molybdenum in the VI, V, and IV oxidation states during catalysis. It is believed that the resting enzyme (Mo(VI)) is initially reduced by substrate in a two-electron process to yield the EPR-silent Mo(IV). A rapid equilibration of electrons between Mo(IV), Fe_2S_2 and FAD centers, governed by the reduction potentials of the various couples, produces the Mo(V) EPR-active species (23).

EPR studies (60-63) have provided insight into the nature and function of the molybdenum coordination environment. Bray (7,8) has observed four major types of EPR signals for the reduced forms of xanthine oxidase: 'very rapid', a reduced form with bound substrate; 'rapid', reduced form without bound substrate; 'slow', arising from cyanolized, desulfo enzyme; and 'inhibited', arising from complexes of the Mo(V) center with certain inhibitors (Table 3). A number of superhyperfine interactions have been observed, most of which have been summarized by Bray (7). The best understood superhyperfine splittings are those originating from proton interactions. An important

Table 3. Molybdenum(V) EPR Data for

Reduced Forms of Xanthine Oxidase(7,8)

Signal	Origin	Reduction Treatment Required	g_{av}
Very Rapid	Native enzyme	Reduction with xanthine at high pH	1.977
Rapid	Native enzyme	Reduction with dithionite	1.973- 1.974
Inhibited	CH_3OH treatment of native enzyme	None	1.973
Slow	Desulfo enzyme	Reduction for 20 min with dithionite	1.965

finding related to these interactions showed that the proton causing the "rapid signal" originates from the C-8 position of xanthine (see structure III) which is believed to be bound to the enzyme during catalysis (7).

EPR spectroscopy has also aided in the determination of the substrate binding site in xanthine oxidase. When reduced xanthine oxidase was treated with NO_3^- the Mo(V) signal was perturbed (67). The experiment was unable to detect whether the anionic binding site was on molybdenum or another site in close proximity to molybdenum. Other experiments pertaining to substrate binding have been performed with the xanthine oxidase inhibitor, allopurinol. The inhibition results from formation of a complex between the reduced enzyme (Mo(IV)) and the product of oxidation of allopurinol, alloxanthine. When this inhibited complex was exposed to the atmosphere a new, broader Mo(V) EPR signal appeared which was attributed to a Mo(V) complex with alloxanthine (68). The spectrum did not exhibit evidence of proton coupling, however treatment with a computer line sharpening technique provided evidence for isotropic coupling (0.36 G) which was attributed to ^{14}N. This was the first reported observation of ^{14}N coupling in a molybdenum enzyme and it suggested that the alloxanthine was bound to molybdenum through N-8 (68). This result was similar to that obtained for the very rapid signal observed for xanthine which is believed to be bound to molybdenum at C-8 via a Mo-O bond (68).

Xanthine Enzyme

Complex

Alloxanthine Enzyme

Complex

Both xanthine oxidase and xanthine dehydrogenase possess a labile sulfide which is necessary for catalytic activity (7,8,69). This is a significant result. Conversion of active or "intact" xanthine oxidase to inactive or "desulfo" forms with cyanide has been shown to involve abstraction of sulfur as thiocyanate:

$$\text{Xanthine oxidase}^{ox} + CN^- \rightarrow \text{Xanthine oxidase}^{red} + SCN^- \qquad (2)$$

$$\qquad\quad \text{(Intact)} \qquad\qquad\qquad\quad \text{(Desulfo)}$$

The "desulfo" form can be restored to the "intact" species by addition of Na_2S to the reduced enzyme. This behavior was used to label xanthine oxidase with ^{33}S (63). The ^{33}S

nucleus was found to couple with the various Mo(V) EPR signals which provided evidence for sulfur coordinated to molybdenum.

A considerable amount of data concerning the molybdenum sites of xanthine oxidase/dehydrogenase has recently been obtained from EXAFS spectroscopy. Initial EXAFS studies on bovine milk xanthine oxidase yielded inconsistent results. Tullius et al. (65) reported 1.5 terminal oxygens at 1.71 Å and 2.1 sulfurs at 2.54 Å coordinated to molybdenum. While Bordas et al. (66) reported a single terminal oxygen at 1.75 Å, two sulfurs at 2.46 Å, and an additional Mo-S interaction at 2.25 Å. Both groups also found a "long" Mo-S interaction at approximately 2.85 Å. Subsequently, Cramer et al. (64) reported an EXAFS study of chicken liver xanthine dehydrogenase. The results of this study indicated terminal oxo and terminal sulfido groups coordinated to molybdenum in the oxidized Mo(VI) state. On reduction, presumably to Mo(IV), the short (2.15 Å) Mo=S bond disappears and an additional thiolate sulfur at 2.38 Å is found. For desulfo (cyanolized) xanthine dehydrogenase, the sulfide (Mo=S) in the oxidized state is replaced with a terminal oxo group (Mo=O), which is consistent with previous results obtained by CN^- treatment of the enzyme (7,8,69). These results on xanthine dehydrogenase are in agreement with the results obtained by Bordas et al. (66) for xanthine oxidase which indicate that both enzymes possess essentially identical molybdenum centers. These results do not

unambiguously exclude the possible presence of other donors (e.g. N,Cl,or P) in either the oxidized Mo(VI) or reduced Mo(IV) states. An oxygen with a Mo-O bond length similar to a Mo-OH (2.04 Å) in the reduced state of the enzyme (64) is in agreement with the data, and in view of EPR evidence for proton coupling, seems highly probable. Proposed structures incorporating conclusions from EXAFS as well as EPR experiments are summarized below (64):

	Oxidized Mo(VI)	Reduced Mo(IV)
xanthine dehydrogenase (native)	O≽Mo(SR)$_2$, Mo=S	O≽Mo(SR)$_2$, Mo-SH
xanthine dehydrogenase (desulfo)	O≽Mo(SR)$_2$, Mo=O	O≽Mo(SR)$_{2\ or\ 3}$, Mo-OH
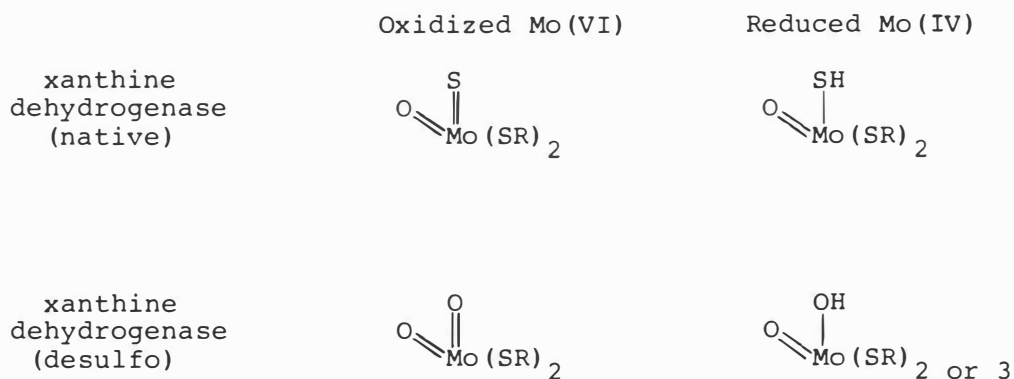
For both native and desulfo forms of xanthine dehydrogenase, it is assumed that the oxo or sulfido group of the oxidized enzyme is converted to an OH or SH group on reduction.

Sulfite Oxidase

Sulfite oxidase has been isolated from a variety of mammalian and avian sources (7,8). The enzyme catalyzes the oxidation of sulfite to sulfate using water as the source of

oxygen and cytochrome c as the physiological electron acceptor (70,71). This process may play a crucial role in mammals as SO_3^{2-} (or SO_2, its gaseous precursor) is toxic while SO_4^{2-} is relatively harmless. Sulfite oxidase exists as a dimer of equivalent 55,000 to 60,000 dalton polypeptide subunits. Each of these subunits possess a molybdenum and cytochrome b-type heme in covalently attached, distinct domains.

EPR studies on sulfite oxidase indicate that the signals are affected by pH (74) and anions (75). Three types of signals are observed (Table 4). The 'low pH' signal exhibits an isotropic ^1H splitting of ~ 10 G with g_{av} = 1.980. When this sample is diluted with $H_2^{17}O$, an ^{17}O splitting of ~ 13 G appears. When the pH is increased, ^1H splitting vanishes and ^{17}O splitting is lowered to ~ 6 G; g_{av} is lowered to 1.968.

When partially reduced sulfite oxidase is treated with ^{17}O labelled PO_4^{3-}, a Mo(V) signal coupled to the ^{17}O is observed; the coupling persisted even after equilibration of the enzyme with H_2O (75). This behavior was attributed to a Mo(V)PO_4^{3-} complex bound by an ^{17}O of the phosphate group. Similar results were obtained when reduced sulfite oxidase was treated with SO_3^{2-}. In this case SO_3^{2-} was proposed to be bound to Mo(V) by a sulfite oxygen (75). Neither of these coupled species exhibited proton coupling.

Table 4. Molybdenum(V) EPR Data for Sulfite
Oxidase (72-74)

| Form | g-values | | | | A_{av} (G) | |
	g_x	g_y	g_z	g_{av}	^1H	^{17}O
'low pH' pH=7.5	2.004	1.972	1.966	1.980	9.8	13
'high pH' pH=9.6	1.987	1.964	1.953	1.968		6
'phosphate bound'	1.992	1.969	1.961	1.974		9

$$\text{Mo}\overset{\text{O}}{\underset{}{\parallel}}\text{—}^{17}\text{O-PO}_3$$

$$\text{Mo}\overset{\text{O}}{\underset{}{\parallel}}\text{—O-SO}_3$$
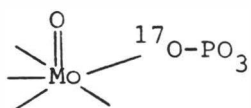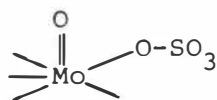
$P^{17}O_4{}^{3-}$ complex $\qquad\qquad$ $SO_3{}^{2-}$ complex

X-ray absorption results for sulfite oxidase (64,75) indicate that there exists a large difference in the absorption edge data for the oxidized and reduced forms. Curve fitting analysis applied to the EXAFS data indicates that there are two oxo groups at ~ 1.68 Å in the oxidized form of the enzyme and a single terminal oxo group at ~ 1.69 Å in the dithionite reduced species. EXAFS data also indicated a set of two or three thiolate sulfurs at 2.42 Å in the oxidized enzyme which change to 2.38 Å in the reduced form with an amplitude best fit by inclusion of three thiolate sulfurs. These results in addition to EPR data suggest the following formulation for the active site of sulfite oxidase:

$$O\overset{\text{O}}{\underset{}{=}}\text{Mo}(SR)_{2 \text{ or } 3}$$

$$O\overset{\text{OH}}{\underset{}{=}}\text{Mo}(SR)_3$$

oxidized $\qquad\qquad\qquad$ reduced
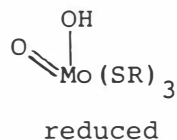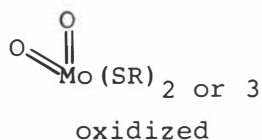
The previous discussion on the structural and physical properties of the molybdenum enzymes has shown that they are dependent upon a molybdenum containing cofactor for enzyme

activity. However, existing biochemical, EXAFS and EPR results have yet to definitively establish the exact donor atom set or geometry of the molybdenum active site. The search for chemical analogues of the molybdenum cofactor in these enzymes has led to significant developments in the syntheses and characterization of model molybdenum complexes (2,21-23). Results from these studies have proven to be useful in interpreting enzyme data and they direct the way towards the design and synthesis of more suitable models.

II. Experimental

A. Materials

A majority of the ligand components (5-X-salicyl-aldehyde (X = NO_2, Cl, Br, H, CH_3O), o-aminobenzenethiol, and 2-aminoethanethiol hydrochloride) were obtained from Aldrich and used without further purification. Thallium(I) acetate, $Tl(CH_3COO)$, was obtained from Fluka and used as received. Ethyldiphenylphosphine ($PEtPh_2$) was obtained from Strem Chemicals and used without further purification. Sodium nitrate ($NaNO_3$) was obtained from Mallinckrodt and used as received. Copper(I) thiocyanate, CuSCN, was obtained from Alfa. Potassium thiocyanate, KSCN, was obtained from J.T. Baker. $Na_2Mo(VI)O_4 \cdot 2H_2O$ and $Mo(VI)O_2Cl_2$ were obtained from Alfa. $Mo(VI)O_2Cl_2$ was stored in a dry box (Vacuum Atmospheres Corp.) to prevent hydrolysis. $Mo(VI)O_2(acac)_2$ ($acac^-$ = acetylacetonate monoanion) was prepared according to the method of Jones (76) and characterized by its IR spectrum. Dimethylsulfoxide (Me_2SO), N,N'-dimethylformamide (DMF) and acetonitrile (CH_3CN) were reagent grade and dried over type 3Å molecular sieves. For substrate reactions high purity DMF (Burdick and Jackson) was purified by an extensive procedure that was initiated by storing the solvent over anhydrous Na_2CO_3 for 2-3 days. The decanted DMF was then distilled under a N_2 atmosphere at reduced pressure. The fraction boiling in the range 38-41°C (~ 20 Torr) was collected and to this fraction

clean sodium metal and anthracene were added. The disodium anthracene-DMF solution was placed in a dry box overnight. The following day DMF was redistilled from this solution under reduced pressure. The middle fraction was isolated and stored over 3Å molecular sieves under dinitrogen in a dry box.

B. Physical Measurements

Cyclic voltammetry measurements were made with a Bioanalytical Systems' (BAS) Model CV-1B potentiostat utilizing a three-electrode cell. The working electrode was a BAS glassy carbon electrode and the auxiliary electrode was a Pt wire. A saturated calomel reference electrode was employed. All potentials are referenced to the ferrocenium/ferrocene couple (0.400 V vs. NHE) (77). The ferrocene concentration was ~ 3×10^{-4} M. All cyclic voltammetry measurements were performed in dry and deaerated DMF with tetrabutylammonium perchlorate (TBAP, ~ 5×10^{-2} M) as the supporting electrolyte and with a molybdenum complex concentration ~ 10^{-3} M. Infrared spectra ($4,000 - 200$ cm^{-1}) were obtained as Nujol mulls with NaCl plates or as KBr disks by using a Perkin Elmer model 283 spectrophotometer. A Beckman Acta M VII spectrophotometer was used to obtain UV-visible data.

C.   Synthesis of Ligands

N-(5-X-salicylidene)-2-aminobenzenethiol, (X = H, Cl, Br, CH₃O); (5-X-SSP-H₂).

These ligands were prepared by reacting equal molar quantities of the appropriate aldehyde and o-aminobenzene thiol in absolute ethanol at 0°C under a dinitrogen atmosphere. The Schiff base condensation reaction took place instantaneously and after stirring for approximately two hours, the ligands were isolated by vacuum filtration. The precipitate was washed with absolute ethanol (2 x 100 ml) and the ligands were allowed to dry in air. Each of these ligands were obtained as pale yellow solids.

N-(5-X-salicylidene)-2-aminoethanethiol, (X = H, Cl, Br, CH₃O); (5-X-SSE-H₂).

These ligands were prepared by an analogous procedure to that described above. The appropriate aldehyde was reacted with the hydrochloride salt of 2-aminoethanethiol which had been converted to the free amine by reaction with one equivalent of triethylamine. Each of the ligands were obtained as pale yellow solids except 5-H-SSE-H$_2$, which was obtained as a yellow oil.

N-(2-thiosalicylidene)-2-aminobenzenethiol; (5-H-SPS-H₂)

(1)   2-Thiocyanatobenzaldehyde (79).

A chilled solution (0°C) of sulfuric acid (13.5 ml in

200 ml H_2O) was added dropwise to a rapidly stirred suspension of 2-aminobenzaldehyde (10.0 g, 0.08 mol) (78) in cold sodium nitrite solution (10.0 g in 500 ml H_2O). The filtrate was added dropwise to a chilled, stirred solution of copper(I) thiocyanate (10.0 g, 0.08 mol) and potassium thiocyanate (100 g) in H_2O (60 ml). The black-green mixture was stirred at room temperature for one hour and then the temperature was raised to 60°C and the reaction stirred for an additional 30 minutes. During this time a golden-yellow solid formed. The mixture was allowed to cool to room temperature and the precipitate was collected by vacuum filtration. The thoroughly dried precipitate was extracted four to five times with boiling petroleum ether (200 ml) to obtain the product as white needles.

(2) 2-Thiosalicylaldehyde (79).

2-thiocyanatobenzaldehyde (2 g, 12 mmol) was added to a freshly prepared solution of sodium hydroxide (10 g in 80 ml H_2O) with rapid stirring. After approximately 10 minutes the mixture was filtered to remove a yellow solid which was discarded. The filtrate was cooled by addition of ice. This solution was acidified with concentrated sulfuric acid (30 ml) and extracted with absolute diethyl ether. The ether layer was isolated and dried over sodium sulfate. The ether solution was reduced to approximately five ml by rotary evaporation, and then chromatographed on Florisil (100-200 mesh) using diethyl ether as the eluant. The

purified 2-thiosalicylaldehyde, approximately 1 g, was stored as an ether solution at 0°C. This compound is unstable with respect to oxidation and was protected as the thallium salt (vide infra).

(3) (Thiosalicylaldehydato)thallium(I) (80).

An ether solution of purified 2-thiosalicylaldehyde (1 g, 7.2 mmol) was reduced to approximately two ml by rotary evaporation. Absolute ethanol (50 ml) was added to this solution. A warm solution of thallium(I) acetate (1.90 g, 7.2 mmol) in absolute ethanol (50 ml) was prepared. 2-thiosalicylaldehyde was added to this solution. There was an immediate formation of an orange-red precipitate. The solution was stirred for 30 min after which time the precipitate was removed by vacuum filtration, washed with ethanol, and allowed to air dry.

(4) [N-(2-thiosalicylidene)-2-aminobenzenethiolato]thallium(I).

(Thiosalicylaldehydato)thallium(I) (0.50 g, 1.5 mmol) was dissolved in boiling 2-methoxyethanol (50 ml) followed by rapid filtration. 2-aminobenzenethiol (0.19 g, 1.5 mmol) dissolved in 2-methoxyethanol (20 ml) was immediately added to the filtrate and the hot solution was stirred rapidly and allowed to cool to room temperature. The orange precipitate which formed was filtered, washed with ethanol, and dried in air.

D. Synthesis of cis-Dioxomolybdenum(VI) Complexes

Cis-dioxo-[N-(5-X-salicylidene)-2-aminobenzenethiolato]mo-
lybdenum(VI); (X = H, Cl, Br, CH$_3$O); (Mo(VI)O$_2$(5-X-SSP).

A sample of the appropriate ligand (1 mmol) was dissolved in 100 ml of absolute ethanol. MoO$_2$(acac)$_2$ (1 mmol) was added as a solid to the ligand solution. The reaction mixture was refluxed for eight hours during which time the product precipitated as a brown solid. The cis-dioxomolybdenum(VI) complex was filtered, washed with ethanol (2 x 100 ml), and allowed to dry in air. The complexes were recrystallized by dissolving in Me$_2$SO followed by addition of H$_2$O until the solution just becomes cloudy, at which time they were left undisturbed. After 1-2 days crystals were obtained.

Cis-dioxo-[N-(5-X-salicylidene)-2-aminoethanethiolato]molyb-
denum(VI), (X = H, Cl, Br, CH$_3$O); Mo(VI)O$_2$(5-X-SSE).

A sample of the appropriate ligand (1 mmol) was dissolved in 100 ml of absolute ethanol. Triethylamine (2 mmol) was added to this solution. Mo(VI)O$_2$Cl$_2$ (1 mmol) was dissolved in a minimum amount of absolute ethanol. The two solutions were mixed and stirred at room temperature for approximately two hours. The cis-dioxomolybdenum(VI) complex precipitated as a red-orange solid and was recrystallized as described above.

Cis-dioxo-[N-(5-X-salicylidene)-2-aminophenolato]-molybdenum(VI), (X = NO_2 Br, H, CH_3O); $Mo(VI)O_2$(5-X-SAP) and cis-dioxo-[N-(5-X-salicylidene)-2-aminoethanolato]molybdenum(VI), (X = NO_2, Cl, Br, H, CH_3O); $Mo(VI)O_2$(5-X-SAE) were prepared as described by Topich (81).

The cis-dioxomolybdenum(VI) complexes were characterized by IR and UV-visible spectroscopies. Elemental analyses were performed by Atlantic Microlab, Atlanta, GA.

The attempted synthesis of a cis-dioxomolybdenum(VI) complex with [N-(2-thiosalicylidene)-2-aminobenzenethiolato]thallium(I) and $MoO_2(acac)_2$ or MoO_2Cl_2 was unsuccessful.

E. Synthesis of oxomolybdenum(IV) Complexes

All oxomolybdenum(IV) complexes are extremely sensitive to air and moisture and therefore all manipulations of these complexes were performed under a dinitrogen atmosphere.

Oxo-[N-(5-H-salicylidene)-2-aminobenzenethiolato]molybdenum(IV); Mo(IV)O(5-H-SSP).

This procedure was adapted from Boyd and Spence (82). $Mo(VI)O_2$(5-H-SSP) (0.36 g, 1.01 mmol) in DMF (5 ml) was added to a solution of $PEtPh_2$ (0.5 ml, 2.3 mmol) in CH_3CN (25 ml). The solution immediately turned dark brown. The solution was stirred at 25°C for 24 hours during which time a dark brown precipitate formed. The complex was filtered

and washed with CH_3CN (2 x 25 ml) and allowed to dry under N_2.

Oxo-[N-(5-H-salicylidene)-2-aminoethanethiolato]molybden-um(IV); Mo(IV)O(5-H-SSE).

This complex was prepared using a procedure analogous to that described above for Mo(IV)O(5-H-SSP).

F. Kinetic Measurements and Activation Parameters for Oxygen Atom Transfer to PEtPh$_2$

All manipulations associated with the kinetic measurements were performed under a dinitrogen atmosphere. Cis-dioxomolybdenum(VI) complex solutions of approximately 10^{-3} M in DMF were employed. Pseudo-first order conditions were used throughout the study of these reactions by maintaining the concentration of PEtPh$_2$ between 25-fold and 100-fold molar excess over the molybdenum concentration. The solutions were maintained at a constant temperature with a thermostated bath. Spectra were recorded for several hours at convenient time intervals, between 650 and 300 nm, using a Beckman Acta M VII spectrophotometer. The pseudo first order rate constants, k_{obs} ($k_{obs} = k_1$ [PEtPh$_2$]), were determined for each reaction from plots of $\ln(A_\infty - A_t)$ versus time. A_t is the optical density at time t. A_∞ was determined as the optical density when the final two spectral traces overlapped. Kinetic experiments were performed at least three times for each molybdenum complex studied, with

the plots in each case being linear over at least three half lives. A plot of ln k_1 versus 1/T yielded the activation energy, E_a, and the frequency factor, A, while a plot of ln(k_1/T) versus 1/T gave the activation ethalpy, $\Delta H^{\ddagger}$. $\Delta S^{\ddagger}$ was obtained from the relationship, ln A = ln RT/Nh + $\Delta S^{\ddagger}$/R + 1, where R = 8.314 J/mol-K and R/Nh = 2.084 x 10^{10} $K^{-1}sec^{-1}$ (83).

III. OXOMOLYBDENUM(VI) CHEMISTRY

Introduction

All known cis-dioxomolybdenum(VI) complexes are six coordinate and possess exclusively the cis-MoO_2^{2+} cation (2). Many of these complexes usually have octahedral geometries with minor distortions which are attributable to polydentate ligand constraints or ligand-ligand repulsions (3). Generally, Mo=O bond distances are between 1.68 and 1.72 Å and O-Mo-O bond angles range from 102 to 108°, see Table 5. The increase in this angle from the expected 90° octahedral value is due to repulsions between the two close Mo=O bonds (i.e., between electrons in their filled bonding orbitals).

The terminal oxo groups of the MoO_2^{2+} core exert a strong _trans_ bond-lengthening effect. In complexes which contain four equivalent donor atoms, those trans to Mo=O are always further from the molybdenum. For example in Mo(VI)-$O_2(SC_6H_5SCH_2CH_2SC_6H_5S)$ the Mo-S bonds _trans_ to Mo=O average 2.69 Å whereas those _cis_ to oxo (and mutually _trans_) average 2.40 Å (84). The _trans_ bond lengthening effect is also observed in the Mo-S distance of 2.78 Å in Mo(VI)$O_2[CH_3SCH_2$-$CH_2N(CH_2CH_2S)_2]$ which contains a weakly donating thioether sulfur in the trans position (75,85). Similar Mo-S bond distances have been found in xanthine oxidase (64) and sulfite oxidase (64,75). In these enzymes such a linkage may possibly arise from a methionine sulfur _trans_ to Mo=O.

Table 5. Representative Structural Studies on Mononuclear
cis-Dioxomolybdenum (VI) Complexes

Compound	Average Mo≡O Distance (Å)	O-Mo-O Angle (°)	Reference
$Mo(VI)O_2(L-cys-OMe)_2$	1.71	108.1	113
$Mo(VI)O_2(S_2CN(C_2H_5)_2)_2$	1.70	105.6	107
$Mo(VI)O_2[(SCH_2CH_2)_2NCH_2CH_2SCH_3]$	1.70	108.6	75
$Mo(VI)O_2[(CH_3)NHCH_2C(CH_3)_2S]_2$	1.72	122.1	114
$Mo(VI)O_2(LNS_2)$	1.69	110.5	126

Spectroscopically characterized cis-dioxomolybden-um(VI) complexes usually exhibit two Mo=O stretching vibrations in the infrared between 1000-850 cm^{-1}. These bands are usually separated by 20-40 cm^{-1} with the lower energy stretch occurring in the 870-910 cm^{-1} range. Since the Mo(VI) oxidation state is formally represented as having a 4d° electronic configuration, the study of EPR, magnetic susceptability or d-d transitions in the electronic spectrum is not possible.

When dissolved in nonaqueous solvents, e.g., DMF or Me_2SO, many cis-dioxomolybdenum(VI) complexes are yellow or orange due to the presence of an electronic absorption band (or bands) near 350 nm. For example, $Mo(VI)O_2(SCH_2CH_2NH_2)_2$ exhibits bands at 350 nm (ε = 6130 $M^{-1}cm^{-1}$), 276 nm (ε = 6180 $M^{-1}cm^{-1}$) and 250 nm (ε = 7250 $M^{-1}cm^{-1}$). The long-wavelength band may be assigned to a S → Mo charge transfer transition although there is insufficient data at this time to make a firm assignment (24). The absorption band at 250-270 nm occurs in all cis-dioxomolybdenum(VI) complexes and has been assigned as an oxo → Mo charge transfer transition (2).

EXAFS results on xanthine oxidase (64) sulfite oxidase (64,75) and nitrate reductase (54) indicate that these enzymes possess similar molybdenum coordination environments. The cis-dioxomolybdenum(VI) complex whose EXAFS spectrum most closely resembles that of sulfite oxidase is $Mo(VI)O_2[CH_3SCH_2CH_2N(CH_2CH_2S)_2]$ reported by Berg

Figure 2. Structure of Mo(VI)O$_2$[CH$_3$SCH$_2$CH$_2$N(CH$_2$CH$_2$S)$_2$],
(reference 24).
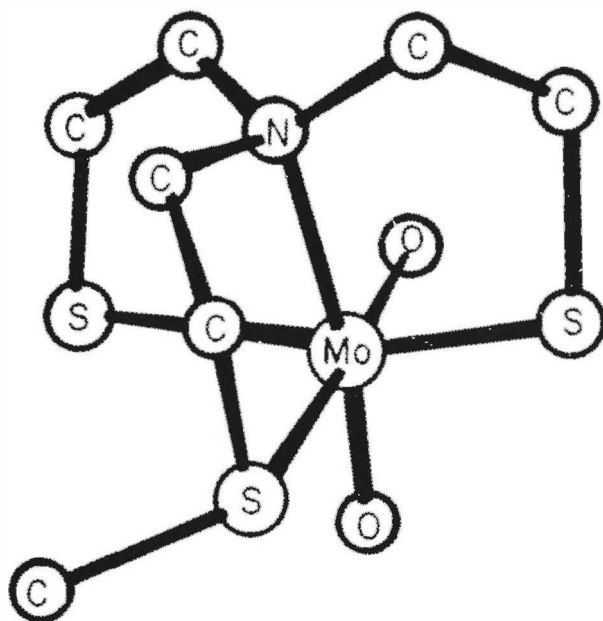
and co-workers (75). X-ray crystallographic studies (75) indicate that this complex has a distorted octahedral geometry with the Mo-N and Mo-S (thioether) of the tripodal ligand trans to oxo groups, Figure 2. The Mo=O and Mo-S (thiolate) bond lengths, 1.695 Å and 2.406 Å, respectively, are very close to those found by EXAFS for sulfite oxidase (i.e., 1.693 Å and 2.401 Å, respectively).

Additional cis-dioxomolybdenum(VI) complexes with ligands containing O, N and/or S donor atoms have also been considered as model compounds. By far the most thoroughly investigated cis-dioxomolybdenum(VI) complexes are the dialkyldithiocarbamates, $Mo(VI)O_2(S_2CNR_2)_2$. Their synthesis (87-92), reactions (92-104), and electrochemistry (105,106) are well documented. Berg and Hodgson (107) have described the crystal structure of $Mo(VI)O_2(S_2CN(C_2H_5)_2)_2$ as a distorted octahedron with Mo=O distances of 1.703 Å and an O=Mo=O angle of 105.61°. These values are consistent with crystallographic results on similar cis-dioxomolybdenum(VI) complexes, see Table 5.

Other series of cis-dioxomolybdenum(VI) complexes which are pertinent from a biomimic standpoint are those prepared from cysteamine ($R_2NCH_2CH_2SH$) and cysteine ester ($RCO_2(NH)CH_2CH_2SH$) ligands. These ligands are bidentate with N and S donor atoms. Like the dialkyldithiocarbamate ligands, these species form cis-dioxomolybdenum(VI) complexes of the $Mo(VI)O_2L_2$ type. Their synthesis, spectroscopic (86,108-112), and structural (111,113,114)

properties have been reported. A few of the cysteamine complexes have been shown to exhibit an unusual structural arrangement. As an example, the structure of $Mo(VI)O_2[(CH_3)NHCH_2C(CH_3)_2S]$ (109,114) is shown in Figure 3 where it can be seen that (1) the structure is not octahedral as is usually observed for cis-dioxomolybdenum(VI) complexes but can be described as an unusual skew-trapezoidal bipyramid, (2) the S atoms are arranged cis to each other at a short distance of 2.76 Å but are nonetheless each 2.42 Å from the molybdenum atom, (3) the Mo=O bond distance is 1.73 Å which is slightly longer than that usually found in most MoO_2^{2+} complexes and the O-Mo-O angle has opened to 122° (4) there are no ligands trans to Mo=O. Apparently, the placement of strongly σ- and π-donating sulfur ligands trans to an oxo is energetically unfavorable requiring the complex to distort to the unusual structure. Preliminary results (111) suggest that the skew trapezoidal bipyramidal structure may have profound effects on the spectroscopic and redox behavior of the complex which may be relevant to the enzymes.

Cis-dioxomolybdenum(VI) complexes possessing tri-(81,115-126) and tetradentate (112,114,118,123,124,127-131) Schiff base ligands have also received a considerable amount of study. Tridentate ligands are of special interest in view of the fact that their complexes have the $Mo(VI)O_2L$ form, possessing a vacant coordination site which is potentially available for substrate binding. Thus, these

Figure 3. Structure of $Mo(VI)O_2[(CH_3)NHCH_2C(CH_3)_2S]_2$, (reference 24).
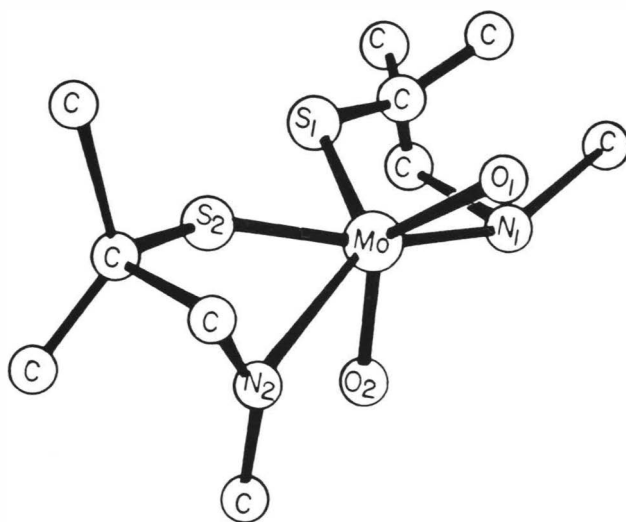
complexes are attractive candidates as active site models for the molybdenum oxidase enzymes.

Rajan and Chakravorty (117) have reported on the synthesis of cis-dioxomolybdenum(VI) complexes with the following tridentate ligands

$X = O$: 5-H-SAP^{2-}
$X = S$: 5-H-SSP^{2-}

$X = O$: 5-X-SAE^{2-}
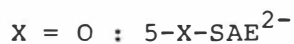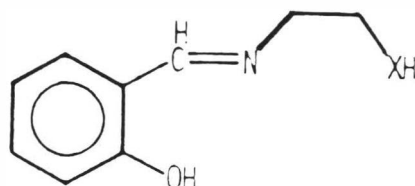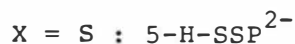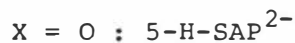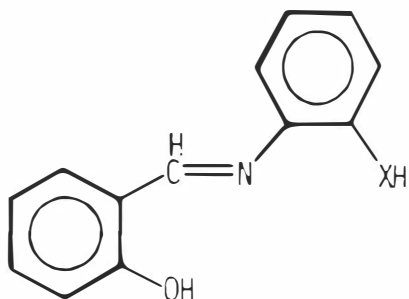
Initially, there was disagreement as to the actual nature and stoichiometry of the molybdenum complexes. Rajan and Chakravorty (117) claimed that the 5-H-SSP^{2-} ligand coordinated to MoO_2^{2+} as a dianionic tridentate ligand producing the $Mo(VI)O_2(5\text{-H-SSP})$ complex, whereas Hill et al. (118) reported that this ligand coordinated as a monoanionic bidentate species yielding $Mo(VI)O_2(5\text{-H-SSP-H})_2$. Recent results obtained by Topich and Lyon (116) on several series of cis-dioxomolybdenum(VI) complexes containing these and similar ligands support the results obtained by Rajan and Chakravorty.

Recently, Rajan et al. (124) reported on the synthesis, spectroscopic, and electrochemical properties of cis-dioxomolybdenum(VI) complexes prepared from the reduced forms of 5-H-SAP^{2-} and 5-H-SSP^{2-} (L'-H$_3$) shown below:

$$X = O, S$$

L'-H$_3$
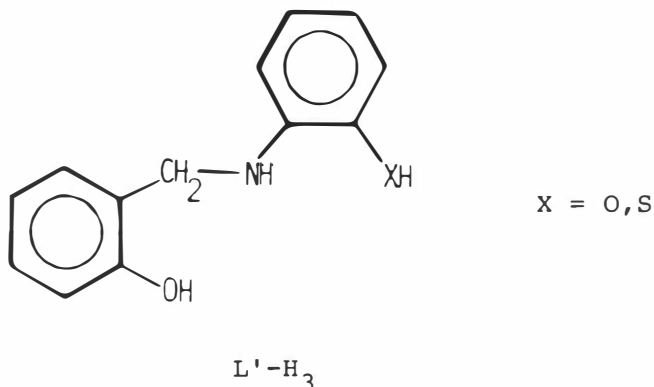
Reaction of Mo(VI)O$_2$(acac)$_2$ with L'-H$_3$ (X=O,S) gave Mo(VI)L'$_2$ complexes which were devoid of both terminal oxo groups. This was attributed to deprotonation of the amino proton during complex formation. Electrochemical reduction of Mo(VI)L'$_2$ indicated that it underwent reversible reduction to Mo(V)L'$_2^-$ and Mo(IV)L'$_2^{-2}$. It is interesting to note that similar ligands which contain two NH groups in the ligand backbone react with Mo(VI)O$_2$(acac)$_2$ to yield complexes of the Mo(VI)O$_2$(L'-H$_2$) type wherein both nitrogens remained protonated. These complexes were reported to undergo irreversible reduction to Mo(V)O(L'-H$_2$)$^-$ wherein nitrogen deprotonation was postulated to occur (132).

Berg and Holm (125) have recently reported the synthesis and X-ray crystallographic results on cis-dioxomolybde-

num(VI) complexes containing the tridentate ligands pyri-
dine-2,6-dimethanethiolate (LNS$_2$), and pyridine-2,6-di-
methanolate (LNO$_2$).

X=S ; LNS$_2$

X=O ; LNO$_2$
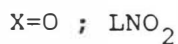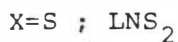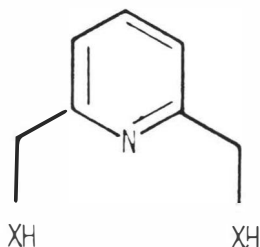
Crystallographic results indicated that the
Mo(VI)O$_2$(L-NO$_2$) complex has an oligomeric structure with
asymmetric trans oxygen bridges as shown below:
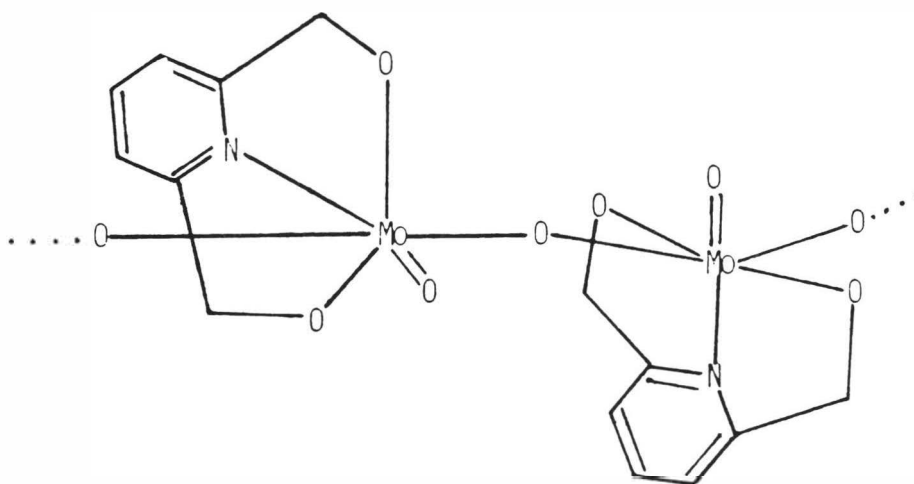
In contrast, the structure of $Mo(VI)O_2(L-NS_2)$, isolated in crystalline form as the tetramethylene sulfoxide (TMSO) adduct, $Mo(VI)O_2(L-NS_2) \cdot TMSO$, revealed well separated mononuclear species with distorted octahedral structures.
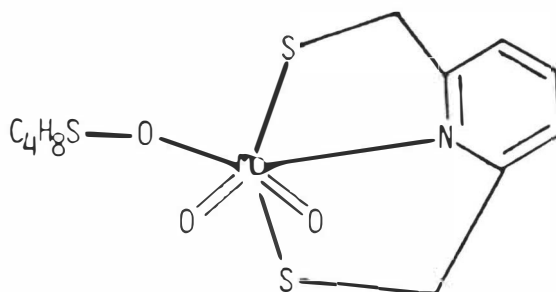
The results obtained in this crystallographic study supported the earlier conclusions reported by Rajan and Chakravorty (117) and Topich and Lyon (116) concerning the structure of cis-dioxomolybdenum(VI) salicylaldimato complexes.

The reactivity of $Mo(VI)O_2(LNS_2)$ in oxo-transfer reactions with PPh_3 was evaluated (125). This complex was found to undergo formation of $Mo(V)_2O_3(C_5H_5N(CH_2S)_2)_2$ dimers under these conditions. This led Berg and Holm (126) to synthesize the related sterically hindered ligands $L'NS_2$ = 2,6-bis(2,2-diphenyl-2-mercaptoethyl)pyridine and $L'NO_2$ = 2,6-bis(2,2-diphenyl-2-hydroxyethyl)pyridine.

$$X=S \; ; \; L'NS_2$$
$$X=O \; ; \; L'NO_2$$
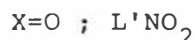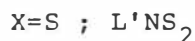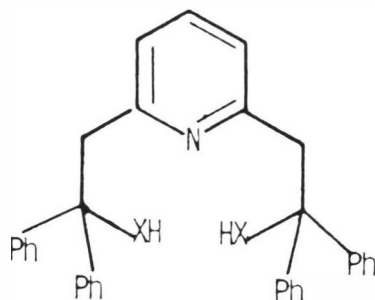
The complexes prepared from these ligands are of the Mo(VI)-O_2L type (L = tridentate ligand). The coordination units possess steric features (i.e. phenyl groups) which are included to suppress formation of μ-oxomolybdenum(V) dimers during reactions of these complexes with organophosphines. Details of these reactions are presented in Chapter V.

Results and Discussion

The objective of this research is to systematically develop molybdenum coordination complexes which attempt to model the active site of the molybdenum oxidoreductase enzymes. The approach used to achieve this objective both by ourselves (81,115,116) and others (125,126) has been termed the synthetic analogue approach. As stated by Ibers and Holm (133): "When reduced to practice, this approach necessitates the synthesis of relatively low molecular

weight complexes, which, ideally are obtainable in crystalline form and approach or duplicate the biological unit in terms of composition, ligand types, structure and oxidation level(s). Such models or synthetic analogues, of course, cannot simulate the environmental effects of an whatever structural constraints are imposed by the normal protein conformation. Indeed, this may be considered an advantage of synthetic analogues, for, being unencumbered by the protein, they should reflect the intrinsic properties of the coordination unit unmodified by the protein milieu".

A suitable synthetic molybdenum oxidoreductase model complex should (a) possess a ligand environment approaching that implicated for the active site in the enzymes as determined by EXAFS and EPR investigations, (b) be interconvertible between the oxidized $Mo(VI)O_2L_n$ and reduced $Mo(IV)-OL_n$ forms, and (c) be mononuclear and not form unreactive, biologically irrelevant, μ-oxo-$Mo_2(V)O_3L_{2n}$ dimers during oxo transfer reactions.

A. Synthesis of cis-Dioxomolybdenum(VI) Complexes

The research effort in this laboratory has focused on the chemical properties of four series of cis-dioxomolybdenum(VI) coordination complexes prepared from the following tridentate Schiff base ligands:

Y=OH; 5-X-SAP-H$_2$ Y=OH; 5-X-SAE-H$_2$

X=NO$_2$,Br,Cl,H,CH$_3$O

Y=SH; 5-X-SSP-H$_2$ Y=SH; 5-X-SSE-H$_2$

X=Br,Cl,H,CH$_3$O
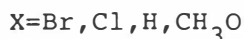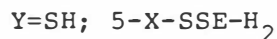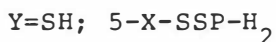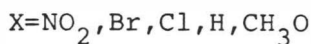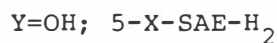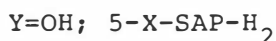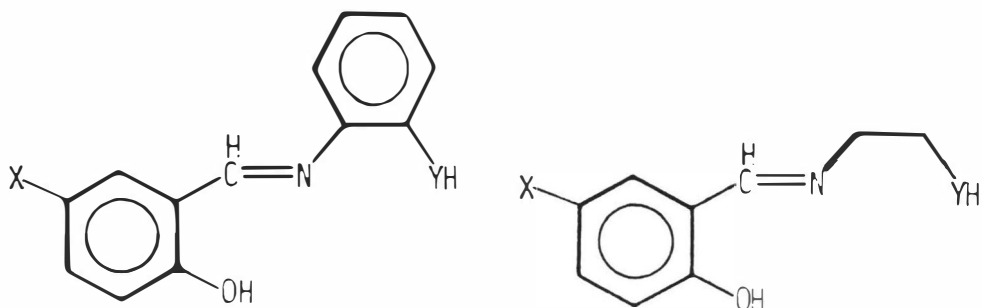
These ligands were designed and synthesized to incorporate
three features that could alter the electronic properties of
the cis-dioxomolybdenum(VI) center and thus its reactivity
in redox reactions. These ligand features include (1) the
X-substituent on the salicylaldehyde portion of each ligand;
(2) the degree of ligand delocalization (5-X-SAP^{2-} and
5-X-SSP^{2-} vs. 5-X-SAE^{2-} and 5-X-SSE^{2-}); and (3) the substi-
tution of a sulfur donor atom in 5-X-SSP^{2-} and 5-X-SSE^{2-} for
an oxygen donor atom in 5-X-SAP^{2-} and 5-X-SAE^{2-}.

The two series of cis-dioxomolybdenum(VI) complexes
containing ONO donor atoms, Mo(VI)O$_2$(5-X-SAP) and Mo(VI)O$_2$-
(5-X-SAE), (X - H, Cl, Br, NO$_2$ and CH$_3$O) were prepared and

characterized as described by Topich (81,115). The two series $Mo(VI)O_2(5-X-SSP)$ and $Mo(VI)O_2(5-X-SSE)$, (X = H, Cl, Br, CH_3O) which contain the ONS donor atom set were prepared by reaction of either $Mo(VI)O_2(acac)_2$ or $Mo(VI)O_2Cl_2$ with the substituted dibasic Schiff base ligand in 1:1 molar ratio in absolute ethanol. The $Mo(VI)O_2(5-H-SSP)$ complex has been described previously in the literature (117,118), however reports with regard to the stoichiometry are inconsistent. Hill et al. (118) claim that 5-H-SSP-H_2 coordinates to the MoO_2^{2+} core as a monoanionic bidentate ligand resulting in the $Mo(VI)O_2(5-H-SSP-H)_2$ stoichiometry. However, Rajan and Chakravorty (117) report that 5-H-SSP-H_2 coordinates to MoO_2^{2+} as a dianionic tridentate ligand to form $Mo(VI)O_2(5-H-SSP)$. Results obtained in this laboratory on $Mo(VI)O_2(5-H-SSP)$ and related complexes support the conclusion of Rajan and Chakravorty as to the stoichiometry of these complexes. Elemental analysis data are provided in Table 6. An idealized cis-dioxomolybdenum(VI) complex structure representing the four series is provided below.

$$X = NO_2, H, Cl, Br, CH_3O$$
$$Y = O, S$$
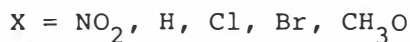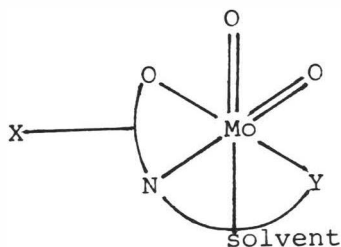
Table 6. Elemental Analyses Data for $Mo(VI)O_2(5-X-SSP)$

and $Mo(VI)O_2(5-X-SSE)$

| Mo COMPLEX | % found (% calc.) | | |
	C	H	N
$Mo(VI)O_2(5-H-SSP)$	44.03 (43.96)	2.62 (2.56)	3.95 (3.94)
$Mo(VI)O_2(5-Cl-SSP)$	40.11 (40.07)	2.12 (2.07)	3.53 (3.59)
$Mo(VI)O_2(5-Br-SSP)$	36.03 (35.97)	1.91 (1.86)	3.20 (3.23)
$Mo(VI)O_2(5-CH_3O-SSP)$	43.43 (43.65)	2.91 (2.88)	3.53 (3.64)
$Mo(VI)O_2(5-H-SSE)$	35.26 (35.19)	2.99 (2.95)	4.51 (4.56)
$Mo(VI)O_2(5-Cl-SSE)$	31.68 (31.64)	2.39 (2.36)	4.09 (4.10)
$Mo(VI)O_2(5-Br-SSE)(H_2O)$	26.66 (26.75)	2.35 (2.49)	3.54 (3.46)
$Mo(VI)O_2(5-CH_3O-SSE)$	35.52 (35.62)	3.36 (3.29)	4.14 (4.15)

Characteristic features of these complexes are (1) the cis arrangement of the oxo groups on the molybdenum which is what is typically observed in MoO_2^{2+} species (2), (2) a tridentate ligand which occupies three meridional sites about the molybdenum and (3) the sixth coordination site trans to Mo=O is labile which allows for potential substrate or solvent coordination.

B. Characterization of cis-Dioxomolybdenum(VI) Complexes

1. Infrared Spectroscopy

The infrared spectra for the two series of Schiff base ligands, $5\text{-}X\text{-}SSP\text{-}H_2$ and $5\text{-}X\text{-}SSE\text{-}H_2$, and their respective coordination complexes, $Mo(VI)O_2(5\text{-}X\text{-}SSP)$ and $Mo(VI)O_2(5\text{-}X\text{-}SSE)$, were obtained in the solid state (KBr disks) between $4000\text{-}200$ cm^{-1}. The infrared spectrum of $5\text{-}H\text{-}SSP\text{-}H_2$ is shown in Figure 4 and is typical for all ligands used in this study. Two features to note concerning this spectrum are (1) the presence of a strong band at ~ 1620 cm^{-1} which is assigned to $\nu(C=N)$ and, (2) the absence of strong bands between $1000\text{-}800$ cm^{-1}. Upon complexation to form $Mo(VI)O_2\text{-}(5\text{-}H\text{-}SSP)$ the $\nu(C=N)$ vibration shifts to lower energy ~ 1605 cm^{-1}, Figure 5. This behavior has been observed previously for a variety of metal complexes with N-aryl-salicylidene-imine ligands (134-137). Usually, IR spectra of Mo(VI) complexes display strong vibrations between $1000\text{-}900$ cm^{-1} due to the MoO_2^{2+} moiety (2). For many of the complexes examined in this study one or more bands in this region were

Figure 4. Infrared spectrum of 5-H-SSP-H$_2$.

80

80

80

60

60

60

40

40

20

20

1000   **800**

SH

N

OH

1600   1400   WAVENUMBER(CM⁻¹)   1000   800   600   400   200

59
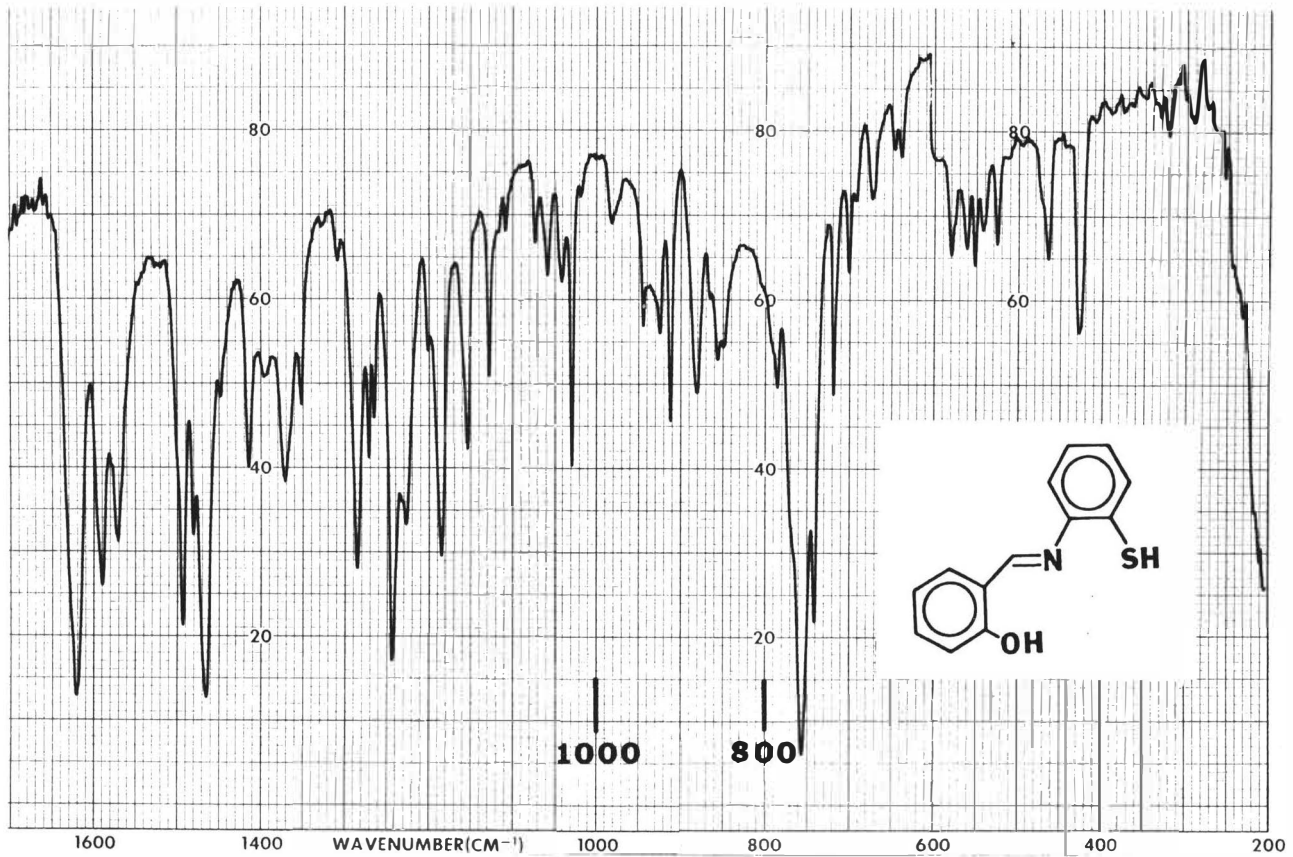
Figure 5. Infrared spectrum of Mo(VI)O$_2$(5-H-SSP).

1000　　800
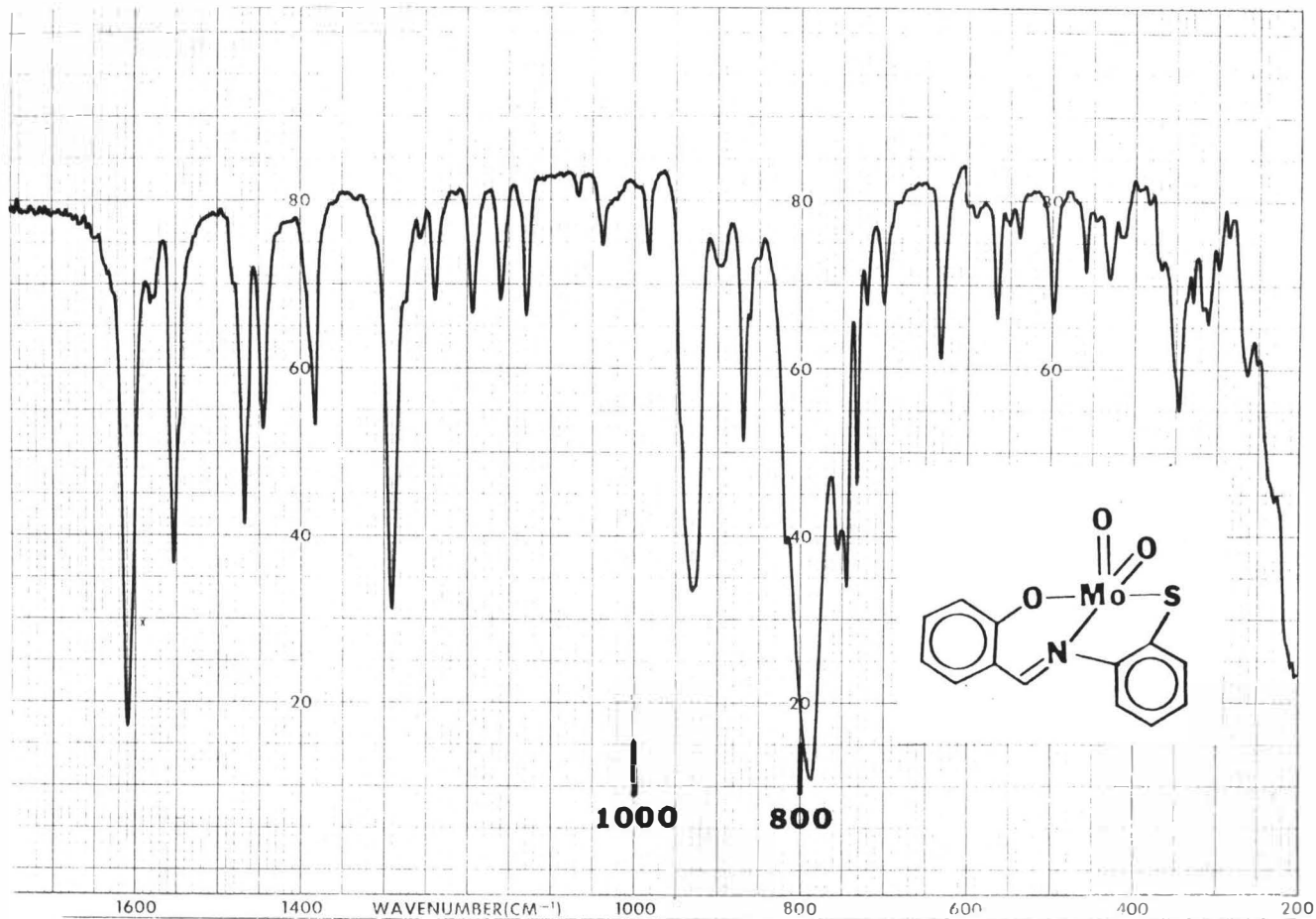
observed. However, in addition to these bands a strong, broad vibration occurring at ~ 800 cm^{-1} was also observed. Rajan and Chakravorty (117) have attributed this vibration to formation of oligomers in the solid state, Figure 6.
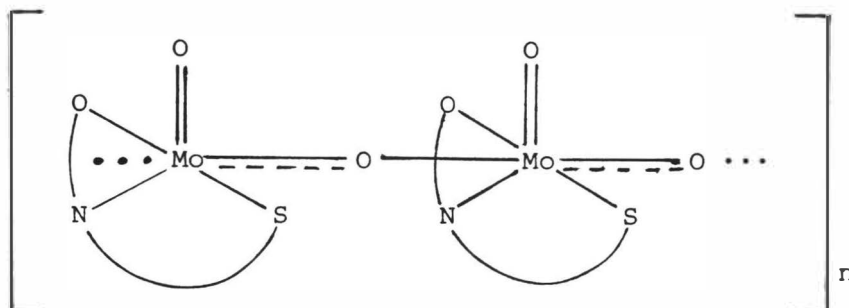
Figure 6. Oligomeric structure of Mo(VI) Complexes in the solid state.

An example of this phenomenon can be seen in the IR spectrum of Mo(VI)O_2(5-H-SSP) in Figure 5. The band at ~ 930 cm^{-1} is assigned to ν(Mo=O) and the broad absorption at ~ 800 cm^{-1} is attributed to the weakened ν(Mo=O) present in the Mo...O→Mo moiety. In donor solvents such as DMF or Me_2SO the oligomeric structure is broken down and monomeric complexes having the Mo(VI)O_2(L)(solvent) stoichiometry are obtained. Infrared data for the two series of complexes, Mo(VI)O_2(5-X-SSP) and Mo(VI)O_2(5-X-SSE), are listed in Table 7.

2. Electronic Spectra

The electronic spectra for the two series of complexes

Table 7. Infrared Data for $Mo(VI)O_2(5-X-SSP)$

and $Mo(VI)O_2(5-X-SSE)$ [a]

Complex	IR $\nu(Mo=O)$, cm^{-1}
$Mo(VI)O_2(5-X-SSP)$	
X = H	925
Cl	934,943
Br	926,940
CH_3O	912
$Mo(VI)O_2(5-X-SSE)$	
X = H	902,947
Cl	918
Br	914,922
CH_3O	887,906,920

(a) KBr disk

Figure 7. UV-Visible spectrum of Mo(VI)O$_2$(5-H-SSP) in Me$_2$SO; C = 3.519 x 10^{-3} M, b = 0.1 cm.
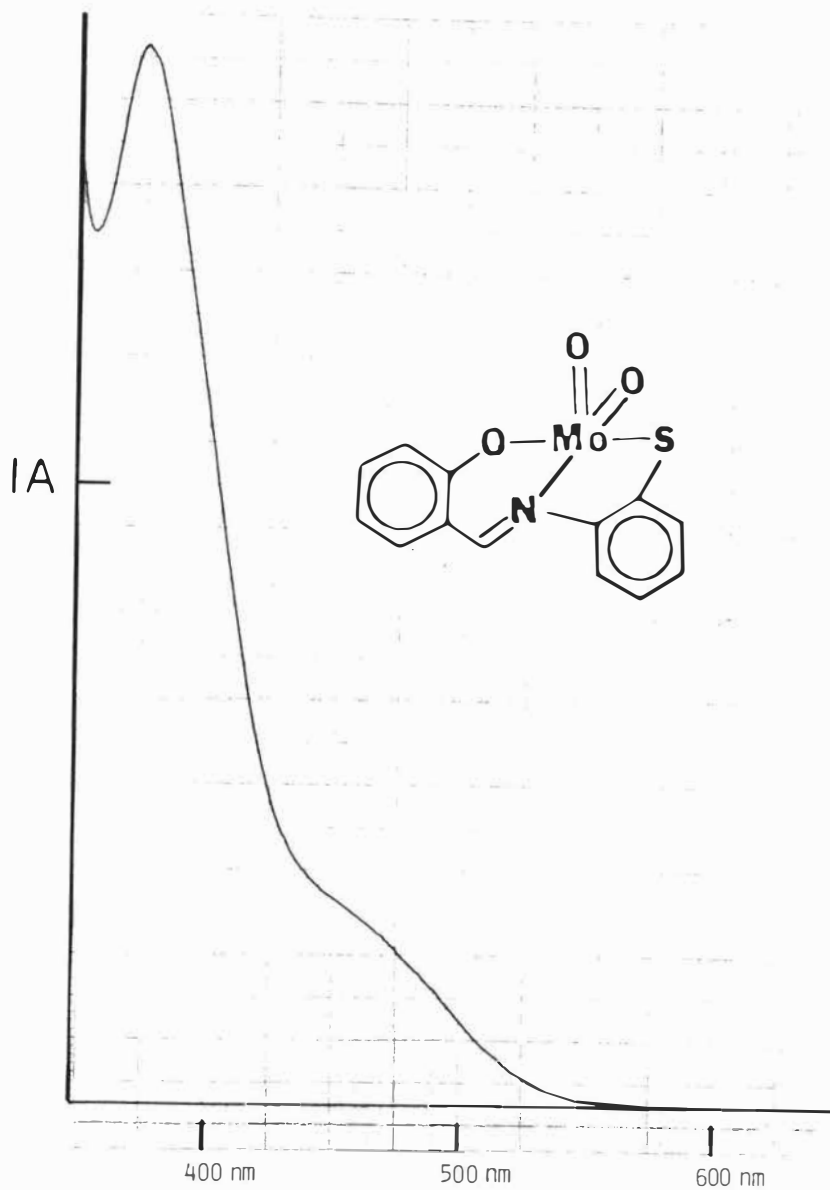
Figure 8. UV-Visible spectrum of Mo(VI)O$_2$(5-H-SSE) in
           Me$_2$SO; C = 4.134 x 10^{-3} M, b = 0.1 cm.
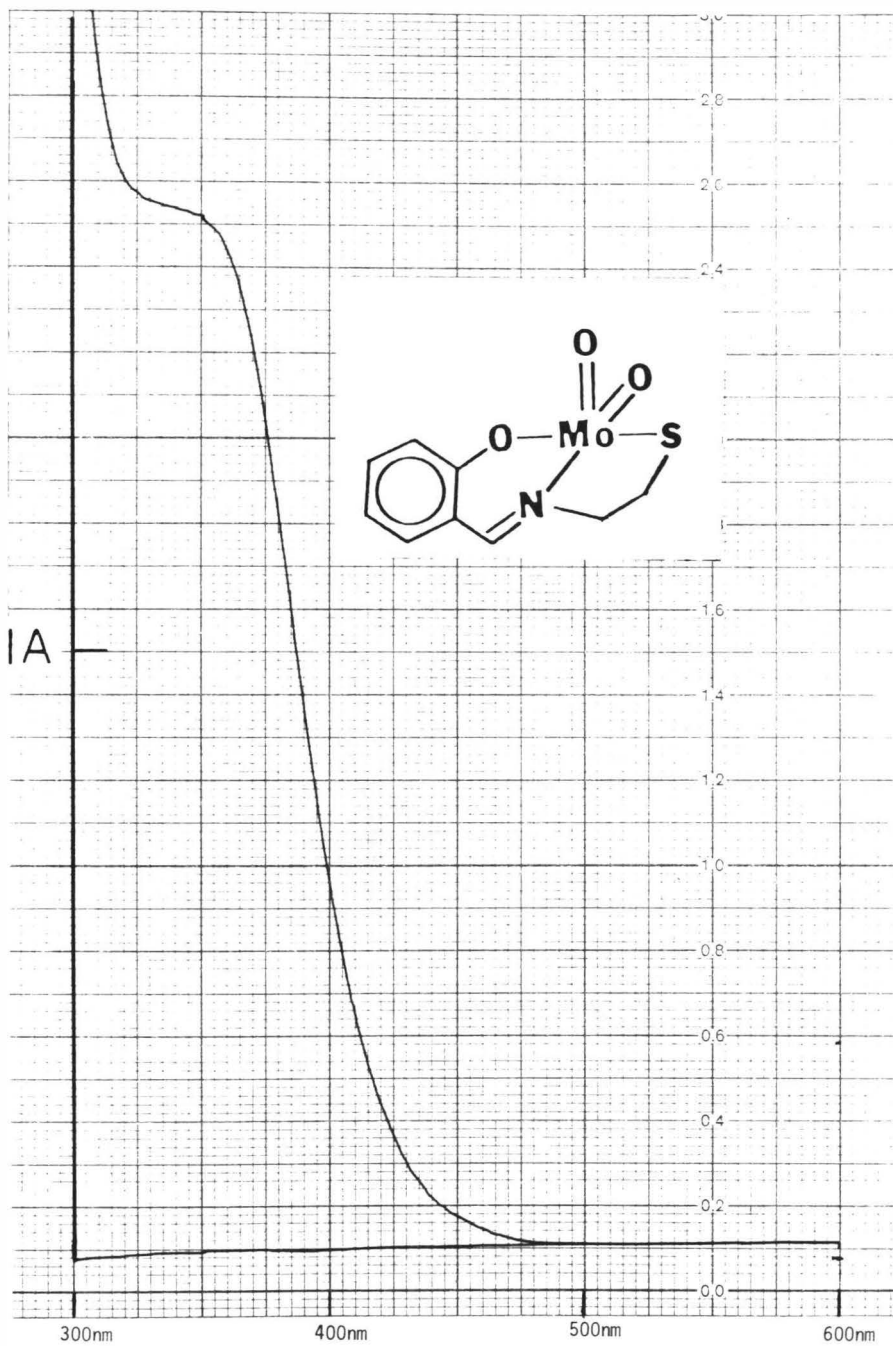
Mo(VI)O$_2$(5-X-SSP) and Mo(VI)O$_2$(5-X-SSE) were recorded be-
tween 650 and 300 nm using either DMF or Me$_2$SO as the
solvent. In each series the free ligands exhibited tran-
sitions below 300 nm. For the two series of complexes, band
placements were shown to be identical in both DMF and Me$_2$SO,
however, small variations in the shape of the bands and
extinction coefficients were noted which may be due to
coordination of Me$_2$SO through the -S=O oxygen and DMF
through the -C=O oxygen atom. The complexes were stable for
extended periods of time (at least two weeks) in both
solvents as evidenced by no change in their electronic
spectra.

The spectra for Mo(VI)O$_2$(5-H-SSP) and Mo(VI)O$_2$(5-H-SSE)
in Me$_2$SO are shown in Figures 7 and 8, respectively.
Mo(VI)O$_2$(5-H-SSP), which forms orange solutions when dis-
solved in Me$_2$SO, exhibits an intense band with λ_{max} = 374 nm
(ε = 6918 M^{-1}cm^{-1}) and a well defined shoulder at ~ 464 nm.
Mo(VI)O$_2$(5-H-SSE) in Me$_2$SO forms a yellow solution and
exhibits a well defined absorption at λ_{max} = 350 nm (ε =
4467 M^{-1}cm^{-1}). UV-visible data for the two series of
complexes, Mo(VI)O$_2$(5-X-SSP) and Mo(VI)O$_2$(5-X-SSE), are
listed in Table 8. Since Mo(VI) is formally represented as
having a 4d° electronic configuration it may be assumed that
the electronic spectra for these complexes are dominated by
ligand to metal charge transfer (LMCT) electronic tran-
sitions. Other intraligand transitions may also be present.
Literature reports containing UV-visible data on complexes

Table 8. UV-Visible Data for $Mo(VI)O_2(5-X-SSP)$

and $Mo(VI)O_2(5-X-SSE)$ in Me_2SO

Molybdenum(VI) Complex	Electronic Spectra λ(nm); ε($M^{-1}cm^{-1}$)
$Mo(VI)O_2(5-X-SSP)$	
X = H	374 (6918), 460 sh
Cl	378 (5623), 453 sh
Br	378 (6471), 456 sh
CH_3O	319 (15,135), 380 (5272), 429 sh, 465 sh
$Mo(VI)O_2(5-X-SSE)$	
X = H	346 (4467)
Cl	349 (4266)
Br	350 (3412), 330 sh
CH_3O	346 (4571)

possessing thiolate ligands have low energy electronic absorptions below ~ 390 nm (84,113,138). These have been assigned to RS^- → Mo(VI) charge transfer transitions. Berg and Holm (126) have recently reported the UV-visible spectrum of $Mo(VI)O_2(LNS_2)$ in DMF. This complex contains two thiolate donor atoms in the molybdenum coordination sphere. The spectrum was shown to exhibit two intense bands at λ_{max} = 449 nm (ε = 3890 $M^{-1}cm^{-1}$) and 385 nm (ε = 4365 $M^{-1}cm^{-1}$) which were assigned to S^- → Mo(VI) charge transfer transitions. In this regard it is interesting that the oxidized Mo(VI) form of the molybdenum cofactor isolated from rat liver sulfite oxidase by Johnson and Rajagopalan (139) also absorbs at relatively low energy with bands at ~ 480 and 350 nm. EXAFS results (64,75) have indicated two or three thiolate ligands in the native enzyme which suggests that these bands are also S^- → Mo(VI) charge transfer transitions.

C. Electrochemical Studies on $Mo(VI)O_2(5-X-SSP)$, $Mo(VI)O_2-$ (5-X-SSE), $Mo(VI)O_2(5-X-SAP)$ and $Mo(VI)O_2(5-X-SAE)$

In view of the fact that all known molybdenum-containing enzymes catalyze oxidation-reduction reactions, electrochemistry is a particularly convenient method for the study of the redox behavior of molybdenum model compounds. Cyclic voltammetry is an electrochemical technique which can be used to determine the electrochemical behavior of a redox couple. Figure 9 is an idealized cyclic voltammogram for a

Figure 9. Simulated cyclic voltammogram for a one electron reversible redox couple ($C=1 \times 10^{-3}$ M, $E°=-1.15$ V, scan rate=100 mV/sec, A=1.0 cm^2, $D=1 \times 10^{-6}$ cm/sec, T=25°C, $\alpha=0.5$, k=1.0, $\Delta E=58$ mV, $i_{pc}=85$ μA, $i_{pa}=-85$ μA, $E_{pc}=-1.178$ V, $E_{pa}=-1.120$ V) (reference 141).

CV SIMULATION
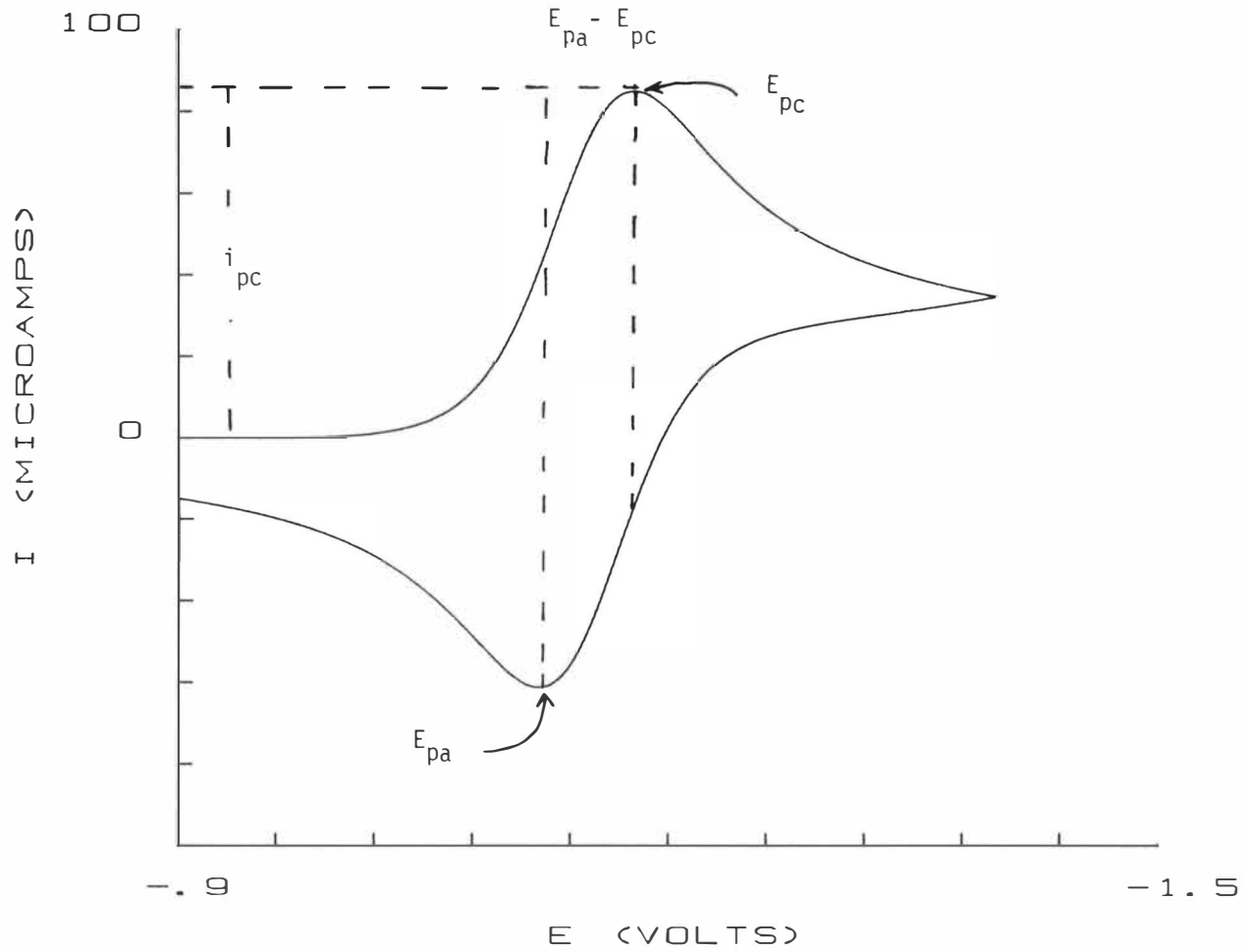
reversible one electron redox process (140,141). E_{pa} and E_{pc} are the potentials corresponding to anodic (oxidation) and cathodic (reduction) processes. i_{pa} and i_{pc} are the measured currents at these potentials. A reversible electrochemical redox couple will possess peak potentials E_{pa} and E_{pc} which are independent of scan rate, a ΔE ($E_{pa}-E_{pc}$) value of $\sim$ 58 mV, and a ratio of cathodic to anodic peak current (i_{pc}/i_{pa}) equal to unity (140).

Electrochemical studies using cyclic voltammetry were carried out on the four series of complexes, $Mo(VI)O_2$(5-X-SSP), $Mo(VI)O_2$(5-X-SSE), $Mo(VI)O_2$(5-X-SAP), and $Mo(VI)O_2$(5-X-SAE). Each cyclic voltammetric experiment was performed in dry, deaerated DMF with tetrabutylammonium perchlorate (TBAP) as the supporting electrolyte. A glassy carbon working electrode was used. Potentials were measured with reference to the ferrocenium/ferrocene redox couple so that errors associated with junction potentials would be minimized.

The four series of complexes examined in this work did not display cyclic voltammograms characteristic of reversible couples. The cyclic voltammogram for $Mo(VI)O_2$(5-H-SSP) (Figure 10) is representative of the CV's obtained for these complexes. Initial cathodic scans (initiated at 0 V vs. NHE) exhibit a well defined reduction peak, however upon reverse anodic scan there is no evidence for a coupled oxidation process. Table 9 contains cathodic peak reduction potentials, (E_{pc}), for $Mo(VI)O_2$(5-X-SSP), $Mo(VI)O_2$(5-X-SSE),

Figure 10.   Cyclic voltammogram for $Mo(VI)O_2(5-H-SSP)$ in DMF ($C=1\times10^{-3}$ M, scan rate=100 mV/sec, A=0.283 cm^2).

2μA

-0.6　　-0.7　　-0.8　　-0.9　　-1.0　　-1.1　　-1.2　　-1.3

Volts vs NHE
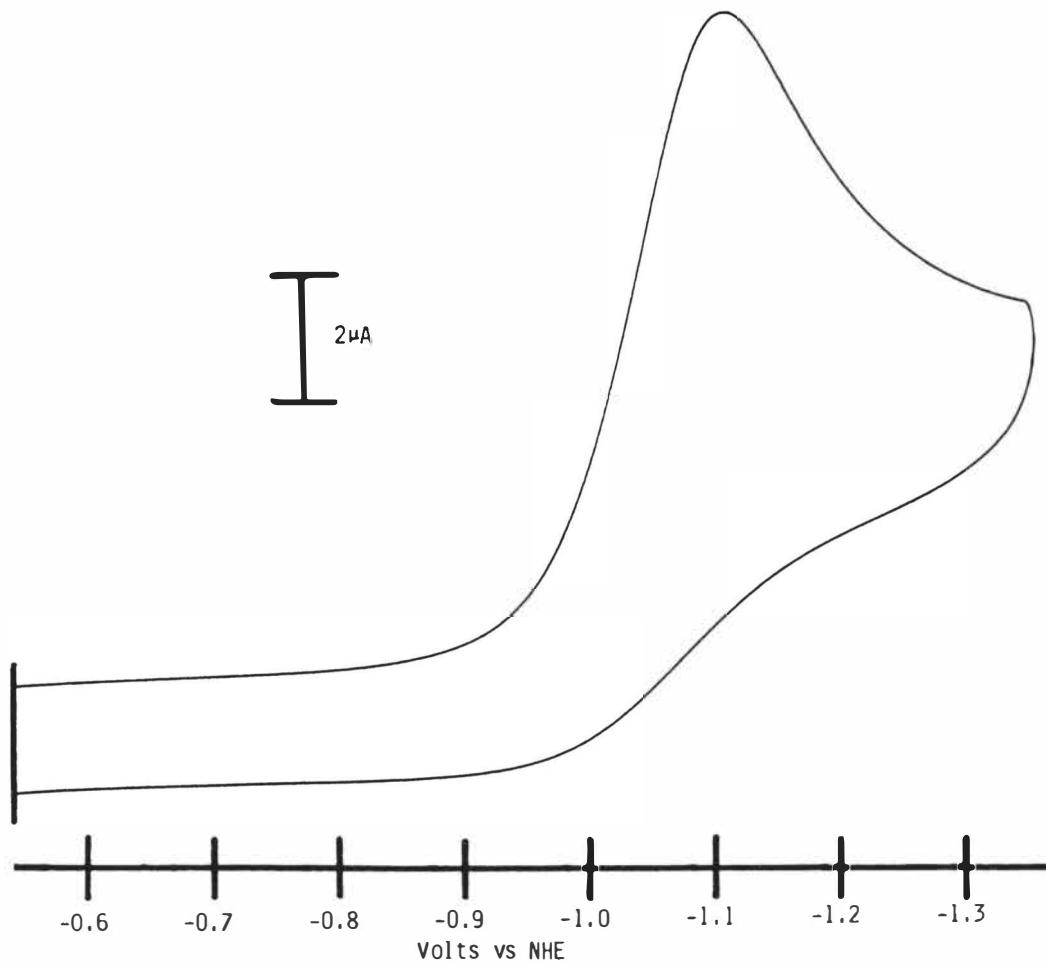
Table 9. Cyclic Voltammetry Data for Cis-

Dioxomolybdenum(VI) Complexes

Mo Complex	E_{pc}, V[a]	Δ, mV[b]
Mo(VI)O$_2$(5-Cl-SSP)	-1.06	+180
Mo(VI)O$_2$(5-Br-SSP)	-1.05	+190
Mo(VI)O$_2$(5-H-SSP)	-1.11	+130
Mo(VI)O$_2$(5-CH$_3$O-SSP)	-1.13	+110
Mo(VI)O$_2$(5-Cl-SSE)	-1.22	+ 20
Mo(VI)O$_2$(5-Br-SSE)	-1.22	+ 20
Mo(VI)O$_2$(5-H-SSE)	-1.25	- 10
Mo(VI)O$_2$(5-CH$_3$O-SSE)	-1.27	- 30
Mo(VI)O$_2$(5-NO$_2$-SAP)	-1.11	+130
Mo(VI)O$_2$(5-Cl-SAP)	-1.17	+ 70
Mo(VI)O$_2$(5-Br-SAP)	-1.17	+ 70
Mo(VI)O$_2$(5-H-SAP)	-1.24	0
Mo(VI)O$_2$(5-CH$_3$O-SAP)	-1.25	- 10
Mo(VI)O$_2$(5-NO$_2$-SAE)	-1.25	- 10
Mo(VI)O$_2$(5-Cl-SAE)	-1.48	-240
Mo(VI)O$_2$(5-Br-SAE)	-1.48	-240
Mo(VI)O$_2$(5-H-SAE)	-1.49	-250
Mo(VI)O$_2$(5-CH$_3$O-SAE)	-1.53	-290

[a]Volts vs. NHE with reference to the Fc^+/Fc redox couple. Scan rate = 100 mV/s.

[b]Δ = E_{pc}(Mo complex) - E_{pc}(Mo(VI)O$_2$(5-H-SAP)).

$Mo(VI)O_2(5-X-SAP)$ and $Mo(VI)O_2(5-X-SAE)$. The cathodic peak reduction potential is the potential measured where the cathodic peak current is at its maximum and the data should not be confused with thermodynamic reduction potentials, $E°$ which are obtained from reversible cyclic voltammograms. It should be noted that the ligands were not electroactive in the potential range where the molybdenum complex reductions are observed.

Scan rate dependence experiments were performed on $Mo(VI)O_2(5-H-SSP)$ between 10 and 500 mV/sec. Plots of i_{pc} vs. $v^{\frac{1}{2}}$ were reasonably linear up to 100 mV/sec (Table 10, Figure 11). At higher scan rates a deviation from linearity was observed. At present it is unclear whether the deviation from linearity at higher scan rates (> 100 mV/sec) is due to a heterogeneous kinetic effect or uncompensated resistance, which could result from the nonaqueous medium or nonideal cell configuration.

Based on these results and also some preliminary data obtained using double potential step chronocoulometry it appears that the complexes are initially reduced in a quasi-reversible electrode process which is followed by a rapid homogeneous chemical reaction (142). This process may be represented by equations (3) and (4)

$$O + ne \rightarrow R \qquad\qquad (3)$$

$$R \rightarrow products \qquad\qquad (4)$$
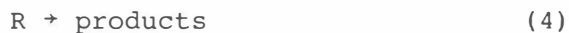
Table 10. Scan Rate Dependence of i_{pc} and E_{pc} for

$Mo(VI)O_2(5\text{-}H\text{-}SSP)$ in DMF^a

Scan Rate v(mV/sec)	$v^{\frac{1}{2}}$	Cathodic Peak Current i_{pc} (μA)	Cathodic Peak Potential E_{pc} (V vs SCE)
10	3.16	2.99	-1.03
20	4.47	4.25	-1.02
50	7.07	6.89	-1.04
100	10.00	9.45	-1.04
200	14.14	12.20	-1.05
500	22.36	17.32	-1.07

[a] Complex concentration was 9.57×10^{-4} M; Electrode Area = 0.283 cm^2

Figure 11. Plot of i_{pc} versus $v^{\frac{1}{2}}$ for $Mo(VI)O_2(5\text{-H-SSP})$ in DMF (v=10,20,50,100,200,500 mV/sec).
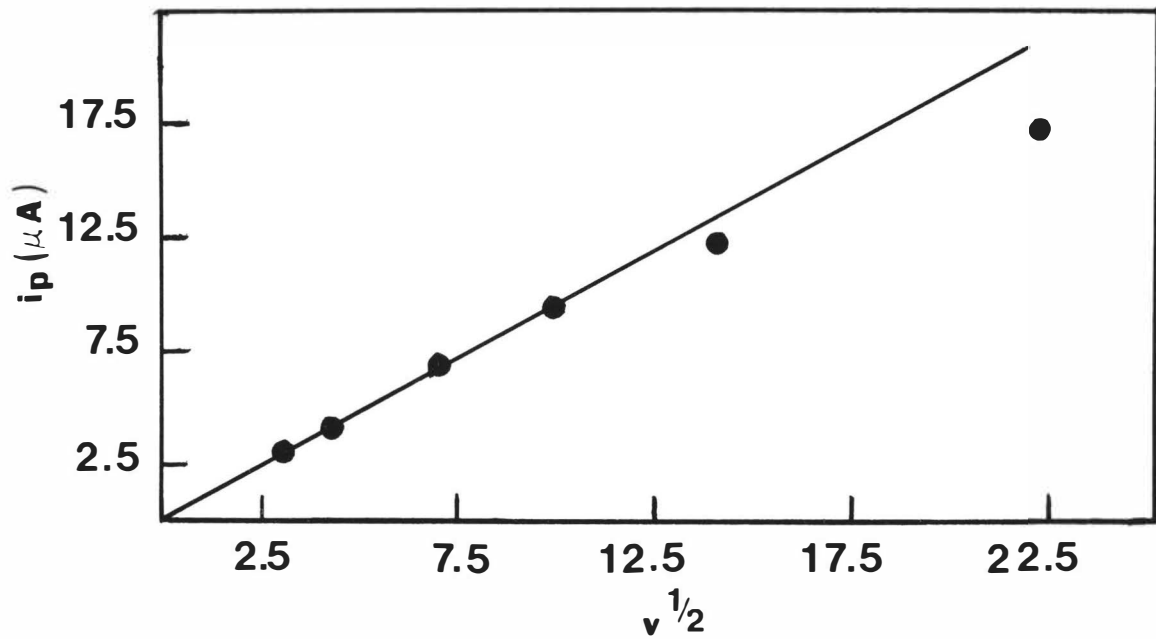
Electrochemical studies (119,126,143-145) on similar cis-dioxomolybdenum(VI) complexes have generally shown irreversible or quasi-reversible behavior. For a series of oxomolybdenum complexes, Taylor et al. have shown (145) that it is impossible to obtain oxomolybdenum(V) monomers by electrochemical reduction of the corresponding cis-dioxomolybdenum(VI) complexes in nonaqueous solvents. Similarly, the oxomolybdenum(V) monomers cannot be electrochemically oxidized to the corresponding cis-dioxomolybdenum(VI) complexes. The failure of these redox processes may be due to the difficulty in adding or removing an oxygen atom from the oxomolybdenum core during the oxidation or reduction process in nonaqueous solvents.

We have been interested in examining how the cathodic reduction potentials for the four series of cis-dioxomolyb-denum(VI) coordination complexes are affected through systematic changes in ligand structure. Studies of substi-tuent effects on metal redox activity in coordination compounds are numerous (146,149), however only a few reports are available with molybdenum as the metal center (81,143,150-152).

Recently, Ghosh and Chakravorty (152) reported on the preparation and electrochemical properties of a series of $Mo(VI)O_2(LRX)$ complexes (LRX = disubstituted hydroxamate), (R = H, CH_3, Ph; and X = CH_3O, CH_3, H, Cl, NO_2).
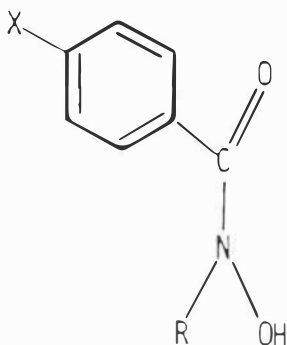
LRX

Each of these complexes was shown to exhibit irreversible electrochemical reductions at a mercury electrode. E_{pc} values obtained from cyclic voltammograms ranged from -0.64 to -1.64 V vs. SCE and linear correlations were noted with Hammett constants.

The cathodic reduction potentials for $Mo(VI)O_2(5-X-SSP)$, $Mo(VI)O_2(5-X-SAP)$, $Mo(VI)O_2(5-X-SSE)$, and $Mo(VI)O_2(5-X-SAE)$ were plotted as a function of the Hammett σ_p parameter (Figure 12). The Hammett para parameter was chosen because the X substituent on the ligand is para to the salicylaldehyde oxygen donor atom. For all four series, the cathodic reduction potentials span a range of -1.53 V to -1.05 V vs. NHE. Within each series the potentials range as follows: $Mo(VI)O_2(5-X-SAP)$, -1.25 to -1.11 V; $Mo(VI)O_2(5-X-SAE)$, -1.53 to -1.25 V; $Mo(VI)O_2(5-X-SSP)$, -1.13 to -1.06 V; $Mo(VI)O_2(5-X-SSE)$, -1.27 to -1.22 V. A linear relation-

Figure 12. Correlation of E_{pc} (V) with the Hammett σ_p parameter for the molybdenum(VI) complexes: □, $Mo(VI)O_2$(5-X-SSP); O, $Mo(VI)O_2$(5-X-SSE); ■, $Mo(VI)O_2$(5-X-SAP); ●, $Mo(VI)O_2$(5-X-SAE); (X=CH_3O,H,Cl,Br,NO_2).
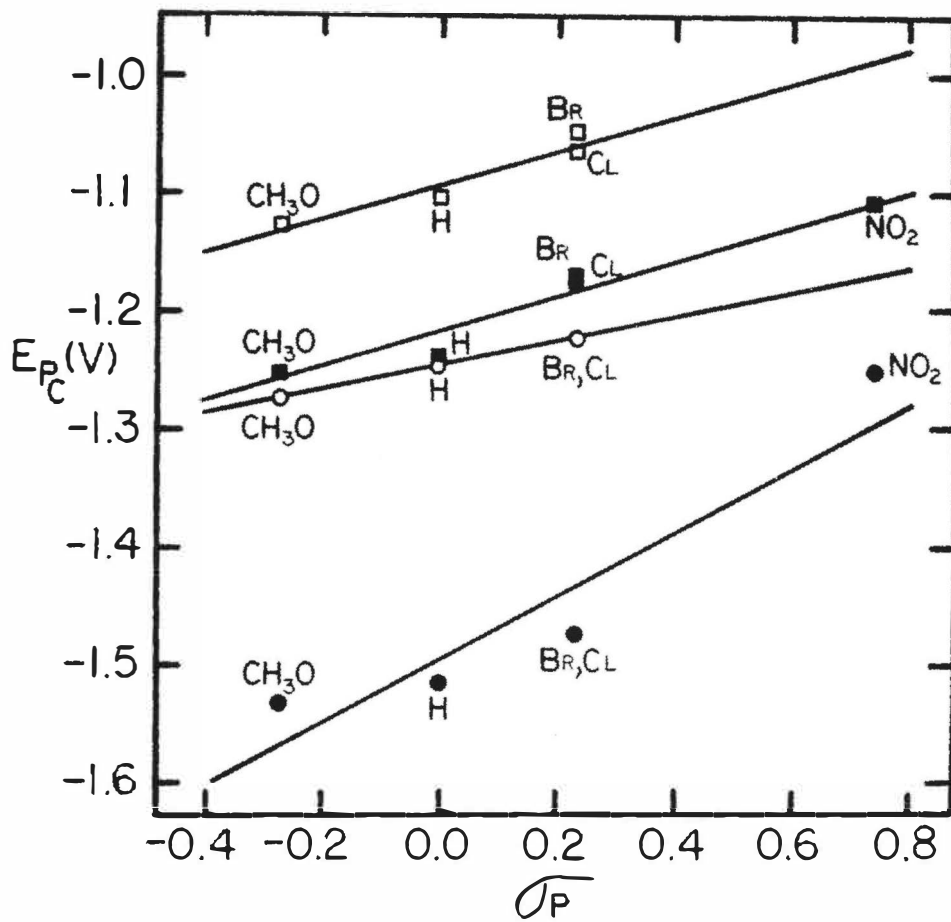
ship between E_{pc} and σ_p for each of the four series of cis-dioxomolybdenum(VI) complexes indicates that the systematic changes in the ligands are bringing about systematic and predictable changes in cathodic reduction potentials. Rajan and Chakravorty (143) reported cyclic voltammetry data on a number of cis-dioxomolybdenum(VI) complexes similar to those described in this study. They defined a parameter $\Delta = (E_{pc})_{complex} - (E_{pc})_{standard}$ to indicate facile or nonfacile reducibility of cis-dioxomolybdenum(VI) complexes as compared to an arbitrary reference complex (i.e., Mo(VI)O$_2$(5-H-SAP)). These Δ values are tabulated in Table 9 along with the E_{pc}'s. A negative Δ value indicates that the molybdenum complex is reduced at a more cathodic potential (more difficult to reduce) than the reference. A positive Δ value indicates that the molybdenum complex is reduced at a more anodic potential (easier to reduce) than the reference.

Even though the reductions observed for the cis-dioxomolybdenum(VI) complexes in this study are not reversible (due to a coupled homogeneous process), there are trends seen in the cathodic reduction potentials both within each series and between series. There are three ligand features whose effect is to systematically alter the cis-dioxomolybdenum(VI) cathodic reduction potential. These include (1) the X-substituent located on the salicylaldehyde portion of each ligand; (2) the degree of ligand delocalization (5-X-SAP^{2-} and 5-X-SSP^{2-} vs. 5-X-SAE^{2-} and 5-X-SSE^{2-}); and (3) the substitution of a sulfur donor atom in 5-X-SSP^{2-}

and $5-X-SSE^{2-}$ for an oxygen donor atom in $5-X-SAP^{2-}$ and $5-X-SAE^{2-}$. Each of these affects will be considered separately with regard to the cis-dioxomolybdenum(VI) cathodic reduction potentials and then their cumulative affect will be discussed.

Within each series, as the X-substituent becomes more electron withdrawing (X = NO_2 > Cl,Br > H > CH_3O) the cis-dioxomolybdenum(VI) E_{pc}'s are shifted to more anodic potentials which means that the cis-dioxomolybdenum(VI) complexes become easier to reduce. The affect of electron withdrawing groups, although not directly bonded to the molybdenum, is to draw electron density away from the metal and hence allow the molybdenum to be more easily reduced. The opposite affect is observed when the substituent is the electron donating CH_3O group.

The $Mo(VI)O_2(5-X-SSP)$ complexes are easier to reduce than the $Mo(VI)O_2(5-X-SSE)$ complexes and the $Mo(VI)O_2(5-X-SAP)$ complexes are easier to reduce than the $Mo(VI)O_2(5-X-SAE)$ complexes. Both $Mo(VI)O_2(5-X-SSP)$ and $Mo(VI)O_2(5-X-SAP)$ are complexes whose ligand systems are completely delocalized with extended π systems. On the other hand, the ligand systems associated with $Mo(VI)O_2(5-X-SSE)$ and $Mo(VI)-O_2(5-X-SAE)$ are not completely delocalized having limited π systems because of the aliphatic amine portion of the ligand. This ease of molybdenum complex reducibility that is observed with delocalized ligand systems can be rationalized as follows. During the reduction process an additional

electron is added to the metal. If this electron can be delocalized throughout the complex, the reduction will be easier to accomplish. An extended ligand π system will facilitate this process. This is in fact what is observed when comparing $Mo(VI)O_2(5-X-SSP)$ and $Mo(VI)O_2(5-X-SAP)$ with $Mo(VI)O_2(5-X-SSE)$ and $Mo(VI)O_2(5-X-SAE)$.

The introduction of a sulfur donor atom in place of an oxygen donor atom on the ligand renders the molybdenum reduction more facile. $Mo(VI)O_2(5-X-SSP)$ is easier to reduce than $Mo(VI)O_2(5-X-SAP)$ and $Mo(VI)O_2(5-X-SSE)$ is easier to reduce than $Mo(VI)O_2(5-X-SAE)$. Smith and Schultz (153) have reported that for a series of eight coordinate molybdenum complexes containing dithiocarbamate, thioxan-thate, and 1,1-disubstituted ethylenedithiolate ligands the molybdenum $3d_{5/2}$ binding energies (obtained from X-ray photoelectron spectroscopy) correlate with $E_{\frac{1}{2}}$ for the $Mo(VI)/Mo(V)$ redox couple. This agreement was attributed to the fact that both the binding energies and redox potentials respond to changes in charge density at the molybdenum site which is controlled by the nature of the ligand.

The more positive cathodic reduction potentials obtained for the two series, $Mo(VI)O_2(5-X-SSP)$ and $Mo(VI)O_2-(5-X-SSE)$, indicate that the sulfur donor atom coordinated to the molybdenum is more effective at reducing charge density at the molybdenum site than complexes which possess analogous oxygen containing ligands.

These three ligand variations by themselves can affect

the molybdenum reduction and when they are found together their effects tend to be cumulative. The easiest cis-dioxomolybdenum(VI) complex to reduce of the four series discussed here should be the one with a ligand having an extended π-system, a sulfur donor atom, and an effective electron withdrawing substituent. Two complexes fall in this category because Cl and Br have the same Hammett σ_p value. They are $Mo(VI)O_2(5-Cl-SSP)$ and $Mo(VI)O_2(5-Br-SSP)$. These two cis-dioxomolybdenum(VI) complexes have the most anodic E_{pc}'s (for X = Cl, E_{pc} = -1.06 V vs. NHE; for X = Br, E_{pc} = -1.05 V vs. NHE) of the eighteen complexes discussed. It is interesting to note that the E_{pc}'s for $Mo(VI)O_2(5-X-SSE)$ and $Mo(VI)O_2(5-X-SAP)$ are similar. This indicates that for these types of cis-dioxomolybdenum(VI) complexes the effect of incorporating a sulfur donor into the ligand is about as effective as including an extended π ligand system in altering cis-dioxomolybdenum(VI) cathodic reduction potentials.

IV.   OXYGEN ATOM TRANSFER CHEMISTRY OF CIS-

DIOXOMOLYBDENUM(VI) COMPLEXES

Introduction

The current understanding of the molybdenum oxidases indicates that the molybdenum cycles between the +6 and +4 oxidation states in their reactions with substrate and subsequent reactivation (126). In examining the reactions carried out by xanthine, sulfite, and aldehyde oxidase and also nitrate reductase (Table 1), one finds that the only difference between the substrate before and after the reaction is the addition or removal of an oxygen atom. The catalytic transformation of substrate may be represented by reactions (5) and (6) which lead to the net transformation of substrate in reaction (7).

$$Mo(VI)O_2L_n + X \rightleftharpoons Mo(IV)OL_n + XO \qquad (5)$$

$$Mo(IV)OL_n + H_2O \rightleftharpoons Mo(VI)O_2L_n + 2H^+ + 2e^- \quad (6)$$

$$X + H_2O \longrightarrow XO + 2H^+ + 2e^- \qquad (7)$$
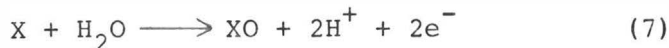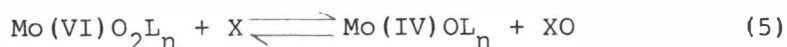
In order to understand the fundamental chemistry associated with the enzymatic active molybdenum site, researchers have sought well characterized synthetic molybdenum coordination complexes which participate in oxygen atom transfer reactions. Several review articles have

appeared which discuss approaches taken by inorganic chemists to attain this objective (21-23).

1. <u>Oxygen Atom Transfer Reactions from Mo(VI)O_2L_n to Substrates as Models for the Molybdenum Oxidase Enzymes</u>

The behavior of Mo(VI)O_2L_n complexes in oxygen atom transfer reactions with substrates (X) of biological interest have been examined, reaction (8),

$$Mo(VI)O_2L_n + X \rightarrow Mo(IV)OL_n + XO \qquad (8)$$

$$X = SO_3^{2-}, RCHO, \text{xanthine}$$
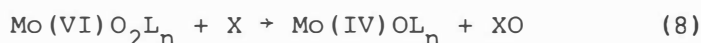
however success in this area has been limited.

(a) <u>Oxidation of Sulfite (SO$_3^{2-}$)</u>

The molybdenum enzyme sulfite oxidase is known to catalyze the oxidation of SO_3^{2-} to SO_4^{2-} using cytochrome <u>c</u> as the physiological electron acceptor (70,71). EPR (72-74) and EXAFS (64,75) evidence suggest that SO_3^{2-} is bound initially at a molybdenum(VI) center.

Spence et al. (132) have reported that Mo(VI)O_2(o-C_6H_4(S)NHCH$_2$)$_2$ is reduced to the Mo(IV)O(o-C_6H_4(S)NHCH$_2$)$_2$ species in the presence of SO_3^{2-}, however the oxidation product of SO_3^{2-} (presumably SO_4^{2-}) was not characterized. Garner et al. (154) have also briefly noted that polystyrene

suspensions of $Mo(VI)O_2(ethyl-L-cysteinate)_2$ in the presence of an aqueous solution of SO_3^{2-} are reduced to $Mo(IV)O-(ethyl-L-cysteinate)_2$, however no details concerning the reaction or characterization of products were provided. Thermochemical studies (155) performed in 1,2-dichloroethane on $Mo(VI)O_2(S_2CNEt_2)_2$ indicate that it should be capable of oxidizing SO_3^{2-}. Nevertheless, it does not oxidize SO_3^{2-} which suggests that the reaction has a large activation energy. At present, no molybdenum model complex exists which is capable of oxidizing SO_3^{2-}.

(b) Oxidation of Aldehydes (RCHO)

        The molybdenum enzymes xanthine oxidase/dehydrogenase and aldehyde oxidase catalyze the oxidation of aldehydes to acids (8,15). In addition, xanthine oxidase catalyzes the oxidation of xanthine to uric acid. Spence and Kroneck (156) initially reported that aldehydes (RCHO), unspecified, were oxidized in DMF by $Mo(VI)O_2(ethyl-L-cysteinate)_2$ to carboxylic acids (RCOOH). This reaction was stated to have occurred based only on the observed appearance during the reaction of a deep red-purple color characteristic of $Mo_2(V)O_3(ethyl-L-cysteinate)_2$. The reaction was reinvestigated in greater detail in two laboratories. Garner et al. (154) indicated that the reaction product of benzaldehyde with $Mo(VI)O_2(ethyl-L-cysteinate)_2$ was not benzoic acid but diethylcystine, formed by oxidation of partially displaced ligand by intact complex (with

intermediate formation of $Mo_2(V)O_3(ethyl-L-cysteinate)_2$).
Miller and Wentworth (157) shortly thereafter reported that
the product of this reaction was neither a benzoic acid or
diethylcystine but a thiazolidine, formed by condensation of
the aldehyde with partially displaced ethyl-L-cysteinate
ligand. In other work, Speier (158) reported on the cata-
lytic aerial oxidation of benzaldehyde to benzoic acid in
the presence of $Mo(VI)O_2(ethyl-L-cysteinate)_2$, however the
exact role of the molybdenum species was not reported.
Although there are apparent contradictions in these results,
it is unlikely that $Mo(VI)O_2(ethyl-L-cysteinate)_2$ oxidizes
aldehydes. Attempts to effect this reaction with other
molybdenum(VI) model compounds have also been unsuccessful
(103). Presently, there are no reports of molybdenum(VI)
complexes which are capable of oxidizing xanthine or other
purines.

(c) Oxidation of Organophosphines (PR_3)

The most thoroughly investigated oxygen atom transfer
reaction involving synthetic $Mo(VI)O_2L_n$ complexes is that
involving organophosphines (PR_3) as reductants (reaction
(9)):

$$Mo(VI)O_2L_n + PR_3 \xrightarrow{k_1} Mo(IV)OL_n + OPR_3 \qquad (9)$$
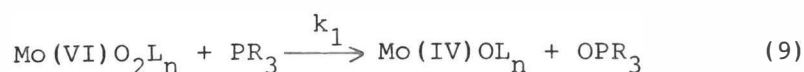
The following equilibrium (reaction (10)) is frequently encountered along with reaction (9)

$$\text{Mo(VI)O}_2\text{L}_n + \text{Mo(IV)OL}_n \; \overset{k_2}{\underset{k_{-2}}{\rightleftharpoons}} \; \text{Mo(V)O}_3\text{L}_{2n} \qquad (10)$$
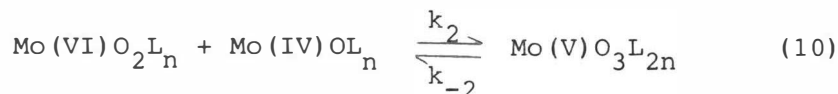
Barral et al. (159) initially observed these types of oxygen atom transfer reactions with $\text{Mo(VI)O}_2\text{L}_n$ (L = dialkyldithiocarbamate), in their development of a system for the catalytic oxidation of triphenylphosphine (PPh_3) with dioxygen. Although organophosphines are not biologi- cally realistic substrates, research on reactions of this type have provided new synthetic routes to oxomolybde- num(V)-(IV) complexes (82,95,126,160-162), kinetic data (94,100,159,163-170), and insights into catalytic systems (159,165) which may be relevant to the enzymes.

2. Synthesis of Oxomolybdenum(V)-(IV) Complexes via Oxygen Atom Transfer Reactions with Organophosphines (PR_3)

Chen et al. (95) have utilized the oxygen atom transfer reactions (9) and (10) as a convenient method for the syntheses of a variety of oxomolybdenum(V), and -(IV) complexes. These workers found that the products obtained in the oxygen atom transfer reaction between several $\text{Mo(VI)O}_2\text{L}_2$ (L = bidentate chelate) and PR_3 (R = phenyl or alkyl) were dependent on the type of ligand involved, i.e., the type of ligand dictated whether reduction would proceed

to $Mo_2(V)O_3L_4$ or $Mo(IV)OL_2$ complexes. For example, when L = methyl-L-cysteinate (cyst-OMe), 8-hydroxyquinoline (ox), and acetylacetone (acac), reduction yielded only the $Mo_2(V)O_3L_4$ complex, even under conditions of excess phosphine. On the other hand, with L = dialkyldithiocarbamate (S_2CNR_2) and dithiophosphinate (S_2PR_2), reduction proceeded to the $Mo(IV)OL_2$ complex under mild conditions. The different reduction behavior exhibited by these two groups of ligands can be explained by the fact that for the former group of ligands, (L = cyst-OMe, ox, acac) the $Mo_2(V)O_3L_4$ complexes do not dissociate (i.e., the visible spectral band at ~ 525 nm obeys Beer's law) which indicates that the equilibrium in reaction (10) lies far to the right. However, for L = S_2CNR_2 and S_2PR_2 Beer's law is not obeyed with the result being that $Mo_2(V)O_3L_4$ is dissociated and exists predominantly as $Mo(VI)O_2L_2$ and $Mo(IV)OL_2$. Analogous results have been obtained by Hyde et al. (161) in their syntheses of oxomolybdenum(IV) thioxanthate complexes, $Mo(IV)O(S_2CSR)_2$ (R = $i-C_3H_7$ and $t-C_4H_9$).

Chen et al. (162) have also reported that a novel atom transfer reaction occurs between $Mo(VI)O_2(acac)_2$ and $Mo(IV)Cl_2(acac)_2$. Instead of obtaining the products expected from a simple oxygen atom transfer (i.e., $Mo(IV)O(acac)_2$ and $Mo(VI)OCl_2(acac)_2$), two moles of the monomeric $Mo(V)OCl(acac)_2$ complex were isolated as shown in equation (11).

$$Mo(VI)O_2(acac)_2 + Mo(IV)Cl_2(acac)_2 \rightarrow 2Mo(VI)OCl(acac)_2 \quad (11)$$

This reaction was unique in that it represented the first reported oxygen-chlorine atom exchange between two different molybdenum complexes. $Mo(V)OCl(acac)_2$ has proven to be very valuable in the synthesis of monomeric molybdenum(V) complexes where facile ligand exchange of $acac^-$ can occur to yield complexes of the type $Mo(V)OClL$, where L = bi-, tri or tetradentate ligands (126,162).

Boyd and Spence (82) have examined the products of the oxo-transfer reaction of $Mo(VI)O_2(mpe)$, (mpe = N,N'-bis(2-mercapto-2-methylpropyl)-ethylenediamine) and $Mo(VI)-O_2(mee)$, (mee = N,N'-bis(2-mercaptoethyl)-ethylenediamine) with ethyldiphenylphosphine, $(PEtPh_2)$. Even though the ligands and oxomolybdenum(VI) complexes are similar, the reduction products were found to be different. While the reduction proceeded successfully in the synthesis of $Mo(IV)O(mpe)$, only the μ-oxo$Mo_2(V)O_3(mee)_2$ dimer was obtained from $Mo(VI)O_2(mee)$. The authors speculated that the different reduction products obtained from the two similar oxomolybdenum(VI) complexes were probably a result of a steric effect associated with the methyl groups on the carbon atoms adjacent to the sulfur donors in mpe. These methyl groups would interact sterically in the μ-oxo dimer, $Mo_2(V)O_3(mpe)_2$, thus destabilizing it and shifting the equilibrium to the left in reaction (10). These results suggest that the synthesis of oxomolybdenum(IV) complexes

by oxo abstraction can be successful if bulky ligands are used to prevent molybdenum(V) dimer formation.

Recently, Berg and Holm (126) reported on the reactivity of cis-dioxomolybdenum(VI) tridentate complexes, $Mo(VI)O_2(LNO_2)$, $(L'NO_2 = 2,6-bis(2,2-diphenyl-2-hydroxy-ethyl)pyridine)$, and $Mo(VI)O_2(L'NS_2)$, $(LNS_2 = 2,6-bis(2,2-diphenyl-2-mercaptoethanyl)pyridine)$ with PPh_3. There being no evident basis for the suppression of reaction (10) by manipulation of electronic factors, these complexes were designed to prevent formation of μ-oxomolybdenum(V) dimers based on steric constraints (i.e., phenyl groups adjacent to sulfur donor atoms). On reaction of $Mo(VI)O_2(LNS_2)$ with PPh_3 only the desired $Mo(IV)O(LNS_2)$ complex was obtained. No reaction occurred with $Mo(VI)O_2(LNO_2)$. Results obtained in their study were consistent with a previous report by Topich and Lyon (168).

Boyd and Spence (82) have also reported the syntheses of tridentate Schiff base oxomolybdenum(IV) complexes, $Mo(IV)O(5-H-SSP)$ and $Mo(IV)O(5-H-SAP)$ from the corresponding oxomolybdenum(VI) complexes and $PEtPh_2$. Apparently the equilibrium reaction (10) does not occur at all during the syntheses of these complexes (based on kinetic results obtained by Topich and Lyon (166-168) described in (Chapter V).

Results and Discussion

Using a procedure similar to that described by Boyd

and Spence (82) we have prepared the oxomolybdenum(IV) complexes Mo(IV)O(5-H-SSP)(DMF) and Mo(IV)O(5-H-SSE). These complexes were synthesized by reacting one equivalent of Mo(VI)O$_2$(5-H-SSP) or Mo(VI)O$_2$(5-H-SSE) with 2-3 equivalents of PEtPh$_2$ in a mixed solvent system, DMF/CH$_3$CN, at room temperature. Each reaction was performed under strictly anaerobic conditions. The complexes were characterized by IR and UV-visible spectroscopy.

The IR spectra for Mo(IV)O(5-H-SSP) and Mo(IV)O(5-H-SSE) were obtained as KBr disks and are shown in Figures 13 and 14, respectively. Each of these complexes in addition to ligand vibrations exhibit ν(Mo=O) bands at ~ 957 cm^{-1} which are in agreement with previously reported values for other oxomolybdenum(IV) complexes (Table 11). In addition, we find that one of the complexes, Mo(IV)O(5-H-SSP)(DMF), contains DMF coordinated to the complex in the solid state. Bands attributed to DMF are located at ~ 1650 cm^{-1}. There was no evidence for DMF coordination for Mo(IV)O(5-H-SSE) in the solid state.

The UV-visible spectra for Mo(IV)O(5-H-SSP)(DMF) and Mo(IV)O(5-H-SSE) were recorded in DMF between 650 and 300 nm. The spectrum of Mo(IV)O(5-H-SSP) (Figure 15) consists of an intense band λ_{max} = 465 nm (ϵ = 10,000 M^{-1} cm^{-1}) and a shoulder at 320 nm. Identical results were reported previously for Mo(IV)O(5-H-SSP) as prepared by Boyd and Spence (82). The spectrum of Mo(IV)O(5-H-SSE) (Figure 16) exhibits an absorption band at λ_{max} = 475 nm (ϵ = 7554

Figure 13. Infrared spectrum of Mo(IV)O(5-H-SSP) (KBr
            disk).

WAVENUMBER(CM⁻¹)
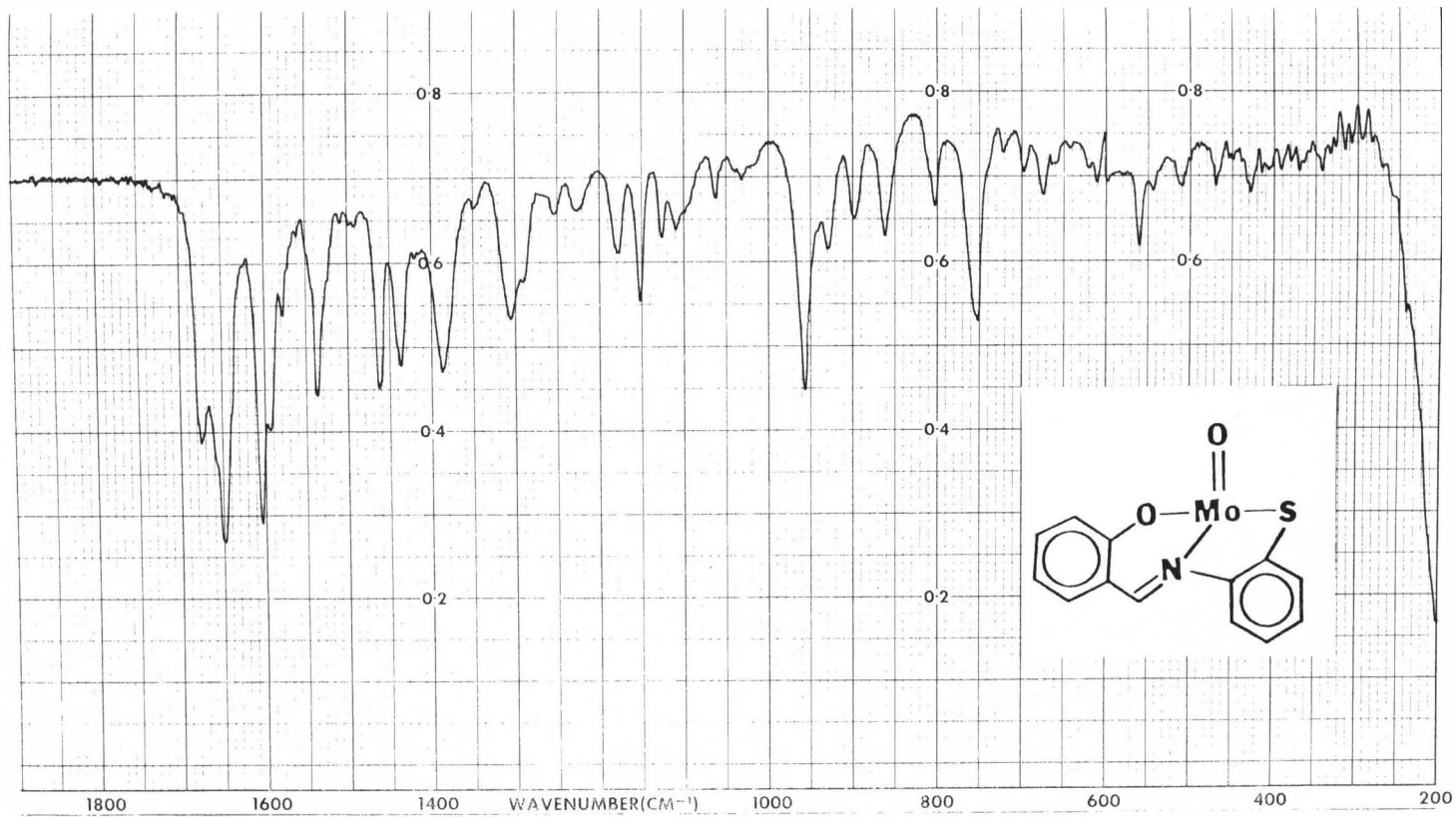
Figure 14.   Infrared spectrum of Mo(IV)O(5-H-SSE) (KBr disk).
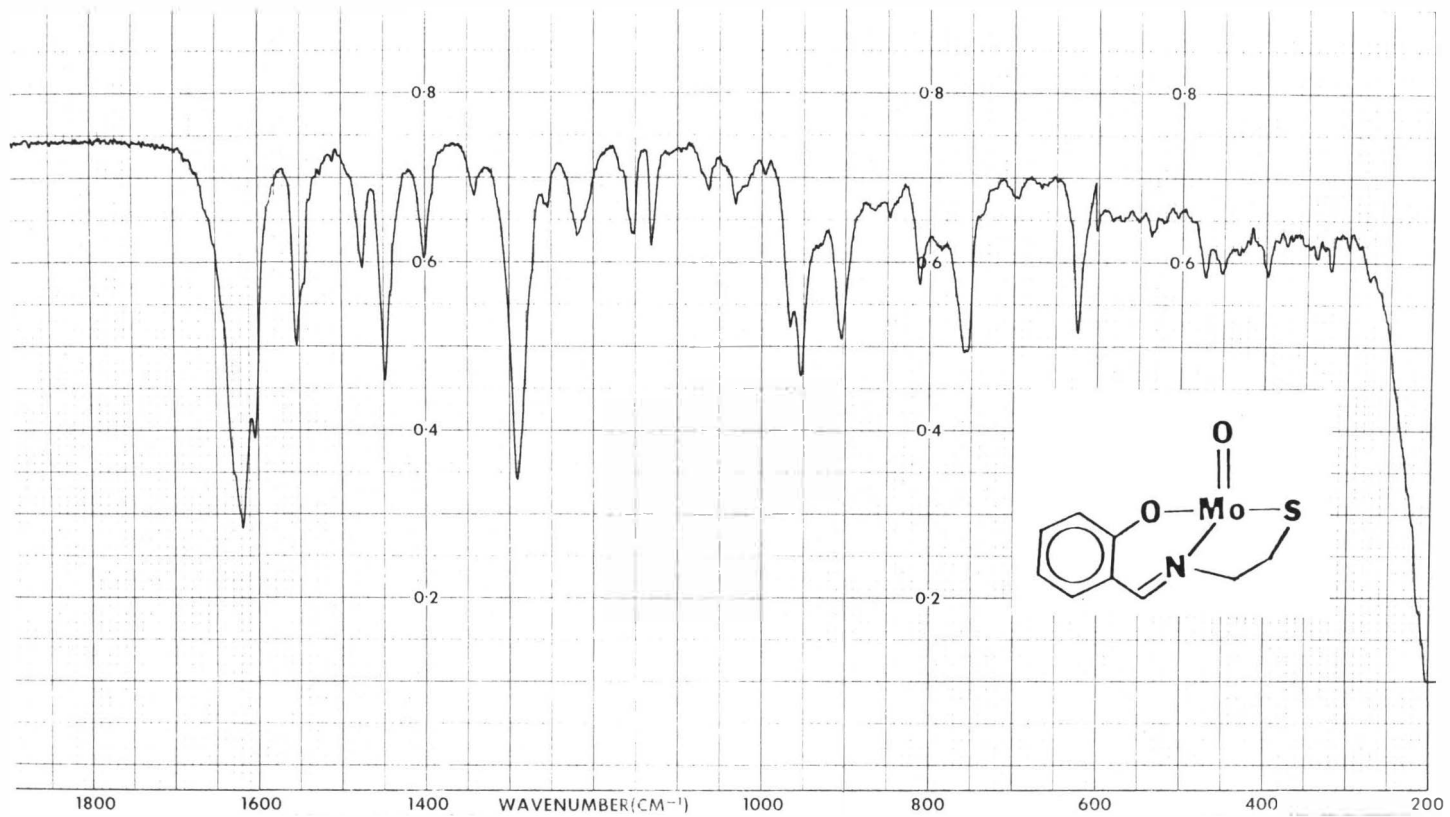
Table 11. Physical Properties of Selected Oxomolybdenum(IV) Complexes

Complex	Infrared absorption ν (Mo=O), cm^{-1}	Absorption maxima, nm (ε, M^{-1}cm^{-1})	Reference
MoO(Et$_2$dtc)$_2$	962	746, 592, 520 388, 313	2
MoO(i-C$_3$H$_7$xan)$_2$	975	518 (355), 395 (1479) 321 (26,915), 289 (19,498)	169
MoO(mpe)	950	368 (3243)	82
MoO(LNS$_2$)(DMF)	945	735 (1174), 529 (6309), 365 (5888)	126

Figure 15.   UV-visible spectrum of Mo(IV)O(5-H-SSP) in DMF.
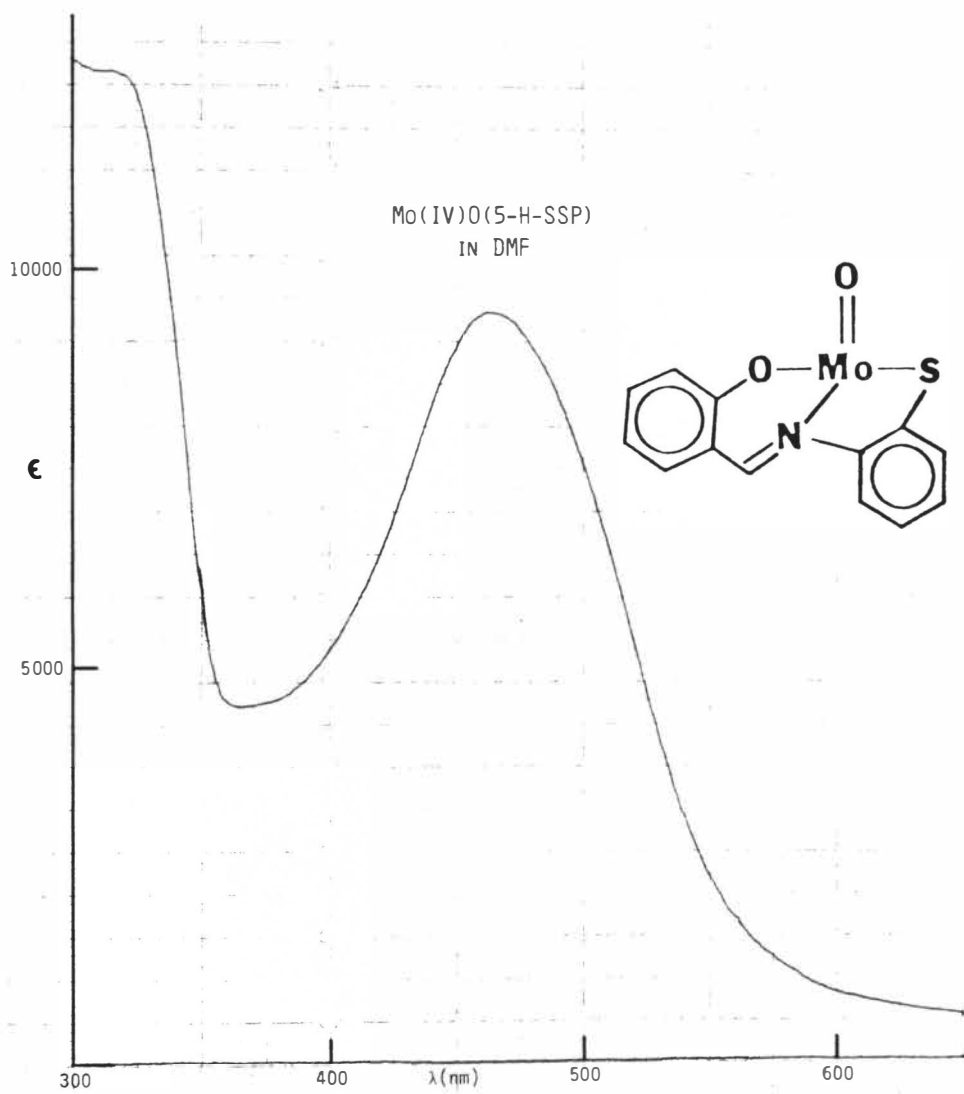
Mo(IV)O(5-H-SSP)
IN DMF

Figure 16. UV-visible spectrum of Mo(IV)O(5-H-SSE) in DMF.

Mo(IV)O(5-H-SSE)
IN DMF
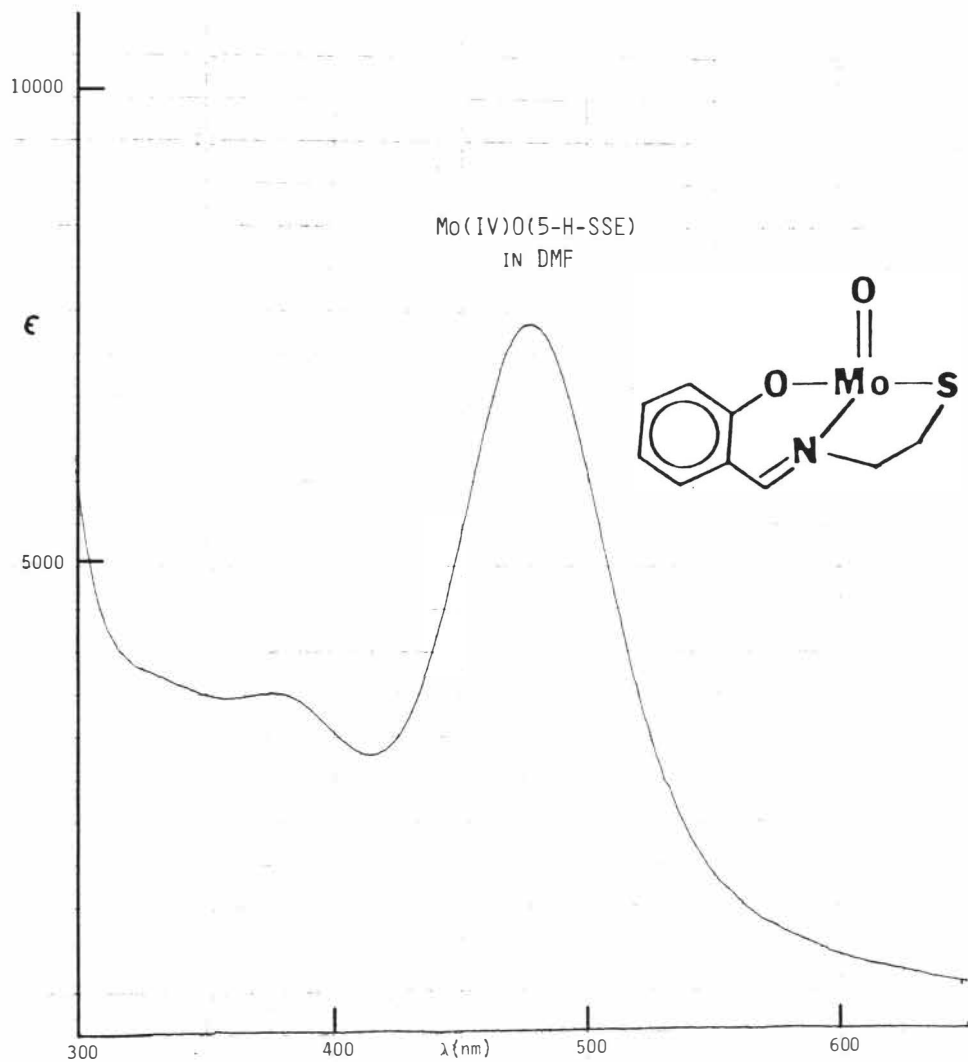
$M^{-1}cm^{-1}$) and a shoulder at ~ 377 nm. UV-visible spectral data for other oxomolybdenum(IV) thiolate complexes often contain intense absorptions in the visible region (Table 11) and both d-d transitions and charge transfer bands are expected. However, detailed assignments of bands for many oxomolybdenum(IV) complexes have been complicated due to the fact that many of these species contain unsaturated ligands whose internal electronic transitions and charge transfer properties induce complex spectra (171).

V. KINETICS OF OXYGEN ATOM TRANSFER TO ORGANOPHOSPHINES

Introduction

The kinetics of oxygen atom transfer reactions (9) and (10) have been examined in some detail for a variety of $Mo(VI)O_2L_n$ complexes with those containing $L = S_2CNR_2$ receiving the most attention.

Barral et al. (159) have reported on the oxidation of PPh_3 by $Mo(VI)O_2(S_2CNPr_2)_2$ in o-dichlorobenzene. At 41°C, the specific rate constant and equilibrium constant were found to be $k_1 = 2.3$ $M^{-1}s^{-1}$ and $K = 4.3 \times 10^3$ M^{-1}, respectively. In addition, it was found that upon introduction of dioxygen into the system, $Mo(IV)O(S_2CNPr_2)_2$ was converted back to $Mo(VI)O_2(S_2CNPr_2)_2$, thus demonstrating that these complexes were capable of catalyzing the aerial oxidation of tertiary phosphines into the corresponding phosphine oxides by dioxygen. The catalytic sequence is depicted in reaction (12).

$$PPh_3 \qquad\qquad OPPh_3$$
$$\overset{k_1}{\searrow}$$
$$Mo(VI)O_2(S_2CNPr_2)_2 + Mo(IV)O(S_2CNPr_2)_2 \overset{K}{\rightleftharpoons} Mo_2(V)O_3(S_2CNPr_2)_4$$
$$\overset{k}{\underset{\tfrac{1}{2}O_2}{\rule{0pt}{0pt}}} \tag{12}$$

McDonald and Schulman (94) have reported that reduction of excess $Mo(VI)O_2(S_2CNEt_2)_2$ by PPh_3 in benzene provided an analytical method for the detection of small amounts of PPh_3. Their procedure was based on the spectrophotometric assessment of the amount of $Mo_2(V)O_3(S_2CNEt_2)_4$ formed as a result of reaction (10). They reported a specific rate constant for this oxidation at 24°C of 0.12 $M^{-1}s^{-1}$. The result of this study led Durant et al. (100) to investigate the oxygen atom transfer kinetic behavior of $Mo(VI)O_2(S_2CNEt_2)_2$ with a greater than tenfold excess of PPh_3 in CH_3CN. At 25°C they reported a specific rate constant of 1.1 $M^{-1}s^{-1}$, $\Delta H^{\ddagger} = 35.2$ kJ-mol^{-1}, and $\Delta S^{\ddagger} = -126$ J-(mol-K)$^{-1}$. It was assumed in this study that under conditions of excess PPh_3 the $Mo(VI)O_2(S_2CNEt_2)_2$ complex was quantitatively reduced to the $Mo(IV)O(S_2CNEt_2)_2$ species. This assumption was based solely on qualitative examination that a minimal spectral absorbance due to $Mo_2(V)O_3(S_2CNEt_2)_4$ occurred.

Deli and Speier (163) have examined the oxidation of PPh_3 by $Mo(VI)O_2(ethyl-L-cysteinate)_2$ in benzene. These authors assumed that the rate of formation of $Mo_2(V)O_3$-(ethyl-L-cysteinate)$_4$ was rapid compared to the rate of oxo abstraction to PPh_3 to produce $Mo(IV)O(ethyl-L-cysteinate)_2$. At 35°C they reported a specific rate constant $k_1 = 2.95 \times 10^{-4}$ $M^{-1}s^{-1}$, $\Delta H^{\ddagger} = 46$ kJ-mol^{-1} and $\Delta S^{\ddagger} = -153$ J-(mol-K)$^{-1}$.

Recently, Berg and Holm (125) reported a kinetic study on the reaction of $Mo(VI)O_2(L'NS_2)$ with PPh_3 in DMF at 23°C. $Mo(VI)O_2(L'NS_2)$ was designed with bulky ligands to suppress μ-oxomolybdenum(V) dimer formation. The reaction of $Mo(VI)O_2(L'NS_2)$ with PPh_3 was monitored spectrophotometrically and the specific rate constant for this reaction k_1 was found to be 7 (±1) x 10^{-3} $M^{-1}s^{-1}$.

There are only a few reports which address specifically the kinetics associated with reaction (10). Matsuda et al. (170) have reported a kinetic study on the disproportionation of $Mo_2(V)O_3(S_2CNEt_2)_4$ (reaction (13)) by the concentration-jump relaxation technique.

$$Mo_2(V)O_3(S_2CNEt_2)_4 \underset{k_{-2}}{\overset{k_2}{\rightleftharpoons}} Mo(VI)O_2(S_2CNEt_2)_2 + \qquad (13)$$

$$Mo(IV)O(S_2CNEt_2)_2$$
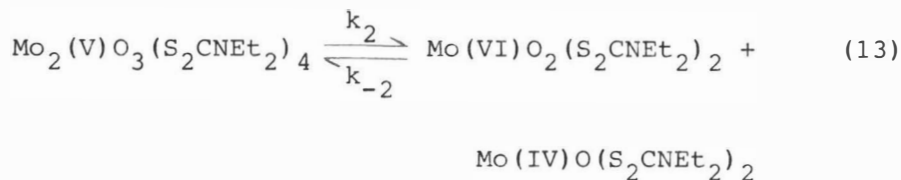
In dichloromethane at 25°C the rate constants for the disproportionation reaction (k_2 = 2.93 (±0.29) s^{-1}) and coupling reaction (k_{-2} = 14.7 (±0.2) x 10^2 $M^{-1}s^{-1}$) in addition to the equilibrium constant (K = 2.0 (±0.2) x 10^{-3} M) were determined.

Durant et al. (100) reported that the value for the specific rate constant in the reaction of $Mo(VI)O_2-(S_2CNEt_2)_2$ with PPh_3 was k_1 = 1.1 $M^{-1}s^{-1}$. The rate constant for this reaction is smaller by three orders of

magnitude than that found by Matsuda et al. (170) for the coupling reaction (13) where k_{-2} = 14.7 x 10^2 $M^{-1}s^{-1}$. The value of the rate constant as reported by Durant et al. (100) is too large because the $Mo(IV)O(S_2CNEt_2)_2$ formed in the oxo abstraction by PPh_3 is rapidly consumed according to reaction (10).

Similar results have been obtained by Miyake et al. (169) in their kinetic study on the disproportionation of μ-oxo-bis[bis(isopropylthioxanthato)oxomolybdenum(V)], $Mo_2(V)O_3(S_2CSPr_i)_4$, reaction (14).

$$Mo_2(V)O_3(S_2CSPr_i)_4 \underset{k_{-1}}{\overset{k_1}{\rightleftarrows}} Mo(IV)O(S_2CSPr_i)_2 + Mo(VI)O_2(S_2CSPr_i)_2$$

$$\text{(14)}$$
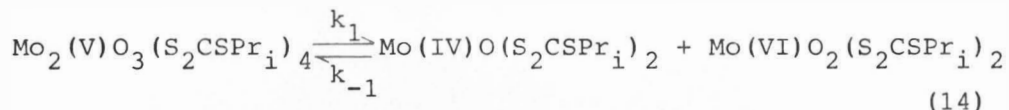
The value for the equilibrium constant (K = 3.81 ± 1.70 x 10^{-4} M) for this reaction is smaller than that found for $Mo_2(V)O_3(S_2CNEt_2)_4$ (K = 2.0 ± 0.2 x 10^{-3} M) (170). This difference was explained on the basis that the thioxanthate ligand is a weaker donor compared to the dithiocarbamate ligand. This effect results from the fact that thioxanthate donates less electron density into the antibonding Mo-O-Mo π orbitals, thus $Mo_2(V)O_3(S_2CSPr_i)_4$ is more stable than $Mo_2(V)O_3(S_2CNEt_2)_4$ with respect to disproportionation.

The kinetic results discussed thus far provided valuable insights into the behavior of molybdenum complexes in oxo transfer reactions. However, examination of reported

specific rate constants (k_1) for reaction (9) under similar conditions (Table (12)) reveals that k_1 varies from 2.94 x 10^{-4} to 2.3 M^{-1} s^{-1}. This range of specific rate constants is too large to be ascribed solely to the differences in solvent, temperature, or R substituent.

Recently, Reynolds et al. (164) reported a detailed kinetic investigation for reactions (15) and (16) in an attempt to clear up some of the discrepancies in the previous kinetic results.

$$Mo(VI)O_2(S_2CNEt_2)_2 + PR_3 \xrightarrow{k_1} Mo(IV)O(S_2CNEt_2)_2 + OPR_3 \quad (15)$$

$$Mo(VI)O_2(S_2CNEt_2)_2 + Mo(IV)O(S_2CNEt_2)_2 \underset{k_{-2}}{\overset{k_2}{\rightleftharpoons}}$$

$$Mo_2(V)O_3(S_2CNEt_2)_4 \quad (16)$$
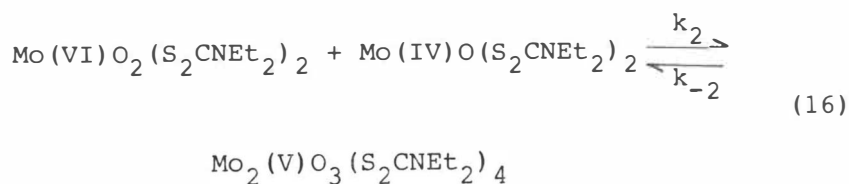
The kinetic treatment of these reactions differed from previous studies (94,100,159,163) in that it was assumed that the equilibrium reaction (16) at all points along the oxo transfer reaction coordinate was very rapid compared to the oxygen atom transfer process occurring in reaction (15) i.e., ($k_2 > k_1$). The specific rate constant for reaction (15) and the equilibrium constant for reaction (16) at 25°C in 1,2-dichloromethane were determined to be 0.071 $M^{-1}s^{-1}$

Table 12. Comparison of Kinetic Data for cis-Dioxomolybdenum(VI)
Complexes in Oxygen Atom Transfer Reactions

Molybdenum(VI) Complex	Solvent	Organophosphine	Temperature (°C)	$k_1 (M^{-1}s^{-1})$	Reference
$Mo(VI)O_2(S_2CNPr_2)_2$	$o-C_6H_4Cl_2$	PPh_3	41	2.3	159
$Mo(VI)O_2(S_2CNEt_2)_2$	C_6H_6	PPh_3	24	0.12	94
$Mo(VI)O_2(S_2CNeEt_2)_2$	CH_3CN	PPh_3	25	1.1	100
$Mo(VI)O_2(Et-L-cys)_2$	C_6H_6	PPh_3	35	2.9×10^{-4}	163

and 1.7×10^{-3} M, respectively. The value of the equilbrium constant is in agreement with that reported previously by Matsuda, $K = 2.0 \times 10^{-3}$ M (170). The results obtained by Reynolds et al. (164) were significant in that for the first time a proper interpretation of kinetic systems which exhibit dimerization reaction (10) was achieved. The demonstration that $Mo_2(V)O_3(S_2CNEt)_4$ is extensively dissociated except at initial commencement of the oxo transfer reaction suggests that previous kinetic results (94,100,159,163) may need reinterpretation.

Results and Discussion

Upon examining the available literature on kinetic treatments of oxygen atom transfer reactions involving cis-dioxomolybdenum(VI) complexes with organophosphines it became apparent that there were few reports concerning the effect of subtle variation in ligand structure on these redox reactions. Since both Mo(IV)O(5-H-SSP) (82) and Mo(IV)O(5-H-SSE) had been synthesized from the corresponding cis-dioxomolybdenum(VI) complexes it was decided to investigate these and other cis-dioxomolybdenum(VI) redox reactions in order to ascertain the effects of systematic variation in ligand structure on the rate of oxygen atom transfer. The following oxygen atom transfer reactions have been studied in detail:

$$\text{Mo(VI)O}_2\text{(5-X-SSP)} + \text{PEtPh}_2 \xrightarrow[\substack{30°\text{C} \\ \text{DMF}}]{k_1} \text{Mo(IV)O(5-X-SSP)} + \text{OPEtPh}_2$$

(17)

$$X = \text{Cl, Br, H, CH}_3\text{O}$$

$$\text{Mo(VI)O}_2\text{(5-X-SSE)} + \text{PEtPh}_2 \xrightarrow[\substack{60°\text{C} \\ \text{DMF}}]{k_1} \text{Mo(IV)O(5-X-SSE)} + \text{OPEtPh}_2$$

(18)
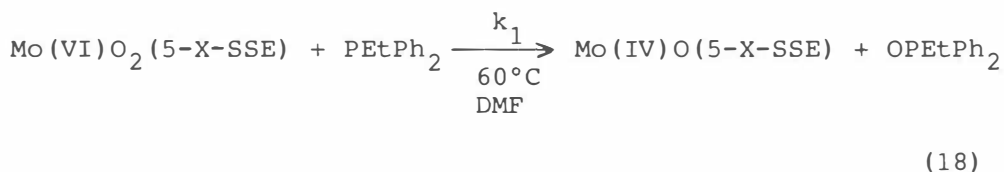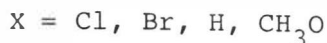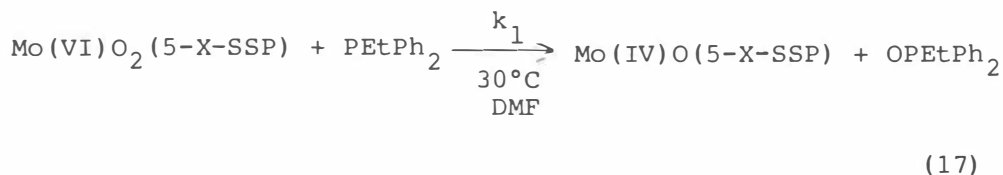
Some comment is necessary concerning the nature of the reduced molybdenum products in reactions (17) and (18). The discussion which follows should support our findings that during the course of these reactions only oxomolybdenum(IV) species are being produced as products without interference from the formation of μ-oxomolybdenum(V) dimers.

The first consideration is that reported UV-visible spectra for a variety of μ-oxomolybdenum(V) dimers usually exhibit electronic transitions above 470 nm (2). A distinctive feature in the electronic spectra of these dimers is the presence of an intense transition at λ = 525 nm with ε ~ 9,000 $M^{-1}cm^{-1}$. This electronic transition is insensitive to the nature of the ligand and is believed to be associated with a charge transfer transition that is localized in the Mo-O-Mo bridge. The electronic transition around 525 nm is

so characteristic of the μ-oxomolybdenum(V) dimer that serious doubts are raised as to its presence if this band is not observed. For reactions (17) and (18) no electronic transitions are observed that are characteristic of μ-oxo-molybdenum(V) dimers. Second, consider the following reaction sequence:

$$Mo(VI)O_2L_n + PR_3 \xrightarrow{k_1} Mo(IV)OL_n + OPR_3 \qquad (19)$$

$$Mo(VI)O_2L_n + Mo(IV)OL_n \xrightarrow{k_2} Mo_2(V)O_3L_{2n} \qquad (20)$$
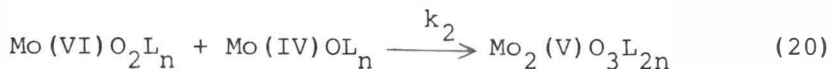
If $k_2 \gg k_1$, then $Mo(VI)O_2L_n$ would be consumed twice as fast as $Mo_2(V)O_3L_{2n}$ would appear even if reaction (19) were the rate-determining step. If $k_2 \ll k_1$ or reaction (20) does not proceed at all, the rate of the disappearance of $Mo(VI)O_2L_n$ would equal that of the appearance of the reduced $Mo(IV)OL_n$ species. Deli and Speier (163) have shown that for L = Et-L-cys, $k_2 \gg k_1$ with the result that $-d[Mo(VI)O_2-(Et-L-cys)_2]/dt = + 2d[Mo_2(V)O_3(Et-L-cys)_4)]/dt$ in which case the μ-oxomolybdenum(V) dimer is being formed rapidly via the oxo abstraction reaction and subsequent dimer formation. For each of the complexes examined in the two series $Mo(VI)O_2(5-X-SSP)$ and $Mo(VI)O_2(5-X-SSE)$ the rate of decrease of the cis-dioxomolybdenum(VI) species was found to equal the rate of appearance of the oxomolybdenum(IV)

species. Third, Boyd and Spence (82) have described the electronic spectrum of the Mo(IV)O(5-H-SSP) complex and they report λ_{max} = 465 nm (ϵ = 10,000 $M^{-1}cm^{-1}$) which is identical to what is observed for the product in the reaction of Mo(VI)O$_2$(5-H-SSP) with PEtPh$_2$. We have repeated their work (Figure 15) and obtained analogous results. In addition, we have independently synthesized the Mo(IV)O(5-H-SSE) complex and obtained its electronic absorption spectrum which is shown in Figure 16. The absorption λ_{max} = 475 nm (ϵ = 7554 $M^{-1}cm^{-1}$) is also identical to what is observed in the reaction of Mo(VI)O$_2$(5-H-SSE) with PEtPh$_2$.

Finally, examination of spectral traces obtained during the course of reactions (17) and (18) (see Figures 17 and 18 for X = H) reveal the presence of well defined isosbestic points in all instances. Usually the appearance of isosbestic points is taken as an indication that only two absorbing species are present in solution, however the existence of isosbestic points alone does not rule out the possibly that other shortlived absorbing species may also be present (172). Shalhoub et al. (173) have indicated that if an absorbing species is present at a low concentration and is equilibrated rapidly relative to the rate of reaction, isosbestic points will still be maintained. Therefore, the appearance of isosbestic points in the spectral traces obtained from reactions (17) and (18) in themselves do not eliminate the possibility that μ-oxomolybdenum(V) dimers are being formed during the course of these reactions. However,

there occurrence taken together with the previously discussed evidence strongly suggests that only oxomolybdenum(IV) species are produced as products of reactions (17) and (18) and that μ-oxomolybdenum(V) dimers are not being formed.

Kinetic Measurements on the Oxygen Atom Transfer Reactions of Mo(VI)O$_2$(5-X-SSP) and Mo(VI)O$_2$(5-X-SSE) (X = Cl, Br, H, CH$_3$O with PEtPh$_2$

All manipulations associated with the kinetic measurements of the reactivity of Mo(VI)O$_2$(5-X-SSP) and Mo(VI)O$_2$-(5-X-SSE) with PEtPh$_2$, reactions (17) and (18), in DMF were carried out under a dinitrogen atmosphere. Pseudo-first-order conditions were used to study these reactions. A greater than 10-fold excess of PEtPh$_2$ was maintained over the concentration of the cis-dioxomolybdenum(VI) complexes ($\sim 10^{-3}$ M). The kinetics for the reaction of the Mo(VI)O$_2$-(5-X-SSP) series with PEtPh$_2$ was examined at 30°C and that of Mo(VI)O$_2$(5-X-SSE) at 60°C. The reason being that the Mo(VI)O$_2$(5-X-SSE) reaction at 30°C is too slow to be conveniently followed. The reactant solutions were thermostated to within $\pm$ 0.1°C in water jacketed cells (1 mm pathlength).

A qualitative examination of reactions (17) and (18) indicated that they could be followed spectrophotometrically by observing changes in their optical spectra. Figures 17 and 18 are spectral traces obtained for the reaction of

Figure 17.   Spectral changes observed during the reaction
of $Mo(VI)O_2$(5-H-SSP) with $PEtPh_2$ in DMF.   The
initial $Mo(VI)O_2$(5-H-SSP) and $PEtPh_2$ concentra-
tions were 3.12×10^{-3} and 3.12×10^{-1} M,
respectively.   Spectra were recorded at 30°C at
30 minute intervals.

Mo(VI)O$_2$(5-H-SSP) + PEtPh$_2$ $\longrightarrow$

Mo(IV)O(5-H-SSP) + OPEtPh$_2$
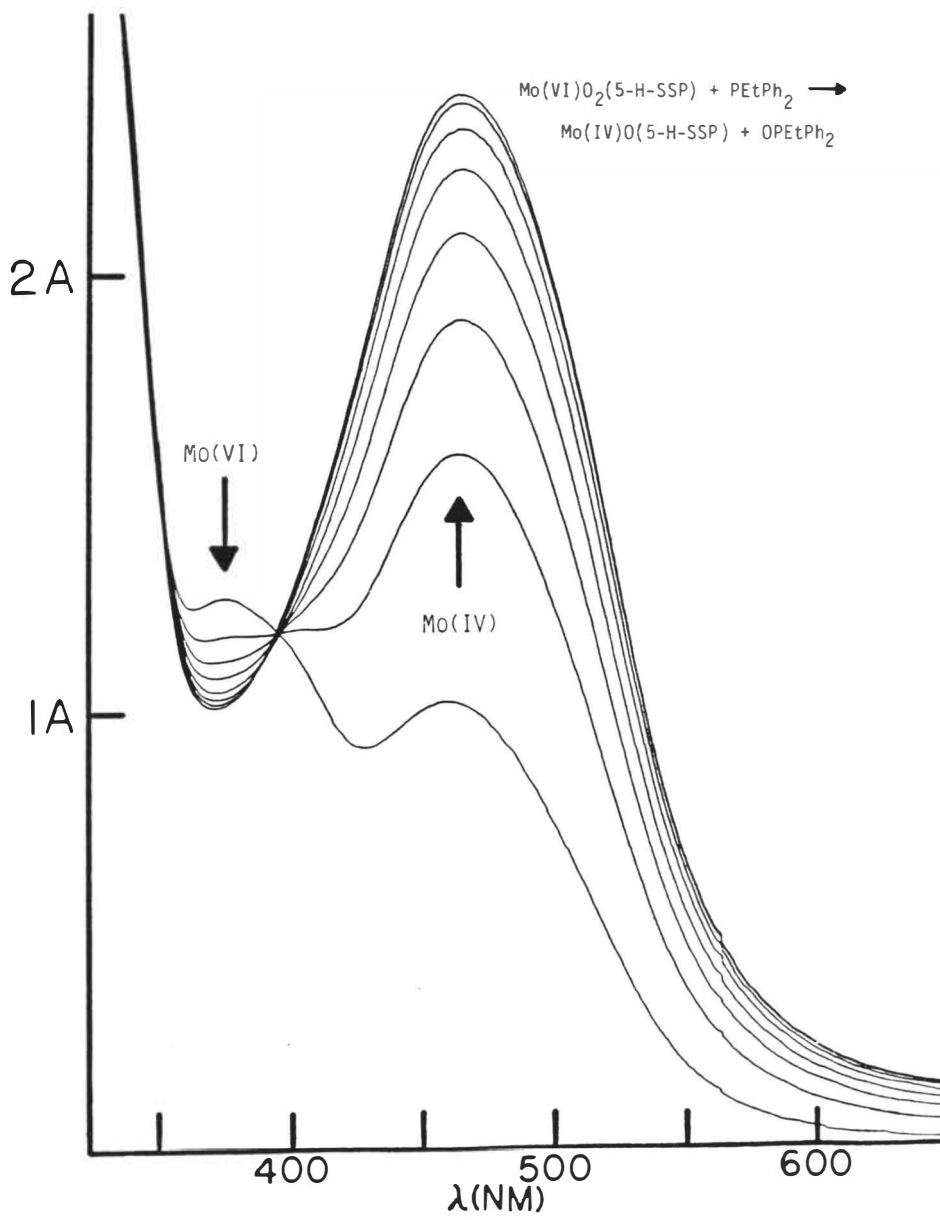
Figure 18. Spectral changes observed during the reaction of Mo(VI)O$_2$(5-H-SSE) with PEtPh$_2$ in DMF. The initial Mo(VI)O$_2$(5-H-SSE) and PEtPh$_2$ concentrations were 2.83 x 10^{-3} and 2.83 x 10^{-1} M, respectively. Spectra were recorded at 60°C at 15 minute intervals.

Mo(VI)O$_2$(5-H-SSE) + PEtPh$_2$ $\longrightarrow$

Mo(IV)O(5-H-SSE) + OPEtPh$_2$

Mo(VI)

IA

Mo(IV)

300   400   500   600

λ (nm)
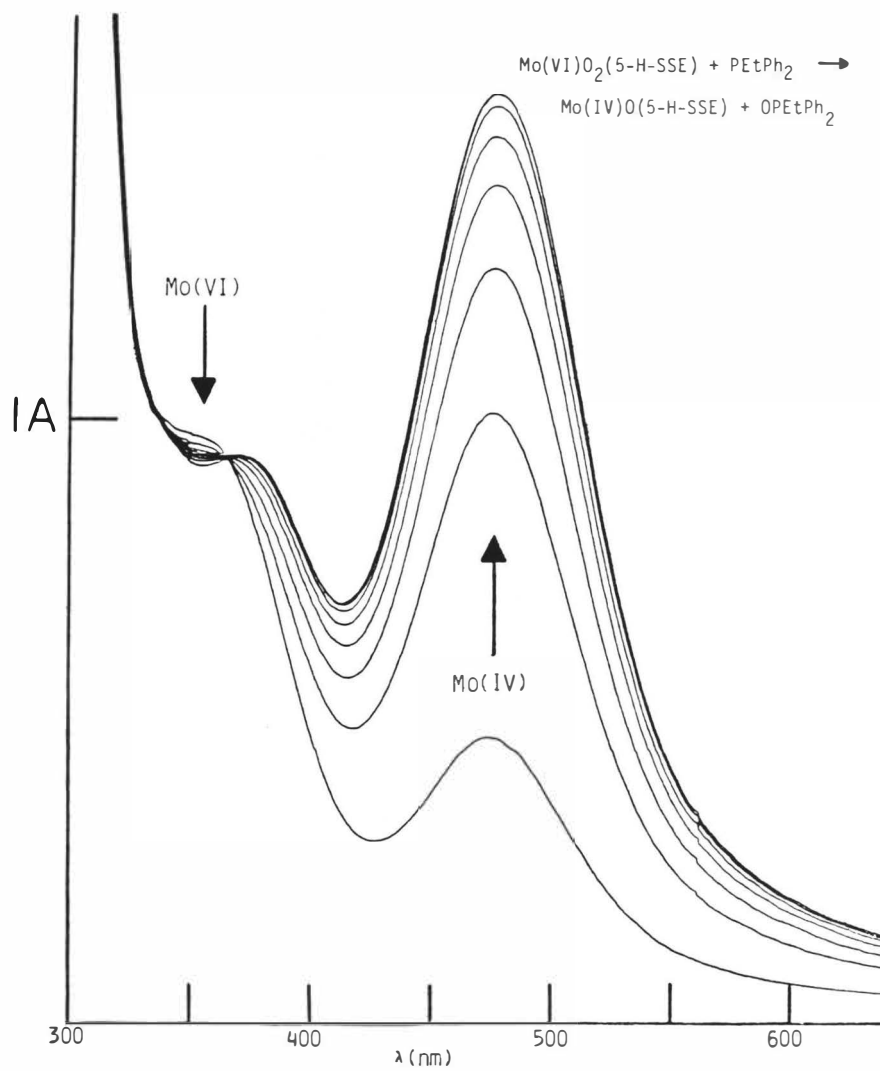
Mo(VI)O$_2$(5-H-SSP) and Mo(VI)O$_2$(5-H-SSE) with PEtPh$_2$ at 30° and 60°C respectively. Similar results were obtained for the other cis-dioxomolybdenum(VI) complexes which belong to these two series. In each experiment spectra were recorded for several hours at 15 to 30 minute intervals between 650 and 300 nm. The progress of reactions (17) and (18) were monitored by observing changes in the absorbance of the oxomolybdenum(IV) complexes at λ_{max} ~ 465 nm for the Mo(IV)O(5-X-SSP) series or λ_{max} ~ 475 nm for the Mo(IV)O(5-X-SSE) series (Figures 17 and 18). The observed first order rate constants (k_{obs}) were determined from the slopes of plots of ln(A$_\infty$-A$_t$) versus time for the two series of complexes. A$_t$ is the optical density at time t. A$_\infty$ was determined as the optical density when the final two spectral traces overlapped. Figure 19 shows a plot of ln(A$_\infty$-A$_t$)$_{465nm}$ versus time for the appearance of Mo(IV)O(5-H-SSP) at 30°C which is representative of the type of plots obtained for the other members of the Mo(VI)O$_2$(5-X-SSP) series reacting with PEtPh$_2$. Analogous plots of ln(A$_\infty$-A$_t$)$_{475\ nm}$ versus time were obtained for the appearance of the Mo(IV)O(5-X-SSE) species at 60°C.

Plots of ln(A$_\infty$-A$_t$) versus time for the appearance of the oxomolybdenum(IV) species in reactions (17) and (18) were generally linear to > 90% completion of the reactions indicating a first order dependence on the concentration of the cis-dioxomolybdenum(VI) complexes in each series. Observed first order rate constants (k_{obs}) were determined

Figure 19. Plot of $\ln(A_\infty - A_t)_{465nm}$ versus time for the appearance of Mo(IV)O(5-H-SSP) at 30°C.

$$Mo(VI)O_2(5\text{-}H\text{-}SSP) + PEtPh_2 \xrightarrow{k_1} Mo(IV)O(5\text{-}H\text{-}SSP) + OPEtPh_2$$

$$rate = k_{obs}\left[Mo(VI)O_2L\right]$$

Time (sec x 10^{-3})
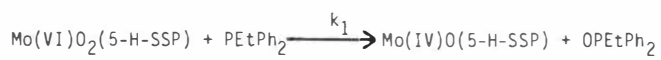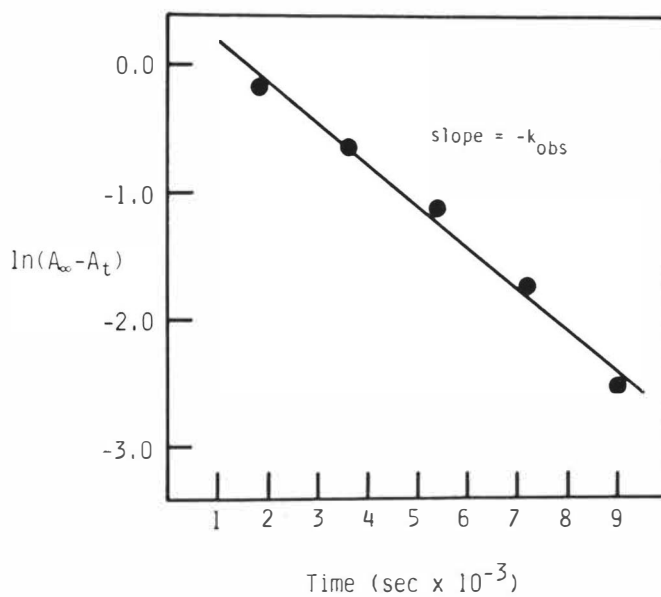
by a least squares analysis of these plots with experiments being performed at least three times for each molybdenum complex studied.

The order of the reaction with respect to $PEtPh_2$ was determined by noting the dependence of k_{obs} on $[PEtPh_2]$. Since these reactions are slow, only the X = Cl complex was examined in the $Mo(VI)O_2(5-X-SSP)$ and $Mo(VI)O_2(5-X-SSE)$ series under conditions of varying $PEtPh_2$ concentrations. Experiments were carried out at 30°C for the $Mo(VI)O_2(5-Cl-SSP)$ complex and 60°C for the $Mo(VI)O_2(5-Cl-SSE)$ complex with the concentration of $PEtPh_2$ being varied at 25, 50 and 100-fold molar excess over the cis-dioxomolybdenum(VI) complex concentration. The dependence of k_{obs} on $[PEtPh_2]$ for $Mo(VI)O_2(5-Cl-SSP)$ is shown in Figure 20. The fit of the data obtained in this plot with y-intercept equal to zero established that the reaction of $Mo(VI)O_2(5-Cl-SSP)$ with $PEtPh_2$ was first order in $PEtPh_2$. An analogous result was obtained in a plot of k_{obs} versus varying concentration of $PEtPh_2$ for $Mo(VI)O_2(5-Cl-SSE)$. Thus these reactions can be considered second order overall and the rate law may be formulated as:

$$\frac{-d[Mo(VI)O_2L]}{dt} = \frac{+d[Mo(IV)OL]}{dt} = k_1[Mo(VI)O_2L][PEtPh_2]$$

$$L = 5-X-SSP \text{ or } 5-X-SSE$$

$$X = H, Cl, Br, CH_3O$$

Figure 20.   Variation of k_{obs} versus [PEtPh$_2$] for the reac-
tion of Mo(VI)O$_2$(5-Cl-SSP) with PEtPh$_2$.
Concentration of PEtPh$_2$ was varied at 25, 50,
and 100-fold molar excess over the
Mo(VI)O$_2$(5-Cl-SSP) concentration.

$$\text{Mo(VI)O}_2\text{(5-Cl-SSP)} + \text{PEtPh}_2 \xrightarrow{\ k_1\ } \text{Mo(IV)O(5-Cl-SSP)} + \text{PEtPh}_2$$

$$k_{obs} = k_1 \left[\text{PEtPh}_2\right]$$
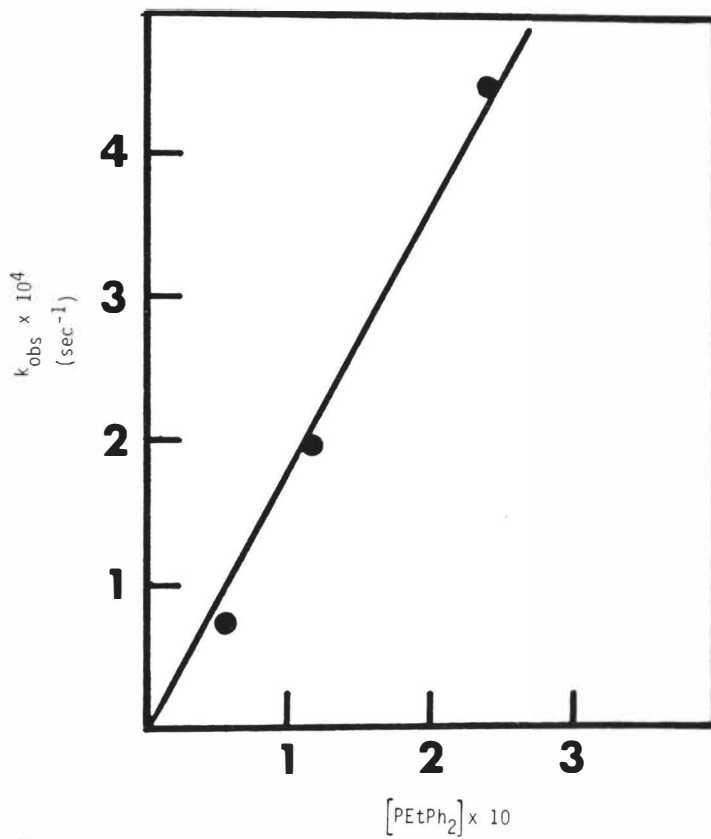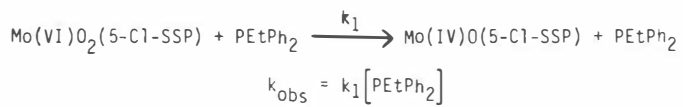
Specific rate constants (k_1) for the two series of
complexes $Mo(VI)O_2(5-X-SSP)$ and $Mo(VI)O_2(5-X-SSE)$ were
determined from the relationship, $k_1 = k_{obs}/[PEtPh_2]$. The
specific rate constants are listed in Table 13. Note that
the k_1's for $Mo(VI)O_2(5-X-SSP)$ were obtained at 30°C while
those for $Mo(VI)O_2(5-X-SSE)$ were obtained at 60°C. Although
$Mo(IV)O(5-H-SAP)$ has been synthesized (82) under refluxing
conditions in DMF/CH_3CN from $Mo(VI)O_2(5-H-SAP)$ and $PEtPh_2$,
neither $Mo(VI)O_2(5-H-SAP)$ nor $Mo(VI)O_2(5-H-SAE)$ reacted with
$PEtPh_2$ at any reasonable rates even at elevated temperatures
(up to 60°C) so no kinetic data are available for these two
series of complexes.

Linear Substituent Effects on k_1

The cis-dioxomolybdenum(VI) complexes, within each
series, contain ligand substituents that span the range from
electron withdrawing (Cl, Br) to electron donating (CH_3O)
(Table 13). Even though the X substituents are not directly
bonded to the molybdenum, their effect is transmitted
through the ligand to the Mo-oxo core. Electron withdrawing
substituents remove electron density from the Mo-oxo core,
making the oxo groups more electrophilic. The opposite
effect is observed for electron donating substituents in
that the oxo groups are less electrophilic. This difference
in the electrophilic character of the $Mo(VI)O_2(5-X-SSP)$ and
$Mo(VI)O_2(5-X-SSE)$ series at 30°C and 60°C, respectively, is
manifested in the systematic variation of the specific rate

Table 13. Specific Rate Constants for the

Reaction of $Mo(VI)O_2(5-X-SSP)$ and

$Mo(VI)O_2(5-X-SSE)$ with $PEtPh_2$

| | k_1 $(M^{-1}sec^{-1})$ x 10^4 | |
Mo Complex	30°C	60°C
$Mo(VI)O_2(5-Br-SSP)$	19.6 (±0.6)	
$Mo(VI)O_2(5-Cl-SSP)$	18.7 (±0.2)	
$Mo(VI)O_2(5-H-SSP)$	10.2 (±0.9)	116.0 (±6.2)
$Mo(VI)O_2(5-CH_3O-SSP)$	8.4 (±0.4)	
$Mo(VI)O_2(5-Br-SSE)$		34.8 (±2.8)
$Mo(VI)O_2(5-Cl-SSE)$		34.6 (±2.7)
$Mo(VI)O_2(5-H-SSE)$	2.1 (±0.2)	28.1 (±1.8)
$Mo(VI)O_2(5-CH_3O-SSE)$		21.4 (±0.6)

constants, k_1, that are obtained for their reactions with PEtPh$_2$.

With the data shown in Table 13 there is a linear dependence of $\log(k_{1X}/k_{1H})$ (where k_{1X} is the specific rate constant for Mo(VI)O$_2$(5-X-SSP) or Mo(VI)O$_2$(5-X-SSE) and k_{1H} is the specific rate constant for Mo(VI)O$_2$(5-H-SSP) or Mo(VI)O$_2$(5-H-SSE) as standards) versus the Hammett σ_p parameter for the X substituent on the ligands for Mo(VI)O$_2$(5-X-SSP) and Mo(VI)O$_2$(5-X-SSE). From plots of $\log(k_{1X}/k_{1H})$ versus σ_p (Figure 21) the reaction constants, ρ, were found to be +0.75 (Mo(VI)O$_2$(5-X-SSP)) and +0.42 (Mo(VI)O$_2$(5-X-SSE)). The positive ρ values are consistent with the reaction mechanism described in a later section. The larger ρ value for Mo(VI)O$_2$(5-X-SSP) indicates that the 5-X-SSP^{2-} ligand with an extended π electron system is more effective than the 5-X-SSE^{2-} ligand in transmitting the electron-withdrawing or electron-donating substituent effect to the Mo-oxo core.

It is also interesting to note the difference in specific rate constants for the two complexes Mo(VI)O$_2$(5-H-SSP) and Mo(VI)O$_2$(5-H-SSE) at 30° and 60°C (Table 13). At these two temperatures the specific rate constant for Mo(VI)O$_2$(5-H-SSP) is approximately a factor of five larger than that found for Mo(VI)O$_2$(5-H-SSE). This behavior can be attributed to the ability of the 5-H-SSP^{2-} ligand to remove electron density from the MoO$_2$$^{2+}$ core to a greater extent than the 5-H-SSE^{2-} ligand. Thus the Mo(VI)O$_2$(5-H-SSP)

Figure 21. Plot of $\log(k_{1X}/k_{1H})$ versus Hammett σ_p for $Mo(VI)O_2(5\text{-}X\text{-}SSP)$ (●) and $Mo(VI)O_2(5\text{-}X\text{-}SSE)$ (■) ($X=Br,Cl,H,CH_3O$).

$$Mo(VI)O_2L + PEtPh_2 \xrightarrow{k_1} Mo(IV)OL + OPEtPh_2$$

$Mo(VI)O_2(5\text{-}X\text{-}SSP)$

$Mo(VI)O_2(5\text{-}X\text{-}SSE)$

$X = Br, Cl, H, CH_3O$

Hammett σ_p

complex is rendered more electrophilic than $Mo(VI)O_2$(5-H-SSE) in its reactivity towards $PEtPh_2$.

E_{pc} and k_1

The relationship between the specific rate constant, k_1, and cathodic reduction potential, E_{pc}, for $Mo(VI)O_2$(5-X-SSP) and $Mo(VI)O_2$(5-X-SSE) is worth considering since both parameters relate to a redox process. Figure 22 shows plots of k_1 (Table 13) versus E_{pc} (Table 9) for the two series $Mo(VI)O_2$(5-X-SSP) (at 30°C) and $Mo(VI)O_2$(5-X-SSE) (at 60°C). It is interesting to note the linear relationship which exists between k_1 and E_{pc} within each series. The same electronic effects which are bringing about systematic changes in the E_{pc}'s for these complexes also alter the electrophilic character of the molybdenum(VI) oxo ligand for its reaction with organophosphines. Within each series, as E_{pc} becomes more anodic the k_1's increase linearly.

It should be pointed out that the magnitude of the cathodic reduction potential itself is not sufficient to establish the rate of the reaction of a cis-dioxomolybdenum(VI) complex towards organophosphines. The E_{pc}'s for $Mo(VI)O_2$(5-X-SAP) and $Mo(VI)O_2$(5-X-SSE) fall into the same range between -1.27 and -1.11 V vs. NHE. Since the $Mo(VI)$-O_2(5-X-SSE) complexes reacted with $PEtPh_2$ at reasonable rates at 60°C, it was expected that $Mo(VI)O_2$(5-X-SAP) would react with $PEtPh_2$ as well because their E_{pc}'s are very similar and even slightly more anodic than those for their

Figure 22. Plot of k_1 versus E_{pc} for $Mo(VI)O_2$(5-X-SSP)
(● ; at 30°C) and $Mo(VI)O_2$(5-X-SSE) (■; at
60°C) (X=Br,Cl,H,CH$_3$O).

Figure showing a plot of $k_1 \times 10^4$ versus E_{pc} (volts vs NHE) for the reaction:

$$\text{Mo(VI)O}_2\text{L} + \text{PEtPh}_2 \xrightarrow{k_1} \text{Mo(IV)OL} + \text{OPEtPh}_2$$

- ● $\text{Mo(VI)O}_2\text{(5-X-SSP)}$ (30°C)
- ■ $\text{Mo(VI)O}_2\text{(5-X-SSE)}$ (60°C)

X = Br, Cl, H, CH_3O

Mo(VI)O$_2$(5-X-SSE) counterparts. This was found not to be the case. There was no appreciable reaction of Mo(VI)-O$_2$(5-X-SAP) with PEtPh$_2$ even at 60°C. The subtle role sulfur exhibits in altering the rates of these chemical reductions goes beyond the electronic effect that alters the electrochemistry. An additional example is seen in the electrochemistry and reactivity of Mo(VI)O$_2$(S$_2$CNEt$_2$)$_2$. In this complex the molybdenum is coordinated by four sulfur donor atoms. The E$_{pc}$ for this complex is -0.93 V vs. NHE when the cyclic voltammogram is measured under identical experimental conditions to those used for all the cis-dioxo-molybdenum(VI) listed in Table 9. The specific rate constant for the reaction of Mo(VI)O$_2$(S$_2$CNEt$_2$)$_2$ with PEtPh$_2$ at 25°C is 0.23 M^{-1}s^{-1} (164). This rate constant is significantly larger than that obtained for Mo(VI)O$_2$(5-Br-SSP) reacting with PEtPh$_2$ (k$_1$ = 19.6 x 10^{-4} M^{-1}s^{-1}; E$_{pc}$ = -1.05 V vs. NHE). One would not have predicted such a large rate constant for Mo(VI)O$_2$(S$_2$CNEt$_2$)$_2$ from just a consideration of its E$_{pc}$.

Activation Parameters for Oxygen Atom Transfer from Mo(VI)-O$_2$(5-H-SSP) and Mo(VI)$_2$(5-H-SSE)

Kinetic data were obtained for the reaction of Mo(VI)O$_2$(5-H-SSP) and Mo(VI)O$_2$(5-H-SSE) with PEtPh$_2$ at 30, 40, 50 and 60°C (Table 14). The activation energy (E$_a$) and the frequency factor (A) were obtained from Arrhenius plots of ln k versus T^{-1} (83). The activation enthalpy ($\Delta H^{\ddagger}$) was

Table 14. Kinetic and Activation Parameter Data

for $Mo(VI)O_2(5-H-SSP)$ and $Mo(VI)O_2(5-H-SSE)$

		$Mo(VI)O_2(5-H-SSP)$	$Mo(VI)O_2(5-H-SSE)$
$k_1 (M^{-1}sec^{-1})$	30°C	$10.2(\pm0.9)\times10^{-4}$	$2.1(\pm0.2)\times10^{-4}$
	40°C	$24.7(\pm1.0)\times10^{-4}$	$6.0(\pm0.2)\times10^{-4}$
	50°C	$56.1(\pm1.5)\times10^{-4}$	$13.9(\pm1.9)\times10^{-4}$
	60°C	$116.0(\pm6.2)\times10^{-4}$	$28.1(\pm1.8)\times10^{-4}$
E_a (kJ/mol)		67.9	73.0
$\Delta H^{\ddagger}$ (kJ/mol)		65.2	70.3
$\Delta S^{\ddagger}$ (J/mol-°k)		-86.5	-82.6

obtained from plots of ln k/T versus T^{-1} (83), and the activation entropy ($\Delta S^{\ddagger}$) was determined from the relationship ln A = ln(RT/Nh) + $\Delta S^{\ddagger}$/R + 1, where R = 8.314 J/(mol-K) and R/Nh = 2.084 x 10^{10} $K^{-1}s^{-1}$ (83). The activation energy (E_a) is the energy necessary for reactants to reach the activated complex. The activation enthalpy ($\Delta H^{\ddagger}$) is a measure of the height of this energy barrier and encompasses the particular bond strengths within and between reactants which must be overcome to reach the activated complex (83). Usually values of the activation energy and activation enthalpy are comparable in magnitude (174). This is what is observed for Mo(VI)O_2(5-H-SSP) and Mo(VI)O_2(5-H-SSE) (Table 14). Comparison of the values for the activation energy and activation enthalpy for Mo(VI)O_2(5-H-SSP) versus Mo(VI)O_2(5-H-SSE) indicates that in each instance the magnitude of these values is larger for Mo(VI)O_2(5-H-SSE). Usually, the larger the value of $\Delta H^{\ddagger}$, the slower the reaction (83), and this is consistent with the kinetic results obtained in this study (note the smaller specific rate constants obtained for Mo(VI)O_2(5-H-SSE) versus Mo(VI)O_2(5-H-SSP)).

The activation entropy ($\Delta S^{\ddagger}$) relates to the probability of reaction. This parameter includes contributions from requirements imposed by the orientation and steric bulk of the reactants and by their solvation (83). The negative values obtained for Mo(VI)O_2(5-H-SSP) and Mo(VI)O_2(5-H-SSE) are consistent with a bimolecular mechanism proposed for

these reactions which is discussed in the following section. Currently, no accurate activation parameter data are available for similar chemical systems to allow for comparisons.

Reaction Mechanism

Reynolds et al. (164) have described the reaction of $Mo(VI)O_2(S_2CNR_2)_2$ with PR_3 as a nucleophilic attack by the organophosphine on the molybdenum oxo group. This mechanism is consistent with the kinetic data presented here for $Mo(VI)O_2(5-X-SSP)$ and $Mo(VI)O_2(5-X-SSE)$. The mechanism may be represented as a simple bimolecular reaction involving the interaction between one $Mo(VI)O_2L$ complex and one $PEtPh_2$ molecule in the activated complex. The formation of the activated complex could lead to transfer of an oxygen atom by way of the donation of the lone pair of electrons of the phosphorus atom into the antibonding Mo-O π^* orbital. This would lead to the formation of the P-O bond and an oxo-molybdenum(IV) complex with a $4dxy^2$ electron configuration. A mechanism of this type is consistent with the values of $\Delta H^{\ddagger}$ obtained for $Mo(VI)O_2(5-X-SSP)$ and $Mo(VI)O_2(5-X-SSE)$ since the formation of the activated complex does not require any significant bond breaking or intramolecular reorganization. The mechanism is outlined in Figure 23.

Figure 23.   Proposed bimolecular mechanism for the reaction
of Mo(VI)O$_2$(5-X-SSP) or Mo(VI)O$_2$(5-X-SSE) with
PEtPh$_2$

VI. OXYGEN ATOM TRANSFER REACTIONS OF

OXOMOLYBDENUM(IV) COMPLEXES

Introduction

Models for the Molybdenum Reductase Enzymes

The transfer of an oxygen atom from substrates (XO) to oxomolybdenum(IV) model complexes (reaction (21)) has not been extensively investigated (95,164,165,175-177).

$$Mo(IV)OL_n + XO \xrightarrow{k} Mo(VI)O_2L_n + X \qquad (21)$$

An undesirable complication of reaction (21) is frequently encountered. This is the formation of μ-oxomolybdenum(V) dimers via reaction (22).

$$Mo(IV)OL_n + Mo(VI)O_2L_n \underset{\longleftarrow}{\overset{K}{\longrightarrow}} Mo_2(V)O_3L_{2n} \qquad (22)$$

Similar behavior has been observed for the reaction of $Mo(VI)O_2L_n$ complexes with various reductants (see Chapter V).

With few exceptions (95,164,165), reactivity of $Mo(IV)OL_n$ complexes with substrates capable of transferring an oxygen atom have only received qualitative examination (175-177). Mitchell and Scarle (176) have reported visual color changes for the oxidation of $Mo(IV)O(S_2CNEt_2)_2$ by various organic oxo donors, XO, in chloroform. In their

142

study it was noted that during the course of reaction (21) with XO = dimethylsulfoxide (Me$_2$SO), dioxygen (O$_2$), triphenylphosphine oxide (Ph$_3$PO), pyridine oxide (C$_5$H$_5$N-O), and dinitrogen oxide (N$_2$O) it was possible to oxidize Mo(IV)O(S$_2$CNEt$_2$)$_2$ to purple Mo$_2$(V)O$_3$(S$_2$CNEt$_2$)$_4$ and finally to yellow Mo(VI)O$_2$(S$_2$CNEt$_2$)$_2$. Chen et al (95) have repeated this work under strictly anerobic conditions for Ph$_3$PO and N$_2$O. The purple color characteristic of Mo$_2$(V)O$_3$(S$_2$CNEt$_2$)$_4$ observed by Mitchell and Scarle (176) in the original experiments could not be reproduced for either of the substrates. It was concluded that these substrates were not capable of oxygen atom transfer to Mo(IV)O(S$_2$CNEt$_2$)$_2$. The purple color of Mo$_2$(V)O$_3$(S$_2$CNEt$_2$)$_4$ observed in the reactions by Mitchell and Scarle (176) may have been due to incomplete anaerobicity.

Recently, Reynolds et al. (164) reported a detailed kinetic study on the reactivity of Mo(IV)O(S$_2$CNEt$_2$)$_4$ with Me$_2$SO and N-methylmorpholine-N-oxide, reactions (23) and (24)

Mo(IV)O(S$_2$CNEt$_2$)$_2$ + Me$_2$SO → Mo(VI)O$_2$(S$_2$CNEt$_2$)$_2$ + Me$_2$S   (23)

Mo(IV)O(S$_2$CNEt$_2$)$_2$ + → Mo(VI)O$_2$(S$_2$CNEt$_2$)$_2$) +

(24)

The oxidation of a 2 mM solution of $Mo(IV)O(S_2CNEt_2)_2$ in 1,2 dichloroethane by Me_2SO (reaction (23)) was shown to be very slow and required a greater than 500 fold excess of substrate. The reaction was monitored spectrophotometrically and the data were analyzed using a detailed kinetic treatment (164). This treatment was analogous to that employed in the kinetic analysis of the reduction of $Mo(VI)-O_2(S_2CNEt_2)_2$ with PPh_3. The specific rate constant for the reaction of Me_2SO with $Mo(IV)O(S_2CNEt_2)_2$ at 25°C was found to be 1.6×10^{-4} $M^{-1}s^{-1}$. This value is several orders of magnitude less than that obtained for PPh_3 oxidation by $Mo(VI)O_2(S_2CNEt_2)_2$ where the specific rate constant was found to be 0.071 $M^{-1}s^{-1}$ (164).

Interestingly, the reaction of a 2 mM solution of $Mo(IV)O(S_2CNEt_2)_2$ with 2.5 equivalents of N-methylmorpholine N-oxide in 1,2-dichloroethane solution, reaction (24), proved to be very rapid and could not be followed spectrophotometrically. Evidence for the occurrence of this reaction was obtained by ^{1}H NMR spectroscopy which indicated N-methylmorpholine as a reaction product. In addition, upon completion of the reaction the solvent was evaporated to leave a solid residue which was confirmed by its IR spectrum to be $Mo(VI)O_2(S_2CNEt_2)_2$. These results taken together provide strong evidence for the occurrence of reaction (24). The differences in the rates of reaction for the two substrates with $Mo(IV)O(S_2CNEt_2)_2$ suggest that breaking of the

bond to oxygen is the factor controlling the rates of these oxo transfer reactions (in the absence of steric effects).

This study by Reynolds et al. (164) represented the first well defined example wherein oxygen atom transfer to a molybdenum(IV) center occurred. However, it should be noted that throughout the course of these reactions the equilibrium reaction (22) was also occurring. Although this equilibrium does not interfere with the reduction of the substrates by $Mo(IV)O(S_2CNEt_2)_2$, systems which lack the equilibrium are far more biologically relevant.

Berg and Holm (165) have examined the reactions of a number of sulfoxides with 2,6-bis(2,2-diphenylethanethiolato)-pyridine-N,N-dimethylformamido-oxomolybdenum(IV), $Mo(IV)O(L'NS_2)(DMF)$ (reaction (25)).

$$Mo(IV)O(L'NS_2) + R_2SO \rightarrow Mo(VI)O_2(L'NS_2) + R_2S \quad (25)$$

During this process an oxo transfer reaction takesplace yielding the cis-dioxomolybdenum(VI) complex and the organic sulfide without the intervention of equilibrium reaction (22). For these reactions they report specific rate constants in DMF at 23°C of ~ 1.5×10^{-2} s^{-1}. The inclusion of the substrate d-biotin-d-sulfoxide is particularly noteworthy in view of the fact that this is believed to be the biological substrate reduced by the recently discovered molybdenum-cofactor-dependent enzyme, d-biotin-d-sulfoxide reductase (178).

In addition to sulfoxides, another substrate of biological interest is nitrate (NO_3^-) which is known to be reduced by the molybdenum containing enzyme nitrate reductase (see Chapter I). The current understanding is that molybdenum in this enzyme cycles between the +6 and +4 oxidation states during catalysis. Although a few reports concerning the interaction of a molybdenum(IV) center with NO_3^- have appeared (165,176,177), in many instances the products, presumably NO_2^- and molybdenum(VI), were not able to be sufficiently characterized.

Results and Discussion

We have been investigating the reaction of Mo(IV)O(5-H-SSP) with NO_3^- and NO_2^- in DMF under a dinitrogen atmosphere. Preliminary experiments (179) indicate that the reaction of Mo(IV)O(5-H-SSP) with NO_3^- in DMF can be followed spectrophotometrically. The spectral progression of the reaction (Figure 24) is the reverse of what is observed for the reaction of Mo(VI)O_2(5-H-SSP) with PEtPh$_2$ (Figure 17). The isosbestic point occurs at the same wavelength, ~ 396 nm. As the reaction proceeds it appears that the Mo(IV)O(5-H-SSP) complex is being converted into its Mo(VI)O_2(5-H-SSP) analogue by way of a two electron oxygen atom transfer redox process. Quantitative determinations (180) of the expected substrate reaction product, NO_2^-, have not produced the expected results for a stoichiometric conversion. The reason for this appears to

Figure 24. Spectral changes observed during the reaction
of Mo(IV)O(5-H-SSP) with NaNO$_3$ in DMF. The
initial concentration of Mo(IV)O(5-H-SSP) was
1.08 x 10^{-3} M and that of NaNO$_3$ was 3.49 x 10^{-4}
M. Spectra were recorded at 30°C at 5 minute
intervals.

$$Mo(IV)O(5\text{-}H\text{-}SSP) + NO_3^- \rightarrow Mo(VI)O_2(5\text{-}H\text{-}SSP) + NO_2^-$$

$$[Mo(IV)OL]_0 = 1.08 \times 10^{-3} \text{ M} \; ; \; [NO_3^-]_0 = 3.49 \times 10^{-4} \text{ M}$$

be a very rapid reaction of Mo(IV)O(5-H-SSP) with NO_2^-
analogous to its reaction with NO_3^-. The reaction appears
to follow the mechanism:

$$Mo(IV)O(5-H-SSP) + NO_3^- \xrightarrow{k_1} Mo(VI)O_2(5-H-SSP) + NO_2^- \qquad (26)$$

$$Mo(IV)O(5-H-SSP) + NO_2^- \xrightarrow{k_2} Mo(VI)O_2(5-H-SSP) + \tfrac{1}{2}N_2O_2^{2-} \quad (27)$$

If this mechanism is correct and one applies a steady state
approximation for the concentration of NO_2^- (which is
consistent with quantitative NO_2^- determinations) the rate
law becomes:

$$\frac{-d[Mo(IV)O(5-H-SSP)]}{dt} = 2k_1[Mo(IV)O(5-H-SSP)][NO_3^-]$$

Using a nonlinear regression analysis (181), k_1 is
calculated to be ~ 10 $M^{-1}s^{-1}$. At present k_2 cannot be
determined. The reaction of Mo(IV)O(5-H-SSP) with NO_2^-
(reaction (27)) is very rapid (i.e., $k_2 \gg k_1$) and cannot be
followed by conventional UV-visible spectroscopy.
Stopped-flow instrumentation is necessary to follow the
kinetic course of this reaction.

SUMMARY AND FUTURE WORK

The current understanding of the molybdenum enzymes, with the exception of nitrogenase, indicates that the molybdenum cycles between the +6 and +4 oxidation states during their reaction with substrate and subsequent reactivation. The enzymes are believed to catalyze reactions that are formally two electron oxygen atom transfer reactions. These reactions are of two types: oxidation, involving the addition of an oxygen atom to substrate, and reduction, involving the removal of an oxygen atom from substrate. Typical enzyme substrate reactions are listed below:

Xanthine Oxidase   Xanthine + [O] $\rightarrow$ Uric Acid

Aldehyde Oxidase   RCHO + [O] $\rightarrow$ RCOOH

Sulfite Oxidase SO_3^{2-} + [O] $\rightarrow$ SO_4^{2-}

Nitrate Reductase NO_3^- $\rightarrow$ [O] + NO_2^-

The objective of this research project was to develop a suitable oxygen atom transfer model complex that would (a) have a ligand donor atom set approaching that of the enzyme; (b) be interconvertible between the oxidized and reduced forms; and (c) be mononuclear and not form unreactive, biologically irrelevant μ-oxo-molybdenum(V) dimers during

150

the oxo transfer process. The chemical properties of four series of cis-dioxomolybdenum(VI) coordination complexes synthesized from the following tridentate Schiff base ligands were investigated with these objectives in mind.

Y=OH; 5-X-SAP-H_2

X=NO_2,Br,Cl,H,CH_3O

Y=SH; 5-X-SSP-H_2

Y=OH; 5-X-SAE-H_2

Y=SH; 5-X-SSE-H_2

X=Br,Cl,H,CH_3O

Cyclic voltammetry was used to obtain cathodic peak reduction potentials (E_{pc}). Kinetic and activation parameter data were obtained between 30° and 60°C for the following oxygen atom transfer reactions:

$$\text{Mo(VI)O}_2(\text{5-X-SSP}) + \text{PEtPh}_2 \xrightarrow[30°C]{k_1} \text{Mo(IV)O(5-X-SSP)} + \text{OPEtPh}_2$$

(28)

$$\text{Mo(VI)O}_2(\text{5-X-SSE}) + \text{PEtPh}_2 \xrightarrow[60°C]{k_1} \text{Mo(IV)O(5-X-SSE)} + \text{OPEtPh}_2$$
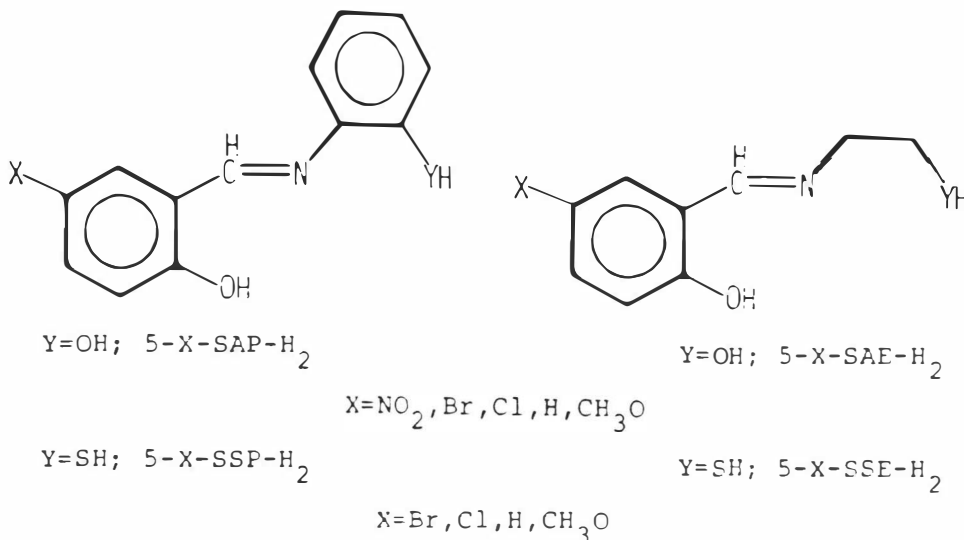
(29)
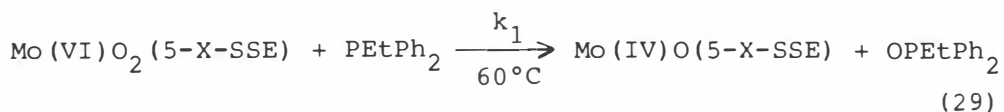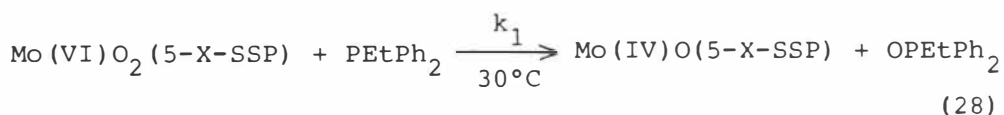
Reactions (28) and (29) have also been used to synthesize the Mo(IV)O(5-H-SSP) and Mo(IV)O(5-H-SSE) species, respectively. The kinetic data were consistent with the rate law, $-d[Mo(VI)O_2L]/dt = +d[Mo(IV)OL]/dt = k[Mo(VI)O_2L][PEtPh_2]$; L = 5-X-SSP or 5-X-SSE. $Mo(VI)O_2(5-X-SAP)$ and $Mo(VI)O_2(5-X-SAE)$ did not react with $PEtPh_2$ at any appreciable rate under the experimental conditions used. During the course of reactions (28) and (29) only oxomolybdenum(IV) species were produced and no μ-oxomolybdenum(V) dimers were formed. This was a significant result and represented the first reported example wherein dimer formation did not accompany reactions of this type.

For the four series of cis-dioxomolybdenum(VI) complexes studied, three ligand features were identified whose effects are to systematically alter both the specific rate constants (chemical reducibility) and cathodic reduction potentials (electrochemical reducibility). These include (1) the X-substituent on the salicylaldehyde portion of each ligand; (2) the degree of ligand π delocalization (5-X-SSP and 5-X-SAP versus 5-X-SSE and 5-X-SAE); and (3) the substitution of a sulfur donor atom in (5-X-SSP and 5-X-SSE) for an oxygen donor atom in (5-X-SAP and 5-X-SAE). Both chemical and electrochemical reductions were shown to be facilitated when the complexes possessed a ligand having an extended π-system, a sulfur donor atom, and an effective electron withdrawing substituent. The results obtained in this study are significant in that they direct the way

towards improving the utility and enhancing the reactivity of molybdenum coordination complexes in important biological redox reactions.

Additional studies which could be carried out as an extension of this project include: (1) examining further the reactivity of the oxomolybdenum(IV) complexes Mo(IV)O(5-H-SSP) and Mo(IV)O(5-H-SSE) with substrates such as NO_3^- and R_2SO using stopped-flow instrumentation. The preliminary spectral results obtained for the reaction of Mo(IV)O(5-H-SSP) with NO_3^- are very encouraging; (2) synthesize new ligands designed to incorporate steric features to prevent μ-oxomolybdenum(V) dimer formation and include substituents which would allow systematic "fine tuning" of the electronic and reactivity properties of the molybdenum center. The information gained in systematic studies of this type will enhance the current understanding of molybdenum's role in important biological reactions.

LIST OF REFERENCES

LIST OF REFERENCES

1. Swedo, K.B.; Enemark, J.H. J. Chem. Educ. 1979, 56, 70.

2. Stiefel, E.I. Prog. Inorg. Chem. 1977, 22, 1, and references therein.

3. Mitchell, P.C.H. "Proceedings of the First International Conference on the Chemistry and Uses of Molybdenum"; Mitchell, P.C.H., Ed., Climax Molybdenum Co.: Ann Arbor, MI, 1973; p. 1.

4. Gates, B.C.; Katzer, J.R.; Schuit, G.C.A. "Chemistry of Catalytic Processes"; McGraw Hill, New York, 1979, p. 390.

5. Hucknall, D.J. "Selective Oxidation of Hydrocarbons", Academic Press, New York, 1974, p. 14.

6. Yavorsky, P.M.; Akhtar, S.; Friedman, S. AIChE Symp. Ser. 137 1975, 70, 101.

7. Bray, R.C. Adv. Enzymol. Relat. Areas Mol. Biol. 1980, 15, 107.

8. Bray, R.C. The Enzymes 1975, 12, 299.

9. Frieden, E. Adv. in Exper. Med. and Biol. 1973, 48, p. 4.

10. Eady, R.R.; Smith, B.E.; Cook, K.A.; Postgate, J.R. Biochem. J. 1972, 128, 655.

11. Eady, R.R.; Smith, B.E. in "Treatise on Dinitrogen Fixation", Hardy, R.W.F., Ed., Wiley, New York, 1979, p. 399.

12. Vincent, S.P.; Bray, R.C. Biochem. J. 1978, 171, 639.

13. Enoch, H.G.; Lester, R.L. J. Biol. Chem. 1975, 250, 6693.

14. Hart, L.I.; McGartoll, M.A.; Chapman, H.R.; Bray, R.C. Biochem. J. 1970, 116, 851.

15. Felsted, R.L.; Chu, A. E.-Y.; Chaykin, S. J. Biol. Chem. 1973, 248, 2580.

16. Cohen, H.J.; Fridovich, I. J. Biol. Chem. 1971, 246, 359.

17. Cohen, H.J.; Fridovich, I. J. Biol. Chem. 1971, 246, 367.

18. Topham, R.W.; Walker, M.C. Fed. Proc. Fed. Am. Soc. Exp. Biol. 1982, 41, 889.

19. Topham, R.W.; Walker, M.C.; Calisch, M.P.; Williams, R.W. Biochemistry 1982, 21, 4529.

20. Johnson, J.L.; Wand, W.R.; Rajagopalan, K.V.; Duran, M.; Beemer, F.A.; Wadman, S.K. Proc. Nat. Acad. Sci. U.S.A. 1980, 77, 3715.

21. Colton, R. Coord. Chem. Rev. 1985, 62, 145.

22. Subramanian, P.; Kaul, B.; Spence, J.T. J. Mol. Catal. 1984, 23, 163.

23. Spence, J.T. Coord. Chem. Rev. 1983, 48, 59.

24. "Molybdenum and Molybdenum-Containing Enzymes"; Coughlan, M.P., Ed.; Pergamon Press, New York, 1980.

25. "Molybdenum Chemistry of Biological Significance"; Newton, W.E., Otsuka, S., Eds.; Plenum Press, New York, 1980.

26. Cramer, S.P. in "Advances in Inorganic and Bioinorganic Mechanisms", Sykes, A.G., Ed., Academic Press, New York, 1983, p. 259.

27. Pienkos, P.T.; Shah, V.K.; Brill, W.J., in reference 24, p. 385.

28. Johnson, J.L., in reference 24, p. 345.

29. Johnson, J.L.; Rajagopalan, K.V. Proc. Nat. Acad. Sci. U.S.A. 1982, 79, 6856.

30. "Nitrogen Fixation"; Newton, W.E. and Orme-Johnson, W.H., Eds.; University Park Press, Baltimore, 1980.

31. "Recent Developments in Nitrogen Fixation"; Newton, W.E.; Postgate, J.R.; Rodriguez-Barrueco, C., Eds., Academic Press, New York, 1977.

32. Benemann, J.R. Science 1973, 181, 164.

33. Carpenter, E.J.; Culliney, J.L. Science 1975, 187, 551.

34. Hageman, R.V.; Burris, R.H. in reference 24, p. 403.

35. Walker, M.N.; Mortenson, L.E. J. Biol. Chem. 1974, 249, 6356.

36. Orme-Johnson, W.H.; Hamilton, W.H.; Jones, T.L.; Tso, M.-Y.N.; Burris, R.H. Proc. Nat. Acad. Sci. U.S.A. 1972, 69, 3142.

37. Smith, B.E.; Lowe, D.J.; Bray, R.C. Biochem. J. 1973, 135, 331.

38. Palmer, G.; Multani, J.S.; Cretney, W.C.; Zumft, W.G.; Mortenson, L.E. Arch. Biochem. Biophys. 1972, 153, 325.

39. Davis, L.C.; Shah, V.K.; Brill, W.J.; Orme-Johnson, W.H. Biochim. Biophys. Acta 1972, 256, 512.

40. Zumft, W.G.; Mortenson, L.E. Biochim. Biophys. Acta 1975, 416, 1.

41. Dilworth, M.J. Biochim. Biophys. Acta 1966, 12, 285.

42. Schrauzer, G.N.; Robinson, P.R.; Moorehead, E.L.; Vickrey, T.M. In "Proceedings of the Second International Conference on the Chemistry and Uses of Molybdenum"; Mitchell, P.C.H. and Seaman, A., Eds., Climax Molybdenum Co.: Ann Arbor, MI, 1976, p. 246.

43. Smith, B.E.; Lang, G. Biochem. J. 1974, 137, 169.

44. Orme-Johnson, W.H.; Davis, L.C. "Iron-Sulfur Proteins", Vol. 3; Lovenberg, W., Ed.; Academic Press: New York, 1977, p. 31.

45. Hoffman, B.M.; Roberts, J.E.; Orme-Johnson, W.H. J. Am. Chem. Soc. 1982, 104, 860.

46. Hoffman, B.M.; Venters, R.A.; Roberts, J.E.; Nelson, M.; Orme-Johnson, W.H. J. Am. Chem. Soc. 1982, 104, 4711.

47. Cramer, S.P.; Eccles, T.K.; Kutzler, F.W.; Hodgson, K.O.; Mortenson, L.E. J. Am. Chem. Soc. 1976, 98, 1287.

48. Cramer, S.P.; Gillam, W.O.; Hodgson, K.O.; Mortenson, L.E.; Stiefel, E.I.; Chisness, J.R.; Brill, W.J.; Shah, V.K. J. Chem. Soc. 1978, 100, 3814.

49. Cramer, S.P.; Hodgson, K.O.; Gillam, W.O.; Mortenson, L.E. J. Am. Chem. Soc. 1978, 100, 7398.

50. Wolff, T.E.; Berg, J.M.; Warrick, C.; Hodgson, K.O.; Holm, R.H.; Frankel, R.B. _J. Am. Chem. Soc._ 1978, _100,_ 4630.

51. Christou, G.; Garner, C.P.; Mabbs, F.E. _Inorg. Chim. Acta_ 1978, _29,_ 189.

52. Howard, W.D.; Solomonson, L.P. _J. Biol. Chem._ 1982, _257,_ 10243.

53. Adams, M.W.W.; Mortenson, L.E. _J. Biol. Chem._ 1982, _257,_ 1791.

54. Cramer, S.P.; Solomson, L.P.; Adams, M.W.W.; Mortenson, L.E. _J. Am. Chem. Soc._ 1984, 106, 1467.

55. Solomonson, L.P.; Barber, M.J.; Howard, W.P.; Johnson, J.L.; Rajagopalan, K.V. _J. Biol. Chem._ 1984, 259, 849.

56. Wahl, W.R.; Rajagopalan, K.V . _Arch. Biochem. Biophys._ 1976, 172, 365.

57. Kaminski, Z.W.; Jezewska, M.M. _Biochem. J._ 1982, 207, 341.

58. Nelson, C.A.; Handler, P. _J. Biol. Chem._ 1968, 243, 5368.

59. Massey, V.; Brumby, P.E.; Komai, H.; Palmer, G. _J. Biol. Chem._ 1969, 244, 1682.

60. Gutteridge, S.; Bray, R.C. _Biochem. J._ 1980, 189, 615.

61. Bray, R.C.; Gutteridge, S. _Biochemistry_ 1982, 21, 5992.

62. Hille, R.; Stewart, R.C.; Fee, J.A.; Massey, V. _J. Biol. Chem._ 1983, 258, 4849.

63. Malthouse, J.P.G.; Bray, R.C. _Biochem. J._ 1980, 191, 265.

64. Cramer, S.P.; Wahl, R.; Rajagopalan, K.V. _J. Am. Chem. Soc._ 1981, 103, 7721.

65. Tullius, T.D.; Kurtz, D.M., Jr.; Conradson, S.D. Hodgson, K.O. _J. Am. Chem. Soc._ 1979, 101, 2776.

66. Bordas, J.; Bray, R.C.; Garner, C.D.; Hasnain, S.S. _Biochem. J._ 1980, 191, 499.

67. Gutteridge, S.; Tanner, S.J.; Bray, R.C.   Biochem. J. 1978, 175, 869.

68. Williams, J.W.; Bray, R.C.   Biochem. J. 1981, 195, 753.

69. Wahl, R.C.; Rajagopalan, K.V.   J. Biol. Chem. 1982, 257, 1354.

70. Cohen, H.J.; Betcher-Lange, S.; Kessler, D.L.; Rajagopalan, K.V.   J. Biol. Chem 1972, 247, 7759.

71. Oshino, N.; Chance, B.   Arch. Biochem. Biophys. 1975, 170, 514.

72. Kessler, D.L.; Rajagopalan, K.V.   Biochim. Biophys. Acta 1974, 370, 389.

73. Lamy, M.T.; Gutteridge, S.; Bray, R.C.   Biochem. J. 1980, 185, 397.

74. Bray, R.C.; Lamy, M.T., Gutteridge, S.; Wilkinson, T. Biochem. J. 1982, 201, 241.

75. Berg, J.M.; Hodgson, K.O.; Cramer, S.P.; Corbin, J.L.; Elsberry, A.; Pariyadath, N.; Stiefel, E.I.   J. Am. Chem. Soc. 1979, 101, 2774.

76. Jones, M.M.   J. Am. Chem. Soc. 1959, 81, 3188.

77. Gagne, R.R.; Koval, C.A.; Lisensky, G.C.   Inorg. Chem. 1980, 19, 2855.

78. Smith, L.I.; Opie, J.W.   "Organic Synthesis. Collection Volume 3", Wiley, London 1955, p 56.

79. Marini, P.J.; Murray, K.S.; West, B.O.   J. Chem. Soc. Dalton Trans 1983, 143.

80. Fallon, G.D.; Gatehouse, B.M.; Marini, P.J.; Murray, K.S.; West, B.O.   J. Chem. Soc. Dalton Trans. 1984, 2733.

81. Topich, J.   Inorg. Chem. 1981, 20, 3704.

82. Boyd, I.W.; Spence, J.T.   Inorg. Chem. 1982, 21, 1602.

83. Espenson, J.H.   "Chemical Kinetics and Reaction Mechanisms", McGraw-Hill: New York, 1981, pp. 117-120.

84. Kaul, B.B.; Enemark, J.H.; Merbs, S.L.; Spence, J.T. J. Am. Chem. Soc. 1985, 107, 2885.

85. Corbin, J.L.; Miller, K.F.; Pariyadath, N.; Wherland, S.; Bruce, A.E.; Stiefel, E.I. Inorg. Chim. Acta 1984, 90, 41.

86. Kay, A.; Mitchell, P.C.H. J. Chem. Soc. (A) 1970, 2421.

87. Moore, F.W.; Larson, M.L. Inorg. Chem. 1967, 6, 998.

88. Jowitt, R.N.; Mitchell, P.C.H. J. Chem. Soc. (A) 1969, 2632.

89. Jowitt, R.N.; Mitchell, P.C.H. J. Chem. Soc. (A) 1970, 1702.

90. Newton, W.E.; Corbin, J.C.; Bravard, D.C.; Searles, J.E.; McDonald, J.W. Inorg. Chem. 1974, 13, 1100.

91. McAuliffe, L.A.; Sayle, B.J. Inorg. Chim. Acta 1978, 30, 35.

92. Newton, W.E.; McDonald, J.W.; Yamanouchi, K.; Enemark, J.H. Inorg. Chem. 1979, 18, 1621.

93. Schneider, P.W.; Bravard, D.C.; McDonald, J.W.; Newton, W.E. J. Am. Chem. Soc. 1972, 94, 8640.

94. McDonald, D.B.; Schulman, J.I. Anal. Chem. 1975, 47, 2023.

95. Chen, G. J-J.; McDonald, J.W.; Newton, W.E. Inorg. Chem. 1976, 15, 2612.

96. Newton, W.E.; Chen, G. J-J.; McDonald, J.W. J. Am. Chem. Soc. 1976, 98, 5387.

97. Chen, G. J-J.; McDonald, J.W.; Newton, W.E. Inorg. Chim. Acta 1976, 19, L67.

98. McDonald, J.W.; Corbin, J.L.; Newton, W.E. Inorg. Chem. 1976, 15, 2056.

99. Dirand-Colin, J.; Schappacher, M.; Ricard, L.; Weiss, R. J. Less-Common Met. 1977, 54, 91.

100. Durant, R.; Garner, C.D.; Hyde, M.R.; Mabbs, F.E. J. Chem. Soc., Dalton Trans. 1977, 955.

101. Maatta, E.A.; Wentworth, R.A.D.; Newton, W.E.; McDonald, J.W.; Watt, G.D. J. Am. Chem. Soc. 1978, 100, 1320.

102. Maatta, E.A.; Wentworth, R.A.D. Inorg. Chem. 1979,

18, 524.

103. Nakamura, A.; Nakayama, M.; Sugihashi, K.; Otsuka, S. Inorg. Chem. 1979, 18, 394.

104. Newton, W.E.; McDonald, J.W.; Corbin, J.C.; Ricard, L.; Weiss, R. Inorg. Chem. 1980, 19, 1997.

105. DeHayes, L.J.; Faulkner, H.C.; Doub, W.H., Jr.; Sawyer, D.T. Inorg. Chem. 1975, 14, 2110.

106. Schultz, F.A.; Ott, V.R.; Rolison, D.S.; Bravard, D.C.; McDonald, J.W.; Newton, W.E. Inorg. Chem. 1978, 17, 1758.

107. Berg, J.M.; Hodgson, K.O. Inorg. Chem. 1980, 19, 2180.

108. Melby, L.R. Inorg. Chem. 1969, 8, 349.

109. Stiefel, E.I.; Miller, K.F.; Bruce, A.E.; Pariyadath, N.; Heinecke, J.; Corbin, J.C.; Berg, J.M.; Hodgson, K.O., in reference 5, p. 279.

110. Stiefel, E.I.; Miller, K.F.; Bruce, A.E.; Corbin, J.L.; Berg, J.M.; Hodgson, K.O. J. Am. Chem. Soc. 1980, 102, 3624.

111. Berg, J.M.; Spira, D.J.; Hodgson, K.O.; Bruce, A.E.; Miller, K.F.; Corbin, J.L.; Stiefel, E.I. Inorg. Chem. 1984, 23, 3412.

112. Corbin, J.L.; Miller, K.F.; Pariyadath, N.; Heinecke, J.; Bruce, A.E.; Wherland, S.; Stiefel, E.I. Inorg. Chem. 1984, 23, 3404.

113. Buchanan, I.; Minelli, M.; Ashby, M.T.; King, T.J.; Enemark, J.H.; Garner, C.D. Inorg. Chem. 1984, 23, 495.

114. Berg, J.M.; Spira, D.; Wo, K.; McCord, B.; Lye, R.; Co, M.S.; Belmont, J.; Barnes, C.; Kosydar, K.; Raybuck, S.; Hodgson, K.O.; Bruce, A.E.; Corbin, J.L.; Stiefel, E.I. Inorg. Chim. Acta 1984, 90, 35.

115. Topich, J. Inorg. Chim. Acta 1980, 46, L37.

116. Topich, J.; Lyon, III, J.T. Polyhedron 1984, 3, 55.

117. Rajan, O.A.; Chakravorty, A. Inorg. Chem. 1981, 20, 660.

118. Hill, W.E.; Ataby, N.; McAuliffe, C.A.; McCullough,

F.P.; Razzoki, S.M. Inorg. Chim. Acta 1979, 35, 35.

119. Subramanian, P.; Spence, J.T.; Ortega, R.; Enemark, J.H. Inorg. Chem. 1984, 23, 2565.

120. Syamal, A.; Maurya, M.R. Trans. Met. Chem. 1985, 10, 45.

121. Goh, W.-K.; Lim, M.-C. Aust. J. Chem. 1984, 37, 2235.

122. Syamal, A.; Niazi, M.A.B. Trans. Met. Chem. 1985, 10, 54.

123. Marabella, C.P.; Enemark, J.H.; Miller, K.F.; Bruce, A.E.; Pariyadeth, N.; Corbin, J.L.; Stiefel, E.I. Inorg. Chem. 1983, 22, 3456.

124. Rajan, O.A.; Spence, J.T.; Leman, C.; Minelli, M.; Sato, M.; Enemark, J.H.; Kroneck, P.M.H.; Sulger, K. Inorg. Chem. 1983, 22, 3065.

125. Berg, J.M.; Holm, R.H. Inorg. Chem. 1983, 22, 1768.

126. Berg, J.M.; Holm, R.H. J. Am. Chem. Soc. 1985, 107, 917.

127. Yamanouchi, K.; Yamada, S. Inorg. Chim. Acta 1974, 9, 161.

128. Gullotti, Pasini, A.; Zanderighi, G.M.; Ciani, G.; Sironi, A. J. Chem. Soc. Dalton Trans. 1981, 902.

129. Pickett, C.; Kumar, S.; Vella, P.A.; Zubieta, J. Inorg. Chem. 1982, 21, 908.

130. Bruce, A.; Corbin, J.L.; Dahlstrom, P.L.; Hyde, J.R.; Minelli, M.; Stiefel, E.I.; Spence, J.T.; Zubieta, J. Inorg. Chem. 1982, 21, 917.

131. Dahlstrom, P.L.; Hyde, J.R.; Vella, P.A.; Zubieta, J. Inorg. Chem. 1982, 21, 927.

132. Spence, J.T.; Minelli, M.; Kroneck, P. J. Am. Chem. Soc. 1980, 102, 4538.

133. Ibers, J.A.; Holm, R.H. Science 1980, 209, 223.

134. Dilworth, J.R.; McAuliffe, C.A.; Sayle, B.J. J. Chem. Soc. Dalton Trans. 1977, 849.

135. Percy, G.C.; Thornton, D.A. J. Inorg. Nucl. Chem. 1972, 34, 3357.

136. Van den Bergen, A.; Murray, K.S.; West, B.O. Aust. J. Chem. 1975, 25, 105.

137. Yamanouchi, K.; Yamada, S. Inorg. Chim. Acta 1975, 12, 9.

138. Buchanan, I.; Garner, C.D.; Clegg, W. J. Chem. Soc. Dalton Trans. 1984, 1333.

139. Johnson, J.L.; Rajagopalan, K.V. J. Biol. Chem. 1977, 252, 2017.

140. Bard, A.J.; Faulkner, L.R. "Electrochemical Methods, Fundamentals and Applications", John Wiley and Sons: New York, 1980, pp. 228-229.

141. Koller, K.B. locally written simulation program.

142. Bard, A.J. Faulkner, L.R. "Electrochemical Methods, Fundamentals and Applications", John Wiley and Sons, New York, 1980, p. 430.

143. Rajan, O.A.; Chakravorty, A. Inorg. Chim. Acta 1979, 37, L503.

144. Isbell, Jr., A.F.; Sawyer, D.T. Inorg. Chem. 1971, 10, 2449.

145. Taylor, R.D.; Street, J.P.; Minelli, M.; Spence, J.T. Inorg. Chem. 1978, 17, 3207.

146. Patterson, G.S.; Holm, R.H. Inorg. Chem. 1972, 11, 2285.

147. Handy, R.F.; Lintredt, R.L. Inorg. Chem. 1974, 13, 893.

148. Walker, F.A.; Beroiz, D.; Kadish, K.M. J. Am. Chem. Soc. 1976, 98, 3484.

149. Kadish, K.M.; Morrison, M.M. Inorg. Chem. 1976, 15, 980.

150. Butler, G.; Chatt, J.; Leish, G.J.; Pickett, C.J. J. Chem. Soc. Dalton Trans. 1979, 113.

151. Chatt, J. Coord. Chem. Rev. 1982, 43, 337.

152. Ghosh, P.; Chakravorty, A. Inorg. Chem. 1983, 22, 1322.

153. Smith, D.A.; Schultz, F.A. Inorg. Chem. 1982, 21, 3035.

154. Garner, C.D.; Durant, R.; Mabbs, F.E. Inorg. Chim. Acta 1977, 24, L29.

155. Watt, G.D.; McDonald, J.W.; Newton, W.E. J. Less-Common Met. 1977, 54, 415.

156. Spence, J.T.; Kroneck, P. J. Less-Common Met. 1974, 36, 465.

157. Miller, K.F.; Wentworth, R.A.D. Inorg. Chem. 1977, 16, 3385.

158. Speier, G. Inorg. Chim. Acta 1979, 33, 139.

159. Barral, R.; Bocard, C.; Se're'e de Roch, I.; Sajus, L. Tetrahedron Lett. 1972, 1693.

160. Newton, W.E.; McDonald, J.W. J. Less-Common Met. 1977, 54, 51.

161. Hyde, J.; Venkatasubramian, K.; Zubieta, J. Inorg. Chem. 1978, 17, 414.

162. Chen, G.J.-J.; McDonald, J.W.; Newton, W.E. Inorg. Chim. Acta 1979, 35, 93.

163. Deli, J.; Speier, G. Transition Met. Chem. 1981, 6, 227.

164. Reynolds, M.S.; Berg, J.M.; Holm, R.H. Inorg. Chem. 1984, 23, 3057.

165. Berg, J.M.; Holm, R.H. J. Am. Chem. Soc. 1985, 107, 925.

166. Topich, J.; Lyon, III, J.T. Inorg. Chim. Acta 1983, 80, L41.

167. Topich, J.; Lyon, III, J.T. Polyhedron 1984, 3, 61.

168. Topich, J.; Lyon, III, J.T. Inorg. Chem. 1984, 23, 3202.

169. Miyake, S.; Tanaka, K.; Tanaka, T. J. Chem. Soc. Dalton Trans. 1981, 292.

170. Matsuda, T.; Tanaka, K.; Tanaka, T. Inorg. Chem. 1979, 18, 454.

171. Steifel, E.I. in reference 24, p. 43.

172. Stynes, D.V. Inorg. Chem. 1975, 14, 453.

173. Shalhoub, G.M.; Reider, C.A.; Melson, G.A. Inorg. Chem. 1982, 21, 1998.

174. Laidler, K.J.; Meiser, J.H. "Physical Chemistry", Benjamin/Cummings: Menlo Park, CA, 1982, p. 380.

175. Durant, R.; Garner, C.D.; Hyde, M.R.; Mabbs, F.E.; Parsons, C.R.; Richens, D.J. J. LessCommon Met. 1977, 54, 459.

176. Mitchell, P.C.H.; Scarle, R. J. Chem. Soc., Dalton Trans. 1975, 2552.

177. Topich, J. Inorg. Chim. Acta 1980, 46, L97.

178. DelCampillo-Campbell, A.; Campbell, A. J. Bacteriol 1982, 149, 469.

179. Topich, J.; Lyon, III, J.T. unpublished results.

180. Shinn, M.B. Ind. Eng. Chem., Anal. Ed. 1941, 13, 33.

181. Dye, J.L.; Nicely, V.A. J. Chem. Ed. 1971, 48, 443, program modified by J. Topich to run on IBM-PC.

VITA